AN ANALYSIS OF HYBRID AND ELECTRIC VEHICLE CRASHES IN THE U.S.

Rong Chen
Virginia Tech
United States

Kyu-Sang Choi
Hyundai Motor Group
Republic of Korea

Allison Daniello
Virginia Tech
United States

Hampton Gabler
Virginia Tech
United States

Paper Number 15-0210

ABSTRACT

The growing popularity of hybrids and electric vehicles in the U.S. has raised questions about whether they might pose a different crash risk than conventional vehicles. In particular, there have been anecdotal reports of fires associated with the battery system in these advanced fuel vehicles. The objective of the study was to characterize the factors that influence the risk of serious to fatal injury in U.S. hybrid and electric passenger vehicle crashes.

Our approach in this study was to compare the crash performance of the conventional passenger vehicle fleet with hybrid/electric passenger vehicles in the U.S. The study was based upon the analysis of three U.S. crash databases: the Fatal Analysis Reporting System (FARS), the National Automotive Sampling System / Crashworthiness Data System (NASS/CDS), and the National Automotive Sampling System / General Estimates System (NASS/GES). Cases recorded by the databases between the years 1999 and 2013, and involving passenger vehicles model year 2000 and newer were extracted from all three databases.

Hybrid vehicles constituted less than 1% of the total vehicle population in all three databases. FARS contained no fatalities in electric vehicles, and less than 0.01 % of cases in NASS/CDS and NASS/GES involved electric vehicles.

The incidence of fire was lower for hybrid vehicles than the conventional fleet in all three databases. Fatal crashes involving fire constituted 2.6% of hybrid vehicle cases and 4.4% of conventional vehicle cases. No cases of fire or electric shock injury associated with hybrid vehicles were found in NASS/CDS. Only 1 case of a hybrid fire was found in NASS/GES and 5 cases of hybrid fire were found in FARS. No fires involving electric vehicles were found in any of the three databases.

Similar crash characteristics were found for both hybrid and conventional vehicle populations. Median longitudinal delta-V was 18 km/hr for hybrid vehicles and 14 km/hr for conventional vehicles. Hybrid vehicle occupants were found to have higher risk of AIS2+ upper extremity injury but lower risk of AIS2+ lower extremity injury than conventional vehicle occupants. Similar risk of AIS2+ head and chest injury was observed between the two groups.

The most notable difference between hybrid vehicles and conventional passenger-vehicles was that occupants of hybrid vehicle were more likely to be older than occupants of conventional vehicles. In FARS, the median age of fatally injured hybrid vehicle occupants was 59 years versus 36 years for conventional vehicle occupants. In NASS/CDS, the median age of hybrid vehicle occupants was 42 years and the median age of conventional vehicle occupants was 29 yrs. In NASS/GES, the median age of hybrid/electric vehicle occupants was 44 years, as compared to the median age of 32 years for conventional vehicle occupants.

The present study characterized the crash and occupants of hybrid and electric vehicles. The comparison between hybrid and conventional vehicle crashes showed little difference in the crash performance and injury outcome between the two groups. The incidence of fire was actually lower in hybrid vehicles than in the rest of the fleet.

INTRODUCTION

Hybrid and electric vehicles have been gaining popularity in the U.S. market since their introduction. Nearly 500,000 hybrid vehicles and 100,000 electric vehicles were sold in the U.S. market in the year 2013 [1]. Although the improved fuel economy offered by hybrid and eletric vehicles have made them very attractive to consumers, the advanced battery systems utilized by these vehicles have raised questions whether they pose a different crash risk than conventional fuel vehicles. It is still unknown whether hybrid and electric vehicles' reliance on heavy battery packs lead to different crash outcomes as compared to similar size conventional vehicles.

Several instances of battery fire associated with hybrid and electric vehicles have been reported. In 2011, The National Highway Traffic Safety Administration (NHTSA) reported that a Chevrolet Volt, which had undergone the side impact pole test as part of the New Car Assessment Program (NCAP), had sustained damage to the lithium-ion battery during the crash test and subsequently experienced a fire [2]. In March 2013, Mitsubishi Motors reported two instances of battery fire associated with the Mitsubishi i-MiEV and Mitsubishi Outlander P-HEV. Both fires occurred at Mitubishi's battery pack assembly plant during testing [3]. Although these fires occurred in unusual conditions, the concern remains that a real world crash of sufficient severity could trigger a fire event.

The objective of this study is to characterize the factors which influence the risk of serious to fatal injury in U.S. hybrid and electric passenger vehicle crashes. Specifically, we would like to answer the following three questions:

1. What is the frequency of fire in these crashes?
2. What are the characteristics of the occupants in these crashes?
3. What types of crashes and injury outcomes are associated with each vehicle fleet?

METHOD

Our approach in this study was to compare the crash performance of the conventional passenger vehicle fleet with the crash performance of hybrid and electric passenger vehicles in the U.S. The study was based upon the analysis of three U.S. crash databases: (1) the Fatal Analysis Reporting System (FARS), (2) the National Automotive Sampling System / Crashworthiness Data System (NASS/CDS), and (3) the National Automotive Sampling System / General Estimates System (NASS/GES).

FARS is a census of all traffic fatalities in the U.S. and was used in this study to determine the characteristics of fatal crashes. NASS/CDS is a sample of 4000-5000 in-depth crash investigations collected each year at 24 sites nationally. NASS/CDS provides exhaustive detail on injuries suffered in these crashes and, in this study, was used to explore the factors associated with injury. To be included in NASS/CDS, cases must involve at least one passenger car or truck and be of sufficient severity that one vehicle was towed from the scene. NASS/GES is a database of approximately 60,000 crashes/year sampled from U.S. police reported crashes, and was used for computation of exposure in this study. Both NASS/CDS and NASS/GES are weighted to be representative of crashes nationally.

Cases were extracted from all three databases using the criteria listed below.

- Case Year 1999-2013
- Model Year (MY) 2000+
- Cars, light trucks, and vans only
- Hybrids identified by Make/Model codes and Fuel Code Variable (hybrid)

These criteria were chosen to include only vehicles with the latest safety technologies. All MY 2000+ passenger vehicles would have been equipped with both driver and right front passenger airbags.

NASS/CDS describes the severity of these injuries based on the Abbreviated Injury Scale (AIS). AIS ranks injuries on a scale of 1-6 based on the threat to the life of the occupant, AIS 1 is a minor injury and AIS 6 is an unsurvivable injury. Here we focused on AIS2+ injured occupants – those occupants with moderate (AIS2) to unsurvivable (AIS6) injuries. Our analysis classified injury severity by the maximum AIS (MAIS) level injury sustained by an occupant. In the analysis which follows, weighted values based on NASS sample weight were used in order to better represent the larger population.

Hybrid and electric vehicles were identified in two ways. For most cases in FARS and NASS/CDS, hybrid and electric cars were identified by using the NASS and FARS FUELCODE variable, which denotes the type of fuel

used in the vehicle. In the event of a missing FUELCODE, the make-model codes of known hybrid and electric vehicles models, e.g. the Toyota Prius and the Chevrolet Volt, were used to identify hybrid and electric vehicles. NASS/GES does not contain a similar FUELCODE variable which describe the type of fuel used in the vehicle. For cases in NASS/GES, make-model codes of known hybrid and electric vehicle models were used to identify hybrid and electric vehicles.

RESULTS

Dataset Composition

Table 1 shows the composition of vehicles in all three databases used in the study. Hybrid vehicles made up approximately 0.3% of the fatal crashes in FARS, 0.7% of the weighted cases in NASS/CDS, and 0.3% of the weighted cases in NASS/GES. No fatalities associated with electric vehicles were found in the FARS databases. Only 2 electric vehicles were found in the NASS/CDS database, representing approximately 0.002% of the weighted vehicle sample, and 18 electric vehicles were found in the NASS/GES database, representing approximately 0.003% of the weighted vehicle sample in NASS/GES. Given the small proportions of electric vehicles in the databases, the following analysis only focuses on the comparison between hybrid and conventional vehicles.

Table 1.
Dataset Composition of Vehicles in All Databases (Case Year 1999-2013)

Database	Hybrid Vehicles (%)	Electric Vehicles (%)	Conventional Vehicles (%)	Total Vehicles (%)
FARS	421 (0.3%)	-	128,119 (99.7%)	128,540 (100%)
NASS/CDS (Unweighted)	377 (0.7%)	2 (0.004%)	55,696 (99.3%)	56,075 (100%)
NASS/CDS (Weighted)	165,932 (0.7%)	553 (0.002%)	25,308,829 (99.3%)	25,475,314 (100%)
NASS/GES (Unweighted)	1,863 (0.3%)	18 (0.003%)	561,812 (99.7%)	563,693 (100%)
NASS/GES (Weighted)	233,796 (0.3%)	2,310 (0.003%)	68,280,880 (99.7%)	68,516,986 (100%)

Dataset Composition

Table 2 shows the distribution of body types for vehicles in the databases. Weighted percentages are shown for NASS/CDS and NASS/GES databases. As shown by the table, conventional vehicles contains approximately equal percentage of cars and LTV, while hybrid vehicles are predominantly passenger cars.

Table 2.
Distribution of Vehicle Body Type in All Databases (Case Year 1999-2013)

Database	Hybrid Vehicles		Conventional Vehicles	
	Cars (%)	LTV (%)	Cars (%)	LTV (%)
FARS	94%	6%	55%	45%
NASS/CDS (Weighted)	87%	13%	57%	43%
NASS/GES (Weighted)	100%	0%	57%	43%

Incidence of Fire in Vehicles

Table 3 shows the number of vehicles involved in crashes with fire in all three databases. In fatal vehicle crashes extracted from FARS, incidence of fire was found in 11 of the 421 hybrid vehicles (2.6%). In comparison, 5,619 of 128,119 conventional vehicles (4.4%) involved in fatal crashes had fire occurrence.

Similar to the FARS analysis, Table 3 shows that vehicle fire was also rare for cases included in NASS/CDS. No hybrid vehicles in the sample experienced a vehicle fire and only 330 of 56,075 conventional vehicles had a fire. Using weighted numbers, this comprised approximately 0.1% of all conventional vehicles in crashes.

The incidence of fire was similarly rare in NASS/GES. Only 1 hybrid vehicle was reported to be involved in a fire, while 974 conventional vehicles were involved in crashes with fire incidences in NASS/GES. Using the NASS/GES weighting factor, fire occurred in 0.03% of all hybrid vehicles and 0.07% of all conventional vehicles.

Table 3.
Vehicles in Crashes Involving Fire in All Databases (Case Year 1999-2013)

Database	Hybrid Vehicles (% of All Hybrid)	Electric Vehicles (% of All Electric)	Conventional Vehicles (% of All Conventional)
FARS	11 (2.6%)	-	5,619 (4.4%)
NASS/CDS (Unweighted)	-	-	330 (0.6%)
NASS/CDS (Weighted)	-	-	37216 (0.1%)
NASS/GES (Unweighted)	1 (0.05%)	-	974 (0.2%)
NASS/GES (Weighted)	61 (0.03%)	-	48,685 (0.07%)

Incidence of Electric Shock

In addition to the incidence of fire, we also searched for any reports of electric shock. Using the sample of crashes from NASS/CDS, AIS codes for all occupants were searched for cases of electric shock. However, no such cases were found in our dataset for either hybrid, electric, or conventional vehicles. Note however, that NASS/CDS only contains vehicles involved in towaway crashes. These results should not be generalized to non-towaway crashes on other non-crash situations.

Occupant Characteristics

Occupant Composition and Gender Table 4 shows the occupant distribution by gender in all three databases. Only weighted gender percentages are shown from both NASS/CDS and NASS/GES datasets. A total of 465 fatally injured hybrid vehicle occupants and 142,821 fatally injured conventional vehicle occupants were found in the FARS data set. Of all fatally injured hybrid vehicle occupants, 58% were male and 42% were female. On the other hand, 62% of all fatally injured conventional vehicle occupants were male and 38% were female.

In NASS/CDS, the distribution of gender between all exposed occupants was almost equal. 43% of hybrid vehicle occupants and 51% of conventional vehicle occupants in NASS/CDS were male. However, only 11% of all MAIS2+ injured hybrid occupants were male, while 47% of all MAIS2+ injured conventional vehicle occupants were male and 53% were female.

Similar to occupants in NASS/CDS, the distribution of gender in NASS/GES was found to be fairly equal. 50% of conventional vehicle occupants were male, while 47% of hybrid occupants were male.

Table 4.
Occupant Count and Gender Distribution in All Databases (Case Year 1999-2013)

Database	Hybrid Vehicle Occupants			Conventional Vehicle Occupants		
	Occ. Count	% Male	% Female	Occ. Count	% Male	% Female
FARS	465	58%	42%	142,821	62%	38%
NASS/CDS (All Occ. Unweighted)	407	-	-	66,037	-	-
NASS/CDS (MAIS2+ Unweighted)	62	-	-	11,430	-	-
NASS/CDS (All Occ. Weighted)	165,070	43%	57%	25,029,076	51%	49%
NASS/CDS (MAIS2+ Weighted)	24,821	11%	89%	1,306,918	47%	53%
NASS/GES (All Occupants Unweighted)	2,523	-	-	802,523	-	-
NASS/GES (All Occupants Weighted)	301,992	47%	53%	94,734,122	50%	50%

Occupant Age The following subsection presents the distribution of occupant age in the three databases. Only occupants with known age are shown in the distributions. Occupants less than one year old are listed as having an age of 0.

Figure 1 shows a summary of median occupant age in all three databases. As shown by the figure, the median age of occupants in hybrid vehicles are generally older than occupants of conventional vehicles. In fatal crashes extracted from FARS, the median age of fatally-injured hybrid occupant was 59 years while the median age of fatally-injured conventional vehicle occupants was 36 years. For all occupants with MAIS2+ injuries in NASS/CDS, the median age for MAIS2+ injured hybrid vehicle occupants was 53 years, and 35 years for conventional vehicle occupants. For all exposed occupants in NASS/CDS, the median age for hybrid occupants was 42 years while the median age for conventional fleet occupants was 29 years. For all occupants in NASS/GES, the median age for conventional vehicle occupants was 32 years while the median age for hybrid occupants was 44 years old.

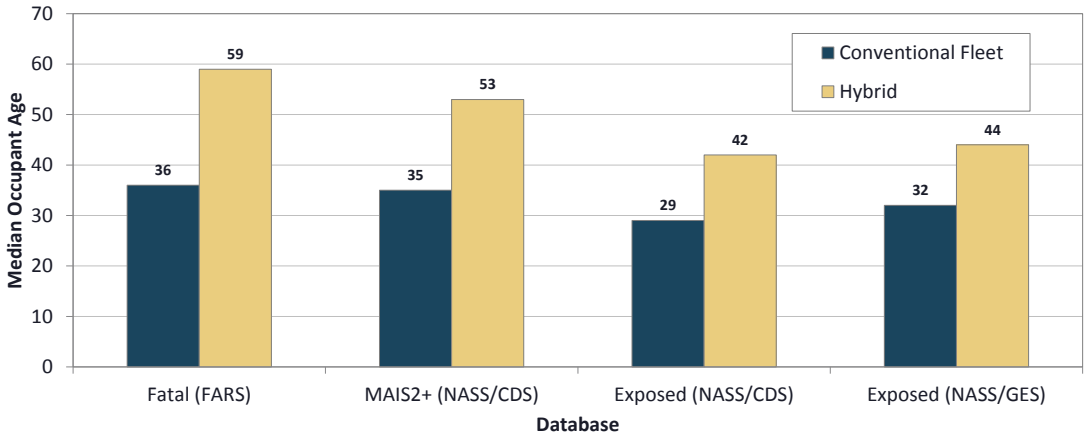

Figure 1. Summary of Median Occupant Age in Crashes (1999-2013)

Occupant Restraint Use The following subsection presents the occupant restraint use in each of the three databases. Only occupants with known restraint use are included in the distributions shown. The "Other" restraint category includes occupant wearing restraint other than lap and shoulder belt or a child restraint, such as lap belt only, shoulder belt only, or wearing the restraint improperly.

Figure 2 shows the distribution of occupant restraint use in fatal crashes extracted from FARS. The comparison between fatalities in hybrid occupants and fatalities in conventional vehicle occupants shows that belt usage was much higher in hybrid fatality crashes. Approximately 75% of occupants in hybrid vehicles were belted, while only 47% of occupants in the conventional fleet were belted.

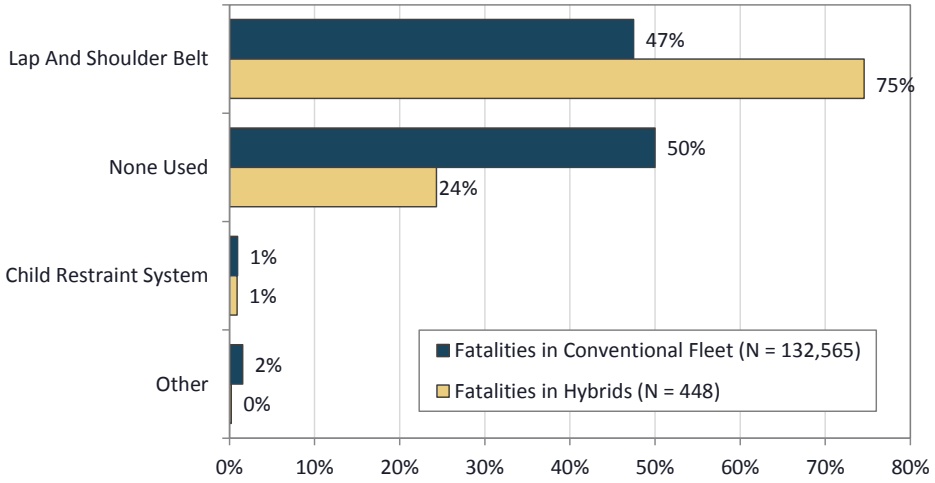

Figure 2. Distribution of Occupant Restraint Use in Fatal Crashes (FARS 1999-2013)

Figure 3 shows the restraint use distribution for all occupants exposed to crashes in NASS/CDS. Approximately 90% of both hybrid and conventional fleet occupants were belted.

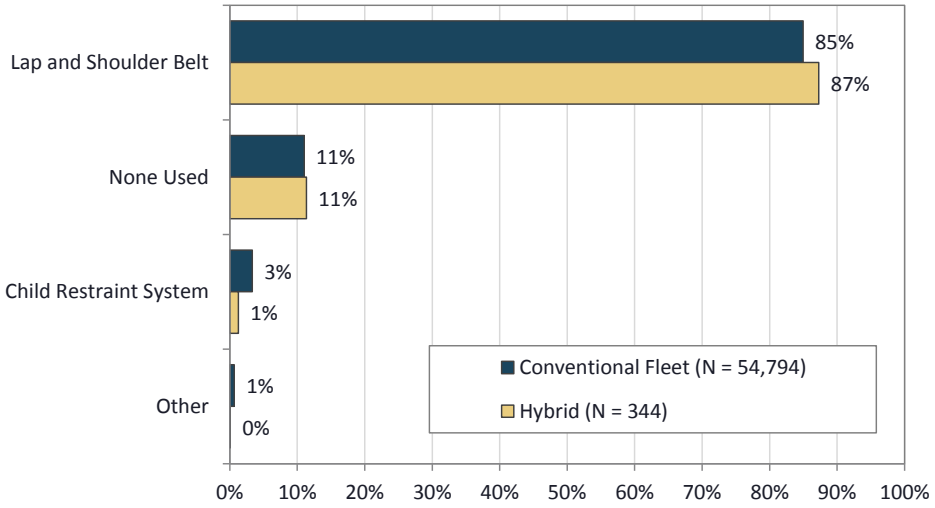

Figure 3. Distribution of Restraint Use in All Exposed Occupants (NASS/CDS 1999-2013)

Figure 4 shows the distribution of distribution of restraint use in MAIS2+ injured occupants in NASS/CDS. Compared to the distribution of all exposed occupants, the restraint use in MAIS2+ injured conventional vehicle occupants decreased from 85% to approximately 67%. On the other hand, the restraint use for hybrid vehicle occupants increased from 87% to 98%.

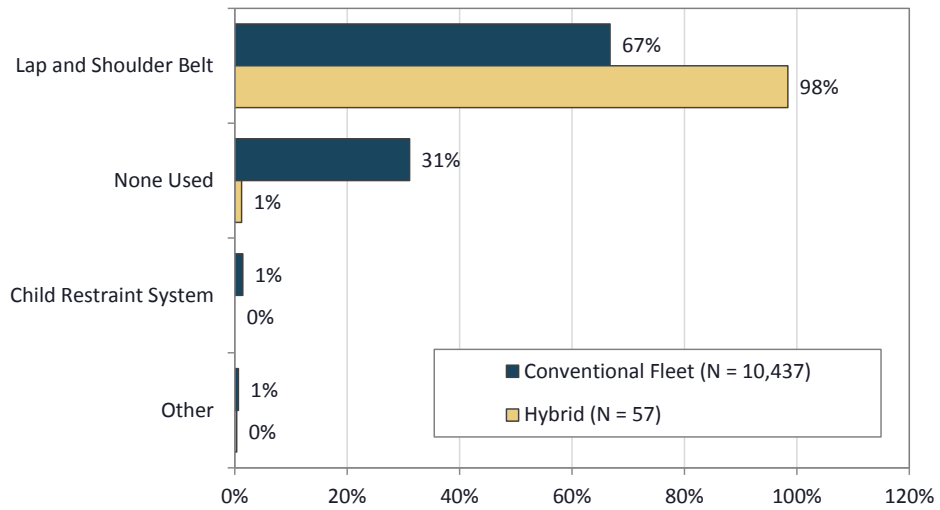

Figure 4. Distribution of Restraint Use in MAIS2+ Injured Occupants (NASS/CDS 1999-2013)

Lastly, Figure 5 shows the distribution of restraint use in all occupants involved in crashes in NASS/GES. As shown from the figure, conventional fleet occupants and hybrid occupants have similar restraint use. Approximately 88% of occupants in the conventional fleet were belted, and about 92% of hybrid occupants were belted.

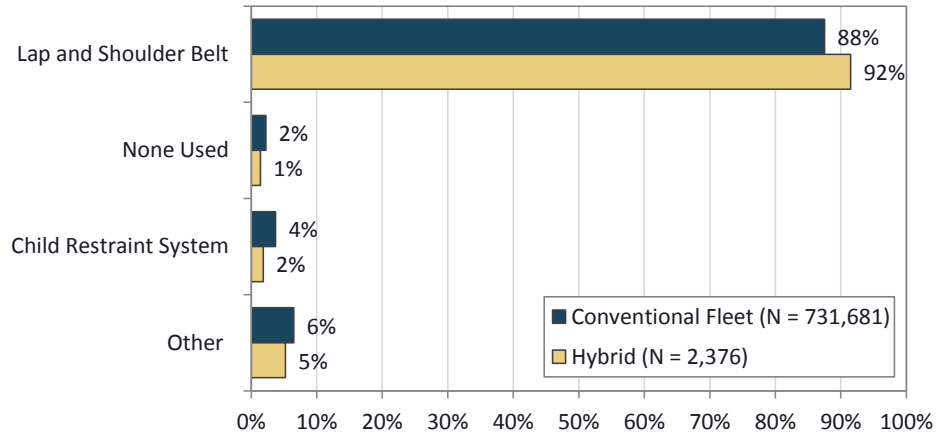

Figure 5. Distribution of Occupant Restraint Use in All Occupants (NASS/GES 1999-2013)

Figure 6 shows the summary of occupant restraint use in all three databases. In the distribution shown, restrained occupant refers to any occupant wearing a lap and shoulder belt, lap belt, shoulder belt, or child restraint. As shown in Figure 6, occupants in hybrid vehicles were generally more likely to be restrained.

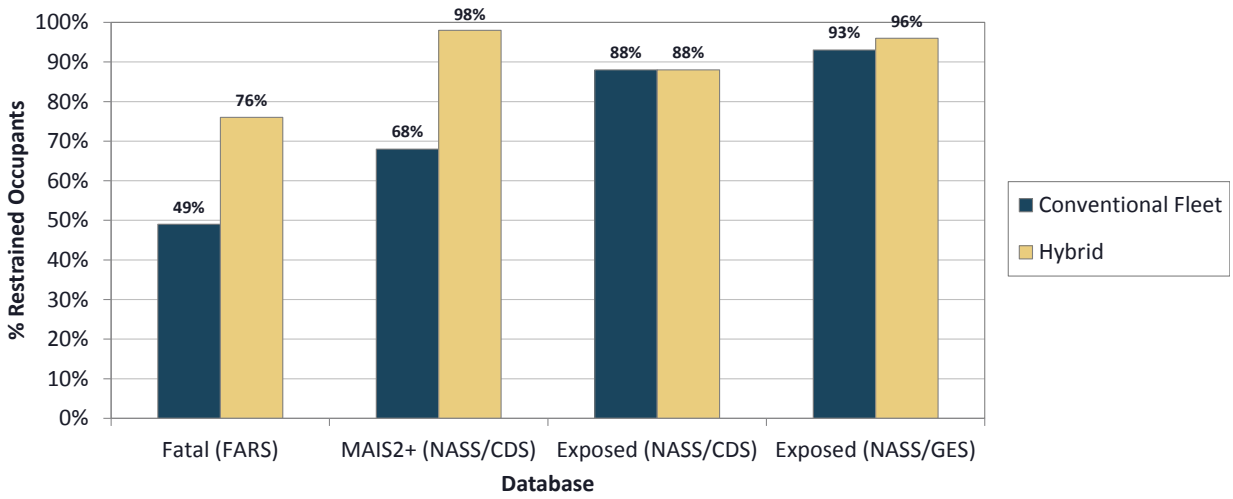

Figure 6. Summary of Occupant Restraint Use (1999-2013)

Occupant Risk of Injury The comparison of occupant injury was conducted using injury information reported from NASS/CDS. In this study, the risk of injury for a particular body region is calculated as fraction of cases at a given severity, as shown in Equation 1.

$$Risk\ of\ Injury = \frac{Number\ of\ Injuries\ to\ Body\ Region}{Total\ Number\ of\ Known\ Injuries} \quad (1)$$

Figure 7 compares the risk of AIS2+ injury by body regions for each occupant of hybrid and conventional vehicles. For both vehicle types, the risk of head injury was very similar (2.5% vs. 2.0%). Similarly, there was little difference in risk of chest injury (1.6% for conventional vehicle occupants and 1.2% for hybrid occupants). However, our sample predicted a higher risk of upper extremity injury for hybrid occupants (2.9% vs. 1.6%), and a lower risk of lower extremity injury for hybrid occupants (0.5% vs. 1.9%). When interpreting this plot, we caution again that the hybrid AIS2+ injuries are based upon a very small number of cases for occupants in hybrid vehicles.

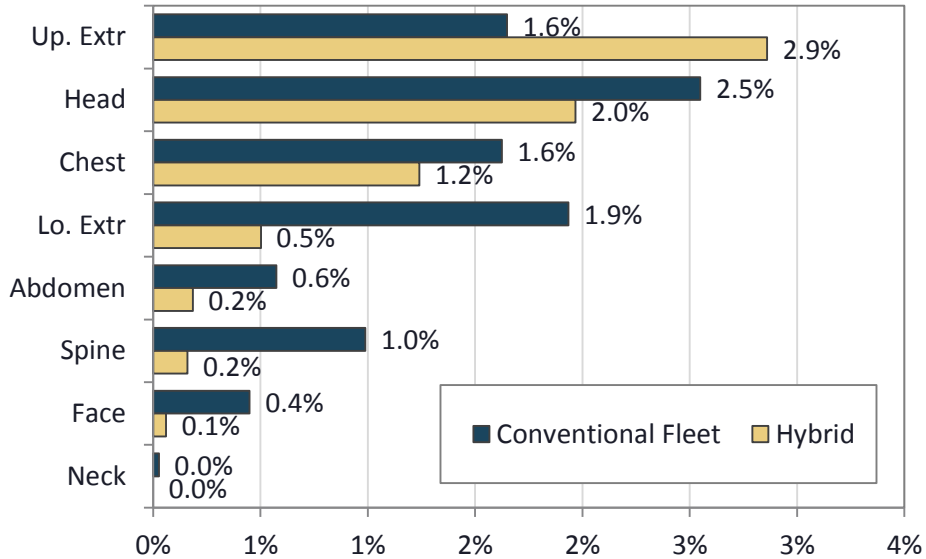

Figure 7. Risk of AIS2+ Injury by Body Region (NASS/CDS 1999-2013)

Crash Characteristics

Crash Mode Figure 8 presents the distribution of fatal crash modes for hybrid and conventional fleet vehicles. The distribution of crash mode is based on the most harmful event during the crash. However, after

year 2011, the definition of crash mode was changed in FARS. Therefore, the distribution shown in Figure 8 is limited to case year 1999-2011.

As shown by the figure, frontal crashes comprise the majority (50%) of fatal crashes, and side impact accounts for the second most common fatal crash mode (28%). For conventional vehicles however, rollover crashes and frontal crashes account for nearly equal percent of fatal crashes (37% and 35%, respectively). The increased incidence of rollover in conventional vehicles may be due to the large number of SUVs and pickup trucks in the fleet, which have a much higher risk of rollover.

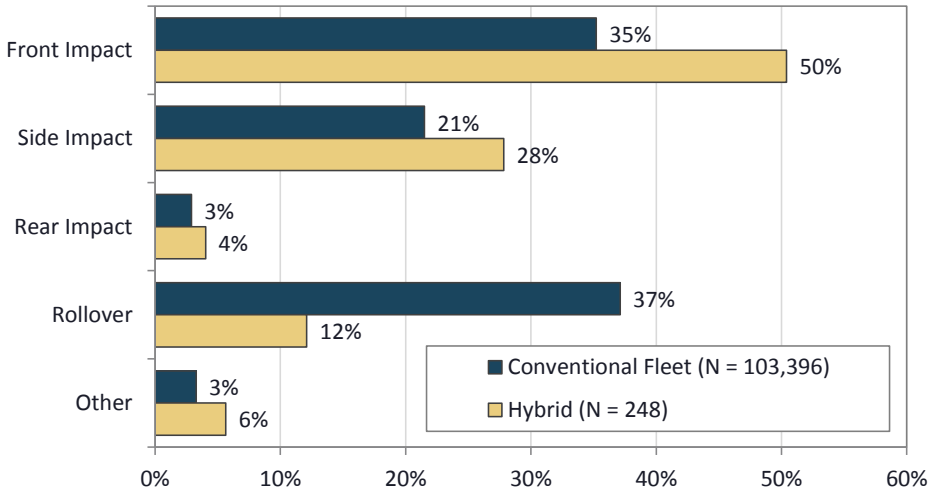

Figure 8. Distribution of Crash Mode in Fatal Crashes (FARS 1999-2011)

In the NASS/CDS dataset, the most common crash mode for MAIS2+ injured occupants in conventional vehicles was frontal impact, as shown by Figure 9. Over half of all MAIS2+ injured occupants in conventional vehicle were involved in a frontal impact. Side impact, including impacts to both the left and right side of the vehicle, was the most frequent crash mode for hybrid vehicles. Over 80% of all MAIS2+ injured hybrid occupants involved in a side impact. Rollover was more frequent in conventional vehicles as compared to hybrid vehicles, with 18% of all MAIS2+ injured conventional vehicle occupants exposed to rollover and less than 1% of all MAIS2+ injured hybrid vehicle occupants were exposed to rollovers.

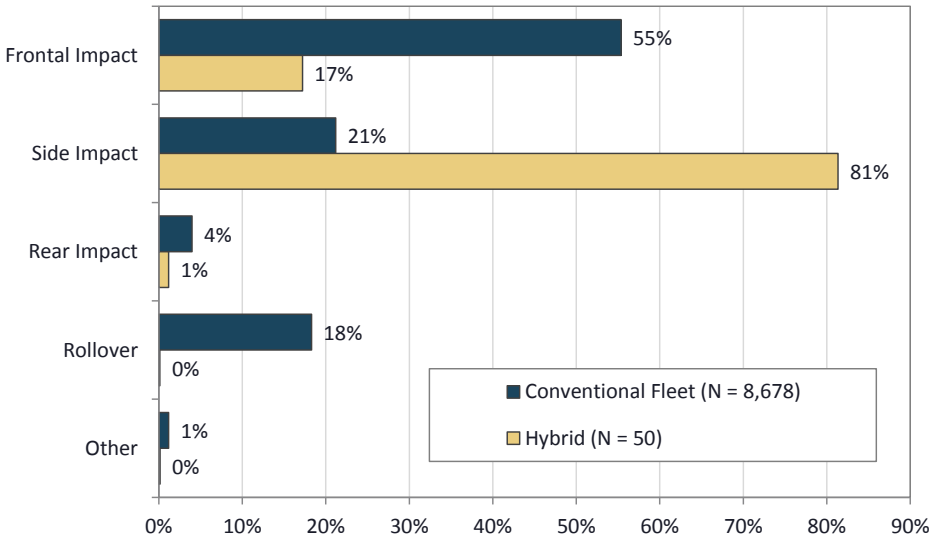

Figure 9. Distribution of Crash Mode in MAIS2+ Injured Crashes (NASS/CDS 1999-2013)

Figure 10 presents the distribution of crash modes in the NASS/GES database. As observed in the FARS and NASS/CDS analyses, frontal impact was the most common crash mode for both vehicle types, and accounted for

approximately 40% of all crashes for both vehicle types. However unlike FARS and NASS/CDS, rear impact was a close second in frequency with 26% of crashed conventional vehicles and 33% of crashes hybrid-vehicles. Rear impact is a common crash mode, but does not carry the injury risk of other crash modes. We hypothesized that rear impact was more common for hybrid vehicles as these are more likely to be drive in urban environments where frequent stop-and-go traffic leads to increase chance of rear end crashes.

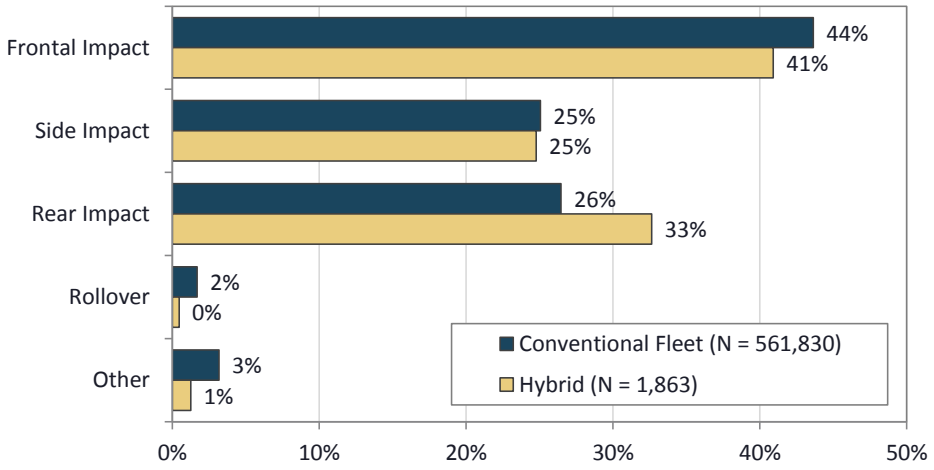

Figure 10. Distribution of Crash Mode in All Crashes (NASS/GES 1999-2013)

Crash Severity The struck vehicle change in velocity, or delta-V, is a widely used measure of crash severity. Longitudinal delta-V for all exposed occupants is presented in Figure 11. The median longitudinal delta-V for hybrid vehicles was 18 km/hr while the median delta-V for conventional vehicles was 14 km/hr. The delta-V for hybrid vehicles was higher as hybrids are in general lighter than conventional vehicles, which include a large number of SUVs and pickup trucks.

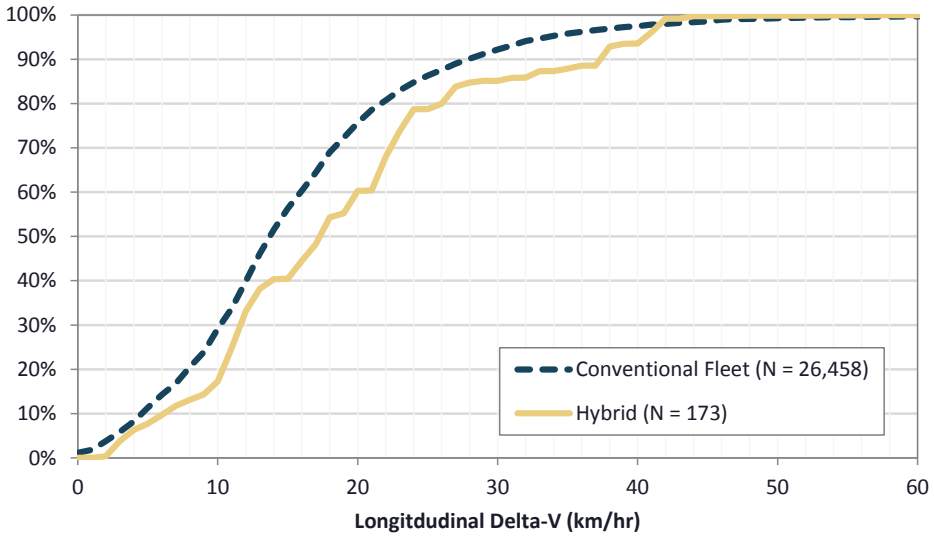

Figure 11. Distribution of Longitudinal Delta-V for All Occupants (NASS/CDS 1999-2013)

The lateral delta-V distribution was very similar for occupants of both hybrid and conventional vehicles. As shown by Figure 12, the median lateral delta-V was approximately 5 km/hr for hybrid vehicles and 3 km/hr for conventional fleet vehicles.

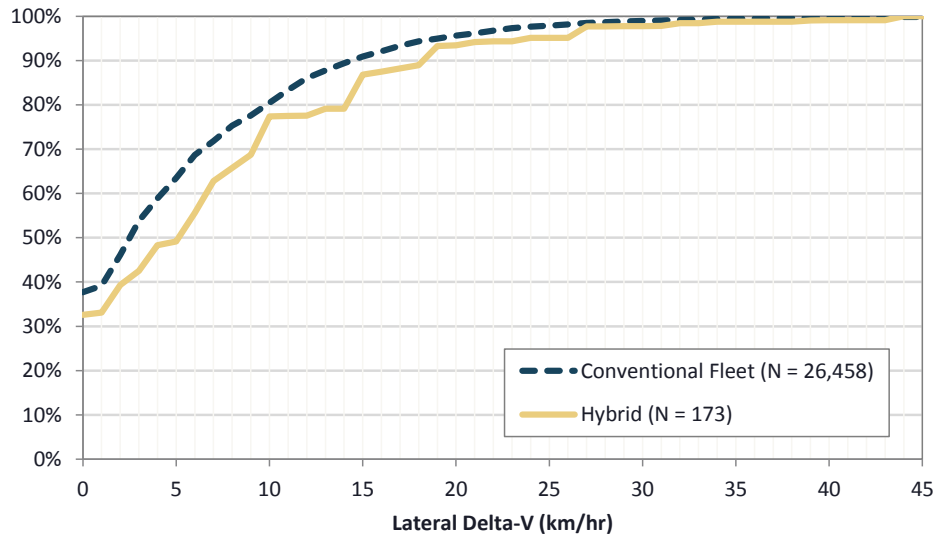

Figure 12. Distribution of Lateral Delta-V for All Occupants (NASS/CDS 1999-2013)

CONCLUSIONS

The goal of this study was to characterize the factors which influence the risk of serious to fatal injury in U.S. hybrid and electric passenger vehicle crashes. The study was based upon the analysis of three U.S. crash databases: (1) the Fatal Analysis Reporting System (FARS), (2) the National Automotive Sampling System / Crashworthiness Data System (NASS/CDS), and (3) the National Automotive Sampling System / General Estimates System (NASS/GES).

The analysis datasets included 421 hybrid vehicles from FARS, 377 hybrid vehicles from NASS/CDS, and 1,863 vehicles from NASS/CDS. Only 2 electric vehicles were found in NASS/CDS, and 18 electric vehicles were found in NASS/GES and, therefore, we could not further investigate electric vehicles in this study.

Fires were rare in both hybrid and conventional vehicles. Fatal crashes involving fire constituted 2.6% of hybrid cases and 4.4% of conventional vehicle cases. No cases of fire or electric shock injury for hybrids in NASS/CDS 1999-2013. Only 1 case of a hybrid fire was found in NASS/GES. The incidence of fire was lower for hybrids than conventional vehicles in all three databases.

The gender of fatally injured hybrid and conventional vehicle occupants was very similar. Males were more likely than females to be fatally-injured. For the population as a whole as described in GES, hybrid occupants were more likely to be female (53%) than conventional vehicle occupants (50%).

Hybrid occupants were more likely to be older than conventional vehicle occupants in all three databases. In FARS, the median age of fatally injured hybrid occupants was 59 yrs vs. 36 years for conventional vehicle occupants. In NASS/CDS, hybrid occupants were more likely to be older (42 yrs) than conventional vehicle occupants (29 yrs). In GES, hybrid occupants were more likely to be older (44 yrs) than conventional vehicle occupants (32 yrs).

The risk of MAIS2+ head and chest injury was very similar for both hybrid and conventional vehicles. Upper extremity injury risk was higher while lower extremity risk was lower for occupants of hybrids than those in conventional vehicles.

Frontal impact was more frequently the fatal crash mode for hybrid (50%) than conventional vehicles (35%). In NASS/CDS, frontal impact was more frequently the injury crash mode for conventional vehicles (53%) than hybrid vehicles (40%). In GES, frontal impact was most frequently the crash mode for both hybrids (41%) and conventional vehicles (44%).

Hybrids and conventional vehicles had similar crash severity based on cases included in NASS/CDS. Longitudinal delta-V for hybrids was 18 km/hr and 14 km/hr for conventional vehicles. Lateral delta-V were similar for both vehicle types.

Our study found little difference between hybrid/electric and conventional vehicle crashes, in either crash performance or injury outcome between the two groups. No unique factors that could influence the crash outcome of these advanced fuel vehicles were found in this study. However, the hybrid/electric vehicle population is currently only a small percentage of the market share. Future studies will benefit from examination of larger population of hybrid/electric vehicles.

ACKNOWLEDGEMENTS

Hyundai Motor Corporation is gratefully acknowledged for providing the funding for this study.

REFERENCES

[1] S. C. Davis, S. W. Diegel, R. G. Boundy, and S. Moore, "2013 Vehicle Technologies Market Report." Oak Ridge National Laboratory, Oak Ridge, TN, 2014.

[2] B. Smith, "Chevrolet Volt Battery Incident Overview Report," DOT HS 811 573, January 2012.

[3] Mitsubishi Motors, "Press Release: Fire of Electric Vehicle Battery Pack in Mizushima Plant," 2013. [Online]. Available: http://www.mitsubishi-motors.com/publish/pressrelease_jp/corporate/2013/news/detaild327.html. [Accessed: 27-Jan-2015].

Thermal modeling of fire propagation in lithium-ion batteries

Johan Anderson[1*], Fredrik Larsson[1,2], Petra Andersson[1] and Bengt-Erik Mellander[2]
[1] SP Technical Research Institute of Sweden, Borås, Sweden
[2] Applied Physics, Chalmers University of Technology, Göteborg, Sweden
[*] E-mail address: johan.anderson.br@sp.se

Paper Number 15-0073

ABSTRACT

The objective of the present work is to assess the risk of spreading of fire between Lithium-ion battery cells initiated by a thermal runaway. In particular it aims at developing means to predict the temperature of cells in the vicinity of an overheated cell during the first 5-7 minutes after the thermal event in a Li-ion cell that has an organic based electrolyte which is flammable. Finite-Element (FE) modelling is used to compute the heat transfer between cells. The spreading model is assessed modeling a scenario where the cells are exposed to a 15 kW propane burner. Two different models where utilized, one that considers the conjugate heat transfer between the surrounding hot gases and the battery cells while the second is a thermal model where the boundary conditions are measured in a mock-up test. The results from the two models are contrasted to experimental data where the heat release rate (HRR) is utilized as an input to the simulation. It is found that the temperature increase in a neighboring cell can be quantitatively estimated in certain cases during the early stages of the fire taking into account the anisotropic thermal conductivity of the cells using the conjugate heat transfer model. Moreover, the thermal model captures the qualitative behavior of the test results, however, the temperature increase is slower in the computational model.

KEYWORDS: lithium-ion, battery, fire, propagation, thermal model, thermal runaway

INTRODUCTION

Lithium-ion (Li-ion) batteries offer great performance in form of e.g. energy and power densities, enabling their use for a wide range of applications including the use in electrified vehicles, an application that is steadily growing. If the temperature in a Li-ion cell is increased beyond a certain threshold, a thermal runaway can occur, resulting in a rapid temperature increase and possibly other adverse effects such as, release of gas, smoke, fire and rupture/explosion. There are numerous types of abuse situations that can result in elevated temperatures inducing a thermal runaway. For example, mechanical abuse, electrical abuse and thermal abuse [1-11]. In case of a thermal runaway in a single Li-ion cell it is important to stop or at least delay its spreading to adjacent cells, since the effects from a cascading thermal runaway scenario of a complete battery pack could be devastating. Battery packs in electrified vehicles can consist of thousands of battery cells. In general, the design of a battery pack plays an important role for fire propagation, e.g. the thermal management system, mechanical support structures cell-to-cell respective module-to-module, use of fire walls and division of the battery pack into different sub-packs are important aspects.

There are relatively many simulation studies regarding general heat generation and cooling of Li-ion batteries during normal cycling (battery charge/discharge) within the battery specifications. Furthermore, Li-ion cells and battery packs with multiple-cells have been simulated during abusive conditions; by external heating in oven, short circuiting, overchargeing and deformation/crash. For example, Spotnitz et. al. [12] performed a numerical study on the influence of various heat transfer modes for the propagation cell-to-cell for a battery pack with 8 cylindrical cells of type 18650.

However, only a limited number of simulations studies of lithium-ion battery fire abuse situations are available. For example, Anderson et. al. [7] used CFD simulations with subsequent thermal modeling to study the fire resistance of a battery pack in a gasoline pool fire test according to UNECE Regulation No. 100.

A heat propagation simulation of cell-to-cell fire propagation for 5 Li-ion cells has recently been performed by Anderson et. Al [8]. That utilized recent experiments performed at SP on five EiG Li-ion 7 Ah cells where a thermal runaway was initiated in a cell using a propane burner. The resulting temperatures were monitored by thermocouples and the experiments are well suited for modelling purposes. However the predicted temperatues were found to be lower than the measured counterparts partly due to the models inability to represent the boundary in the fire test.

The present work continues this work by utilizing additional measurements of the fire load on the batteries. The aim of this work is to develop a model suitable for predicting the propagation of thermal runaways in stacked Li-ion cells. The modelling was done using the COMSOL Multiphysics software package that can model conjugate heat transfer. The software is a Finite-Element (FE) tool and in order to successfully model the experimental set-up appropriate boundary conditions are needed for reliable results. The long term goal is to be able to study protective measures mitigating the propagation of a thermal runaway event. In this paper we will extend previous work done in Anderson et al. [8] where we make use of fire abuse tests of commercial Li-ion cells where detailed measurements of the temperatures between the cells as a result of the thermal runaway response of the cells were performed. These tests may be utilized to fine tune a numerical model of the phenomena.

RESULTS FROM THE FIRE TESTS

Commercial Li-ion (EiG ePLB-F007A 7 Ah) pouch cells were exposed to a 15kW propane burner that initiated a thermal runaway event in the cell closest to the burner. During the tests heat release rates and temperatures, measured by thermocouples between the cells, were measured. The resulting HRRs have been published as well as one preliminary study on modeling one of the tests [6,8]. The tested EiG cell had a lithium-iron phosphate, $LiFePO_4$, cathode and a carbon based anode. Each of the tests consisted of five cells tightly packed together with steel wires, see Figure 1 (left). Also in Figure 1 (right), the mock-up used in to determine the impact from the burner can be seen and is described in detail below.

Figure 1. Fire test on EiG 7 Ah LFP pouch cells (left) and measurement of the impact on a mock-up (right).

The cell terminals (tabs) were cut-off prior to the tests for all but the middle cell. In the tests the thermal runaway was initiated by a LPG burner of approximately 15 kW placed underneath the packed cells, see Figure 1. Several tests with varying state of charge was done yielding cases with varying reactivity. The HRRs are presented in Figure 2, however in this paper we will focus on modeling the case with 75% state of charge (SOC) indicated by a dashed line, previously the case with 100% SOC was used.

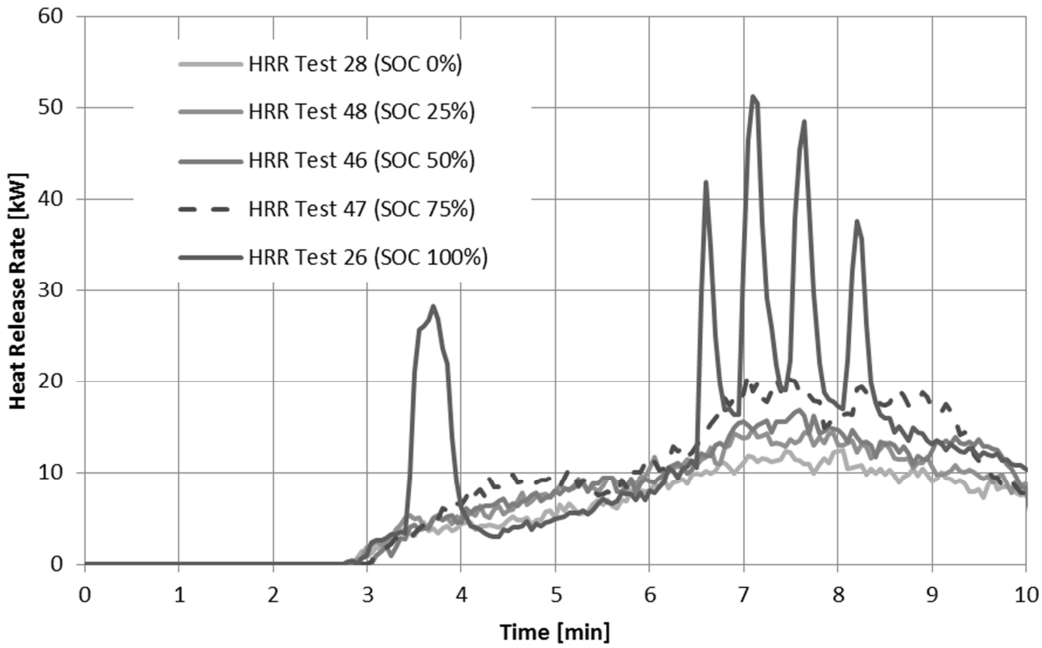

Figure 2. The heat release rate of the EiG 7 Ah LFP pouch cells where the heat from the burner is subtracted.

Additional quantities of interest was measured in each test such as cell voltage of the mid cell however this is out of the scope of the present work. We noted that the measured voltage breakdowns occurred earlier for increasing SOC values, in accordance with faster thermal response for increasing SOC shown by temperature and HRR measurements. During the test temperatures between some of the cells were carefully monitored in four positions, see Figure 3.

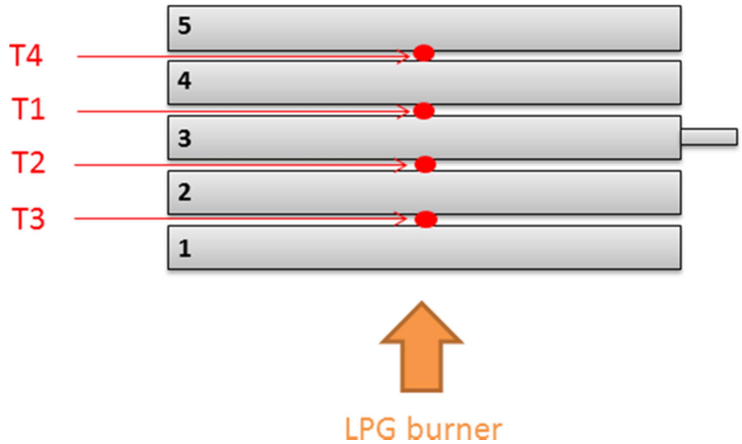

Figure 3. The placement of thermocouples in the live fire test.

In the previous paper by Anderson et al [8] it was identified that a well defined fire source is needed in order to more accurately describe the evolution of the temperatures between the cells. For modeling purposes one test with a

mock-up was performed where the impact of the burned was assessed. To achieve this the mock-up shown in Figure 1 was constructed of promatect clad with custom made plate thermometers. Although the moisture level in promatect is very low it was dried for around 48 h further reducing the moisture content. The plate thermometers were approximately 40 mm x 100 mm in size to fit on the side of the mock-up. The objective of the mock-up test is to estimate the fire source's impact on each side of the mock-up by measuring the adiabatic surface temperature (AST). The AST is an artificial effective temperature that replaces the gas and radiation temperature that describe the local conditions around the test object. It is defined as the temperature of a surface that cannot absorb any heat. However, due to the limitations of the physical extensions of the object the size of the plate thermometers were smaller than usual indicating that they may experience somewhat different convection radiation equlibrium since the estimation of the AST becomes more sensitive with smaller devices.

THE SET-UP OF NUMERICAL SIMULATIONS

The modeling was performed in two stages; the first stage covered the fluid-structure interaction in a conjugate heat transfer model; the second stage was a thermal model where the boundary conditions were taken from measurements. Common in both models was to use the measured HRR produced in the thermal runaway event. The models were built in the multi-physics software COMSOL suitable for studying heat transfer problems. In the models the five battery cells have been implemented where bulk values of the density, specific heat and thermal conductivity are specified. Below we present the particulars of the models.

The conjugate heat transfer model

The software solves the heat transport taking into account heat conduction and radiation as well as solving for the Navier-Stokes equations to assess the convection around the cells coming from the fluid movement of air around the cells. The software is a Finite-Element (FE) code and the Reynolds number is assumed to be small, such that turbulent fluctuations can be neglected. The model consists of around 10000 elements in order to have sufficient convergence and accuracy. The solution time of the model is about 10 minutes on an ordinary personal computer. A simplified 2D geometrical model was constructed for this work. In the model, the battery cells are in the same ambient conditions (T0) as the surroundings of that particular test and the cells are assumed to always be in perfect contact to each other. The ambient conditions give the boundary conditions for the thermal exchange between the cells and the surroundings by conduction, convection and radiation. The 15 kW heat of the propane burner was assumed as a boundary heat source placed directly beneath the first battery cell. The measured heat release rate was used as input in the model for the thermal energy which was deposited homogenously into the bottom cell. The heat generated by the propane burner was taken into account, however, the extra buoyancy of the exhaust gases from the burner was omitted since numerical instabilities occurred.

The thermal model

Similarly to the conjugate heat transfer model the thermal model was built in COMSOL. The test specimen was modelled in 3D with half the amount of cells compared to the other model. The thermal model is considerably faster with runtimes of a few minutes. The boundary conditions were estimated by assuming a heat flow in to the specimen determined by the AST (T_{AST}) in the following manner,

$$\dot{q}'' = h(T_{AST} - T).$$

Here the heat flow is determined per unit of time and area where h is the heat transfer coefficient. The heat transfer coefficient is taken from Eurocode standard [13] to be h = 25 W/(m^2 K). No assumption was necessary for the propane burner since this is included in the AST. Otherwise the model had a similar set-up as the conjugate heat transfer model.

Bulk material data

The physical structure of the pouch cells is complex with a repeatable layering of anode and cathode material. The total numbers of layers is of the order of 150 layers. The thermal properties of the materials vary significantly in terms of thermal conductivity, density and specific heat along and across the cell due to the layered structure. To be

able to accurately compute the temperatures in the 5-cell-pack realistic values of the thermal properties are needed in combination with a well-defined fire source in terms of the measured heat release rate. This complex structure of the cell makes detailed modeling impractical however for our purposes bulk values of the thermal properties are enough to capture the essential propagative features. In the present study these values are estimated from literature values by Spotnitz and Franklin, Fan et al., Wu et al and Chacko et al, [12], [14] –[16]. Ideally, careful measurements of these quantities at elevated temperatures are needed but generally difficult to obtain. The heat conductivity coefficient, k, was varied in the simulations since the multi-layered structure of the battery cell allows for this value to be highly anisotropic. Table 1 shows the thermal material properties of the cells used in the thermal simulations.

Table 1. Values of the thermal properties of the cell used for the simulations.

Notation used in this paper	Density ρ [kg/m^3]	Specific heat C_p [J/(kg K)]	Thermal conductivity k [W/(m K)]
Anisotropic k=13	1895	700	k_x = 13 and k_z = 0.4
Anisotropic k=27	1895	700	k_x = 27 and k_z = 0.8

RESULTS FROM THE NUMERICAL SIMULATIONS

In this section we will present the numerical results found using the developed models. We have chosen the test with 75% SOC as a representative case in the test series for corroborating the simulations. In this test four time series with temperature data, T1-T4, were recorded. In Figure 4, the results by comparing the experimental data with the simulations using isotropic (a) and anisotropic (b) thermal conductivity are presented using the conjugate heat transfer model. It is found that T1 and T2 of the middle cell can be modeled as described previously [8], but the temperatures are lower than the experimentally measured values. However, T3 at the top of the initiating (bottom) cell that undergoes thermal runaway deviates quite early.

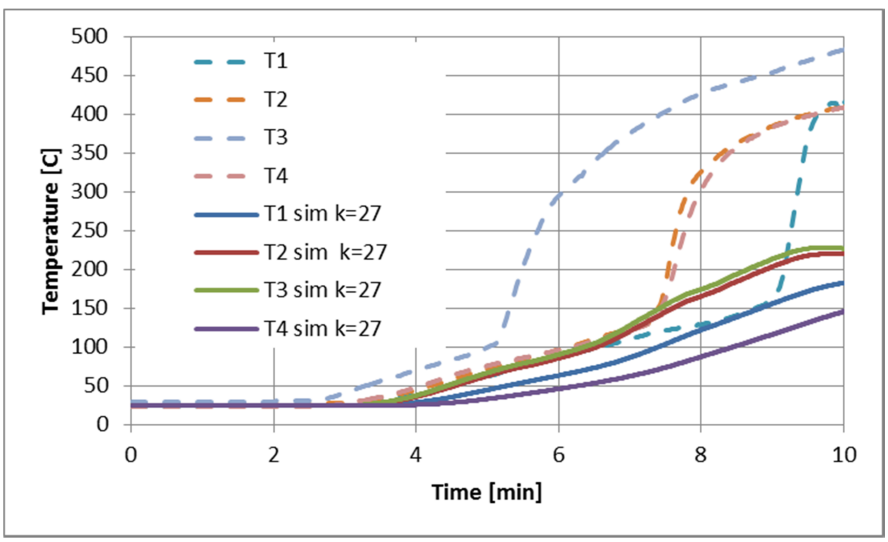

Figure 4. Comparison between test results and simulated temperatures at 75% SOC using the conjugate heat transfer model. A comparison of temperatures T1, T2, T3 and T4 found in the experiment and the simulation assuming anisotropic heat conductivity k=27 (kx =27 W/(m K) and kz = 0.8 W/(m K)).

In Figure 5, the same test is modelled using the thermal model with the AST used as boundary conditions however the same HRR is used. We find also in this case that the model yield lower temperatures compared to the experimental values. Interestingly, a higher value of the heat conductivity would yield lower temperatures through the whole test specimen.

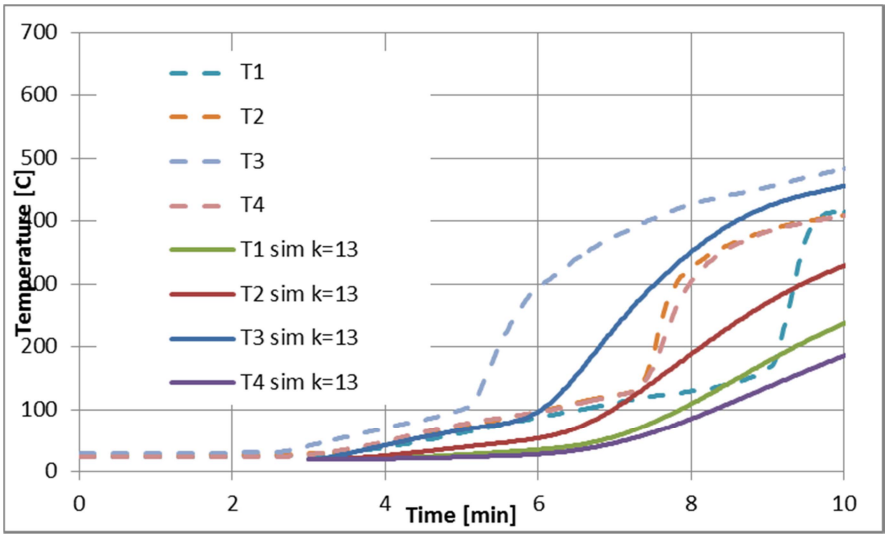

Figure 5. Comparison between test results and simulated temperatures at 75% SOC using the thermal model. A comparison of temperatures T1, T2, T3 and T4 found in the experiment and the simulation assuming anisotropic heat conductivity k=13 (kx =13 W/(m K) and kz = 0.4 W/(m K)).

However, the qualitative behavior is considerably better in the thermal model and it is very likely that using values corresponding to a lower thermal inertia would give a much better correspondence with the experimental results. In particular, the value for the specific heat and density may decrease considerably as the reactions progress. We note that in the experiment the measured temperature closest to the top is elevated, T4 is close to T2, indicating a significant amount of heat coming in from the top surface.

DISCUSSION

This paper presents an attempt to predict the progress of a thermal runaway/fire in a cell to neighboring cell by simulating the temperature development on neighboring cells in the same lines as in our previous work, Anderson et al. [8]. Simulations and experiments have been conducted for varying SOC, this paper focuses on the case with 75% SOC as an example of results.

Modeling battery cells in such harsh conditions as that of a fire is a rather difficult task due to the lack of knowledge of the precise local conditions around the test object. This gives an uncertainty in the boundary conditions to be used. Another difficulty is the lack of knowledge of the material data. In order to have a reliable model the precise temperature dependency of the heat conductivity, specific heat and density are needed.

Using the conjugate heat transfer model we find that the model captures the first minutes of the test however as the runaway event progresses large deviations are found, this is partly due to that the thermal exposure in that case is only assumed to be underneath the cells and not around the entire object. In the thermal model a good qualitative match between the test and model is found however the thermal inertia in the model seems to be larger compared to the actual cell case. The thermal model uses the measured AST values as input however it is uncertain how representative this measurement is as in the real case the boundaries are not smooth/edges are sharp creating a complex convective heat transfer. Furthermore, radiative losses at the top surface are likely since the flames are rather thin resulting in a different boundary.

The simulations are in reasonable agreement with the experimental result up to the point where the thermal runaway is initiated but still the simulations under-predict the temperature in the neighboring cell somewhat in all cases.

However the model can be further developed by:

1. A two stage simulation using the methodology in Anderson et al [7] is likely to be a more proper representation of the turbulent driven convective heat transfer process.
2. Investigate in more detail different boundary conditions. Since the dimensions of the battery pack is rather small the influence of the boundary is important and can be a source for uncertainties. Both geometry at the edges and different forced convection boundaries should be investigated.
3. Simulating different contacts between the cells using a thin contact element with variable thermal resistance should be investigated.
4. More adequate values of the thermal properties data including temperature variation.

With these improvements there is great potential for the simulations to be able to better predict the temperature development in a neighboring cell. A conservative model of the propagation is desirable to be on the safe side in the predictions.

ACKNOWLEDGMENTS

The Swedish Energy Agency is greatly acknowledgment for its financial support. Several technical staff colleagues at the Fire technology have contributed to this work.

REFERENCES

[1] Roth EP, Doughty DH. Thermal abuse performance of high-power 18650 Li-ion cells. J Power Sources 2004; 128:308-318.

[2] Roth EP. Abuse response of 18650 Li-ion cells with different cathodes using EC:EMC/$LiPF_6$ and EC:PC:DMC/$LiPF_6$ electrolytes. ECS Transactions. 2008; 11(19):19-41.

[3] Jeevarajan J. Safety of commercial lithium-ion cells and batteries In: Gianfranco Pistoia (ed) Lithium-Ion Batteries Advances and Applications. Elsevier. Amsterdam. The Netherlands. 2014, p. 387-407.

[4] Zhang Z, Ramadass P, Fang W. Safety of lithium-ion batteries In: Gianfranco Pistoia (ed) Lithium-Ion Batteries Advances and Applications, Elsevier, Amsterdam, The Netherlands, 2014, p. 409-435.

[5] Doughty D, Roth EP. The Electrochem. Soc. Interface, summer 2012. 2012; 37-44.

[6] Andersson P, Blomqvist P, Lorén A, Larsson F. Investigation of fire emissions from Li-ion batteries. SP Report 2013:15, SP Technical Research Institute of Sweden, Borås; 2013.

[7] Anderson J, Sjöström J, Andersson P, Amon F, Albrektsson J. Experimental and numerical characterization of an electrically propelled vehicles battery casing including battery module. Journal of Thermal Science and Engineering Applications. 2014 Dec; 6: 041015-1 - 041015-7.

[8] Anderson J, Larsson F, Andersson P, Mellander BE. Fire spread due to thermal runaway in a lithium-ion battery cell. Conference proceedings of Fires in vehicles (FIVE) 2014, Andersson P, Sundström B, eds. SP Technical Research Institute of Sweden, Borås, Sweden; 2014: 268-271.

[9] Larsson F, Mellander BE. Abuse by external heating, overcharge and short circuiting of commercial lithium-ion battery cells. Journal of the Electrochem. Soc, 2014: 161 (10); A1611-A1617.

[10] Larsson F, Andersson P, Mellander BE. Battery Aspects on Fires in Electrified Vehicles. Conference proceedings of Fires in vehicles (FIVE) 2014, Andersson P, Sundström B, eds. SP Technical Research Institute of Sweden, Borås, Sweden; 2014: 209-220.

[11] Larsson F, Andersson P, Mellander BE. Are electric vehicles safer than combustion engine vehicles? In: Sandén B, Wallgren P, eds. Systems perspectives on Electromobility. Chalmers University of Technology. Göteborg. ISBN 978-91-980973-9-9; 2014:33-44.

[12] Spotnitz R, Franklin J. Abuse behavior of high-power, lithium-ion cells. Journal of Power Sources. 2003; 113:81-100.

[13] Eurocode EN 1991-1-2.

[14] Wu W, Xiao X, Huang X. The effect of battery design parameters on heat generation and utilization in a Li-ion cell. Electrochimica Acta 2012; 83:227-240.

[15] Chacko S, Chung YM. Thermal modelling of Li-ion polymer battery for electric vehicle drive cycles. 2012; 213:296-303.

[16] Fan L, Khodadadi JM, Pesaran AA. A parametric study on thermal management of an air-cooled lithium-ion battery module for plug-in hybrid electric vehicles. J Power Sources. 2013; 238:301-312.

Protection of Lithium-Ion Traction Batteries in the Electric Car

Michael Funcke
Forschungsgesellschaft Kraftfahrwesen Aachen mbH
Germany
Sebastian Lovski
Sebastian Schäfer
Institute for Automotive Engineering RWTH Aachen University
Germany
David Sturk
Dominique Dufaut
Hakan Sundmark
Kyriakos Vavalidis
Per Gustafsson
Autoliv
Sweden

Paper Number 15-0234

ABSTRACT

The storage elements in an electric vehicle (EV) remain a key challenge to wide-scale, successful deployment of EVs that are appealing to customers and are adequately functional (e.g. in terms of range and drivability). State-of-the-art electric storage systems are lithium-ion batteries, offering approximately 0.5 km driving range per 1 kg of battery pack mass (see Funcke et al [1]). However, these battery packs require high level safety measures to avoid e.g. mechanical damage of the cells, which increases the pack mass again. In order to make a reliable statement about the battery safety at an early stage of development, detailed knowledge of the mechanical behavior of the cells as well as its reproduction in the virtual development process is necessary.
Based on a sample design of a main battery structure, the development process of the cell model is explained. The first steps are the integration of the design in a full vehicle and the determination of the dominant cell deformations, which are transferred to cell load cases. These mechanical abuse tests of cells deliver the input data for generating an adequate finite-element (FE) model, which offers the opportunity to dimension the battery pack and to add safety measures. With this simulation model inflatable structures as well as passive reinforcements for the traction battery are investigated.
To validate the simulation results, component tests on system level, i.e. complete battery packs, are conducted. The test is based on the full vehicle reference design load case, in this case the EuroNCAP pole side impact with a modified pole position and an impact velocity of 50 km/h. An analysis of the impact position is needed since the vulnerabilty to intrusion of the battery pack and the stiffness of the vehicle structure varies along the vehicle longitudinal axis.
These component tests confirm the simulation results and show the potential of inflatable structures and passive protection systems. Furthermore, it is possible to generate a FE model for lithium-ion batteries, which is applicable to full vehicle simulations.
Although it is possible to map the mechanical characteristics to the generated cell model, this model is limited to the investigated load cases, which have been the result of the battery position within the vehicle and the corresponding critical design load case. Since the battery may be placed in another position within the vehicle and the arrangement of the cells may change, the cell model is not universal. However, it is extensible to other load cases.
Overall, the results from the study with the inflatable elements show clearly the benefit of those structures. With low additional mass a high positive effect (e.g. lower intrusion) is achieved, which means the ratio of the incorporated mass to the reached protective effect is lower than with passive protection systems.

INTRODUCTION

In the field of electric vehicles, lithium-ion batteries are widely utilized. In general three major types of battery cells are used: prismatic, cylindrical and pouch cells. A representative prismatic cell is protected by a case made of metal or hard plastic. Cylindrical cell cases often consist of aluminium. Pouch cells use lightweight cases made of layered foil consisting of sheets of polymer and aluminium jointed at the edges of the flat cell. Usually multiple cells are grouped into modules and several modules are grouped into a battery pack. Using different circuit conditions (in parallel, in series) different voltages or different capacities at the same voltage are achievable. The assembled main battery pack (MBP) is installed within the electric vehicle, mostly in the safest position e.g. in the tunnel area.

Sahraei et al [2] as well as Choi et al [3] reported their effort on modelling lithium-ion pouch cells using FE. Sahrei et al [2] model covered the force-displacement behaviour for 3-point bending as well as for axial and through thickness compressions. The FE model of Choi et al [3] focussed on a more detailed behaviour of the cell layers e.g. local stress and strain. Therefore three-layered shell elements were used, which represented the pure metal substrate (Al or Cu) and the coating (e.g. Cobalt or Carbon coating). The electrolyte layers, which nodally connects the shell layers, were modeled using link elements. However, both simulation models are limited to the tests used for the validation which do not necessarily represent the loads acting when the MBP is placed in an electric vehicle. In addition, the high number of nodes and elements restricts the use of the model to cell tests. With the aim to design a MBP and to apply a passive as well as an active protection system, in means of inflatable elements, for the OSTLER project a battery model was needed which was applicable to full vehicle simulations.
The following study was part of the european founded project OSTLER which focused on the development of smart concepts for physical integration of battery packs in electric vehicles. For this purpose, the MBP was placed outside the common safe zone in an area that presents higher frequency of intrusions – i.e. MBP under the front seats, transverse to the driving direction and stretching out into areas close to the vehicle sill. Using a simplified battery cell model, for the given battery location relevant full vehicle load cases as well as associated cell load cases were derived using a simplified FE cell model. For these load cases mechanical tests were carried out and gradually built up a full vehicle-enabled cell model, which enabled the investigation of inflatable elements and passive systems to provide protection to the battery. Using systems tests, the final design of the systems was validated against the simulation results. The following investigation was carried out using the explicit solver LS-DYNA.

DEVELOPMENT OF A FE MODEL FOR LITHIUM-ION POUCH CELL

First, the selection of cell type for this study was carried out. For this purpose, it was necessary to determine the full vehicle load cases, which had to be considered for the crash simulations. By analysing the German In-Depth Database (GIDAS) (see Funcke et al [1]) the impact velocity, direction and the impacting object of the 2 % of accidents with the highest intrusion was evaluated.

Relevant Full Vehicle Load Cases And Derivation of Cell Load Cases

The 2 %-tile area consisted of 82 collisions. If the incident direction is numbered according clockwise, with 12 clock corresponds to a frontal impact, it was found that in 45 cases the impact object was another vehicle with the predominant impact direction between 12 and clockwise to 7. In the other cases the impact object was an object which were predominant in the area between 8 and 2 with major peaks at 9 and 12.
Beside the impact direction the impact velocities were analysed with the result that to cover at least 50 % of all crashes the following load cases had to be considered within the project:

- EuroNCAP ODB
- FMVSS 208 (56 km/h, 0° impact, 50 % male dummies)
- FMVSS 301
- EuroNCAP pole side impact with 50 km/h and varied pole position

First draft designs for MBP, containing the three different cell types each, were installed as part of the electrification process in the FE model of a Toyota Yaris model which was publicly available. Placing the MBP transverse underneath the frontal seats meant the battery reaches in an area where frequently deformations occur in case of an accident. Performing the four load cases and analysing the deformations of the MBP housing as well as the deformation of the cells inside, the pouch cell was identified as cell with the highest deformation and most critical cell type for this MBP location and design. Due to the location relevant intrusions only occurred within the high speed EuroNCAP pole side impact. Out of the occurring cell deformations as well as the plastic strains within the cells (*see Figure 1*), three load cases were identified, which the simulation model of the cells had to fulfil and which were used for the built-up process. Specifically, these were the load cases through thickness compression, three-point bending and the clamped cell. Within the last-mentioned load case the pouch cell is clamped according to the installation condition in the MBP between two frames.
For the following study, lithium-ion pouch cells with a capacity of 40 Ah and 3.7 V were used, which were fully charged for the tests. This enabled to detect whether a short circuit or internal damage occurs during the

test. To avoid personal injury and to increase security the cell tests were carried out using a freestanding and foreclosed housed test bench, which enables the application of a maximum force of 30 kN. Any escaping gas could get vacuumed by the built-in ventilation.

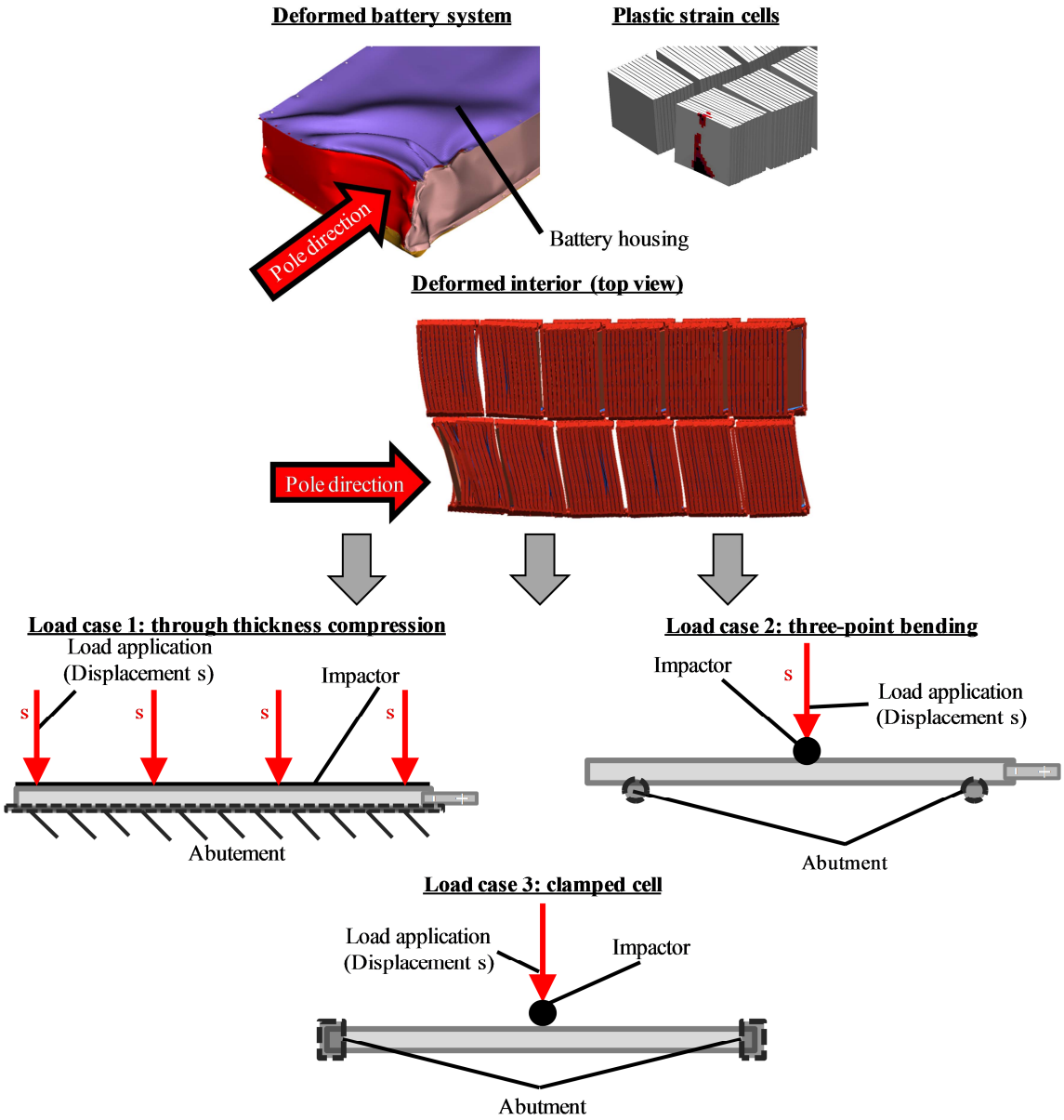

Figure1. Determination of cell load cases.

Based on the experiences made by Sahraei et al [2] the test series began with the through thickness compression in order to determine the material parameters for the solid layers representing the electrolyte. Therefore, the assumption was made that the other layers do not contribute to the overall performance within this load case. Starting from this load case, the simulation model was gradually expanded.

Through Thickness Compression Test

Although a pouch cell consists of a high number of layers (e.g. ~205, Choi et al [3]), the number of layers was reduced in order to reduce simulation time and to generate a simulation model applicable to full vehicle simulation. The simulation time step, which depends on the smallest element length within the simulation model and is called courant criterion [4], should not be lower than the value $1.112e^{-6}$ s, which was the time

step defined in the full vehicle simulation. The cell model (*see Figure 2*) consisted of five solid layers representing the electrolyte layers, six layers of aluminum representing the pure metal layers, a layer representing the border area of the cell which was used for clamping the cell as an element row closing the cell at the sides. The different layers were not coincident connected using shared nodes, like done by Sahraei et al [2]. Instead, the layers could slide to each other using a common LS-DYNA single surface contact [5]. As input for the material model MAT_83 served a stress-strain curve which was calculated out of the testing force-displacement-curves.

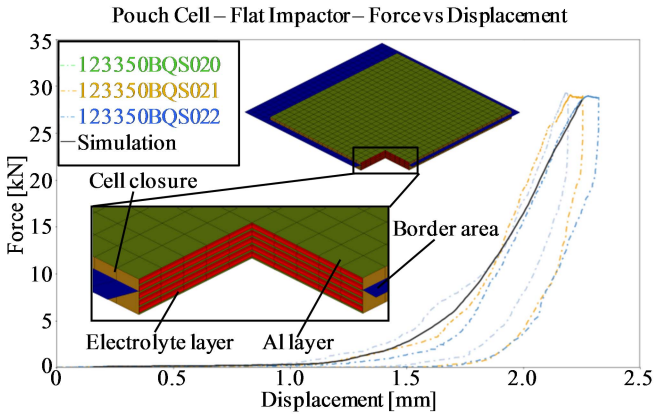

Figure2. Cell modeling and through thickness compression test results vs. simulation.

Using this approach provided very good results which can be seen comparing the force-displacement curves of the simulation compared to the three tests (*see Figure 2*).

Three-Point Bending Test

The determination of the Al layer thickness, the contact parameters between the electrolyte and the Al layers as well as the cell closure thickness formed the next step. For this purpose, the three-point bending test was the best choice since the cell surrounding does not contribute, or only to a very small part, to the bending stiffness within this load case. As abutment as well as impactor served round profiles with 40 mm diameter (*see Figure3*), which covered the entire width of the battery cell. The bending load case was carried out as in the entire vehicle occurring about the vertical axis in parallel to the electrical contact areas of the cell. Using a layer thickness of 0.4 mm for the pure metal layers, a thickness of 0.04 mm for the closure and a friction of 0.15 between the layers it was noted that a good correlation between simulation results and the tests was achieved. Both the force-displacement curves as well as the qualitative behavior were in good agreement.

Clamped Battery Test

In the last validation step, the cell was fitted under mounting conditions between two frames similar to the MBP (*see Figure4*). As required by the cell manufacturer, the through the frames transmitted clamping force was applied only to the border area of the battery. Since the behavior of the battery should be examined and the mechanical effect of the framework should be kept as low as possible, an impactor with a length of 100 mm and a diameter of 40 mm was used, which was placed centered in height and width of the battery. During the load application, on the one hand the battery slid out of the frames; on the other hand the battery was locally deformed in the impact area as well as in the border area. As a result, the material and the thickness of the border area could be determined as well as the friction parameters between border and frame. The highest agreement with the experimental results could be achieved by using a Part_Composite [5], which enables to apply multiple materials and associated thicknesses to one single layer of shell elements. Most suitable was a layout consisting of a layer of aluminum (thickness 0.4 mm) surrounded by a layer of a plastic material (thickness 0.25 mm).

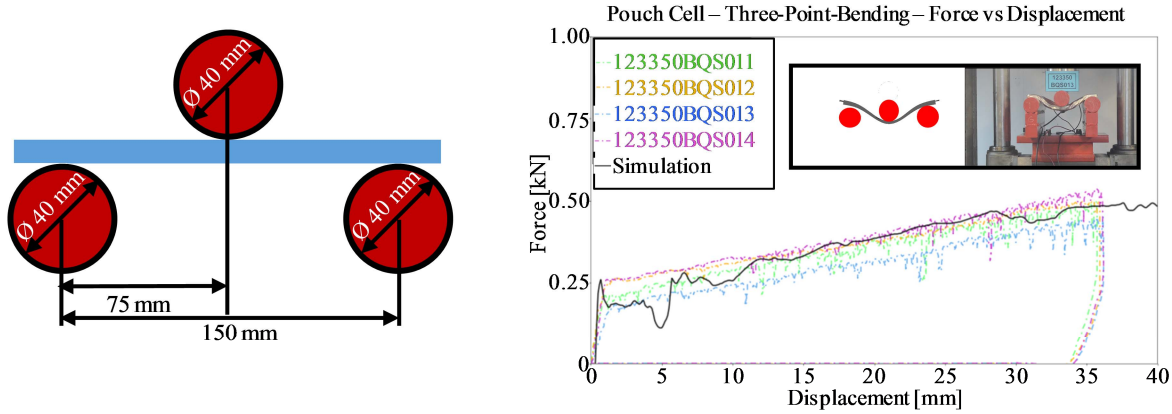

Figure3. Results testing vs. simulation three-point bending.

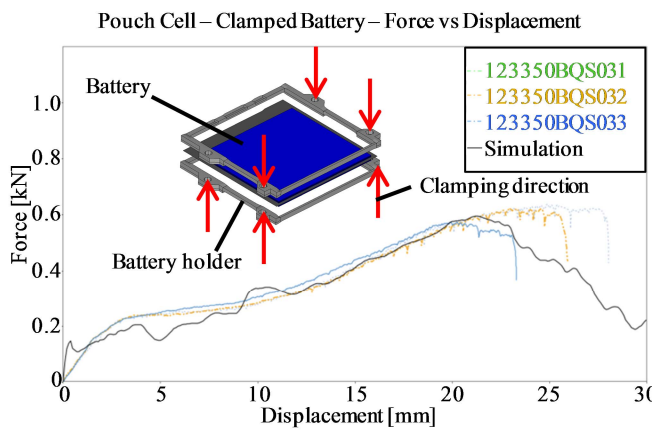

Figure4. Results testing vs. simulation clamped battery.

Both initial force and the force-displacement curves of simulation and experiments were in a good agreement (*see Figure4*). It must nevertheless be noted, that the simulation model considered no strain rate as well as temperature effects. After generating a simulation model for the pouch cells the design process of the inflatable element and the passive reinforcement as battery pack protection started.

PROTECTION OF BATTERY SYSTEMS USING INFLATABLE ELEMENTS

Including the gained CAE model of the pouch cells into the full vehicle simulation model, the loads as well as the geometrical interaction between battery system and the surrounding vehicle structure were analysed using different impact points of the pole. In this analysis, it was found the highest intrusion into the battery system occurred when the pole hits the center of the modules. Another finding was that the vehicle structure in means of the inner sill hit the battery with a velocity of 9 ms/s and thereby increased the pole diameter due to the wrapping to 325 mm (see Funcke et al [1]). These parameters were transferred into a battery system test, where the vehicle structure was skipped and the battery was hit directly by the pole with the higher diameter. This test was used to further speedup the virtual design process as well as to run the final physical evaluation of the protection concepts.
Since the development of a passive protection is state of the art in protecting battery systems, the following passages focus on the development process of the active protection system. Nevertheless, there is some information included since the passive protection was used as benchmark for the active system.

Concept of Passive Protection

The passive reinforcement consisted of three stages compared to the unreinforced battery pack; an increased wall thickniss, an additional load path by adding longitunal beams within the battery housing and an energy

absorbing foam block between the battery and the vehicle structure. After the virtual optimisation of the named measures, the passive reinforcement caused a weight increase of 37 kg but reduced the intrusion into the main battery pack (MBP) from 157 mm to 66 mm (58 %) compared to the unreinforced reference structure. The reduction within the simulation loop was predicted with 69 % (from 157 mm to 48 mm). Since the intrusion of the unreinforced battery pack was predicted with a high accuracy, the reason for the inconsistency is not located in the cell model. Rather, the reason is suspected in other model parameters.

Concept of Active Protection using Inflatable Elements

The installation of inflatable elements made it possible to create new energy absorption paths and to reduce the load onto the MBP.
As a consequence it was possible to reduce the deformation and the stress of the cells in case of a crash. As shown in *Figure5*, in the case of a pole side impact with a current lateral in-crash sensing, the active solution of battery pack protection consisted of a "structural" airbag, which provided both a certain structural rigidity against intrusions as well as good energy absorption potential.

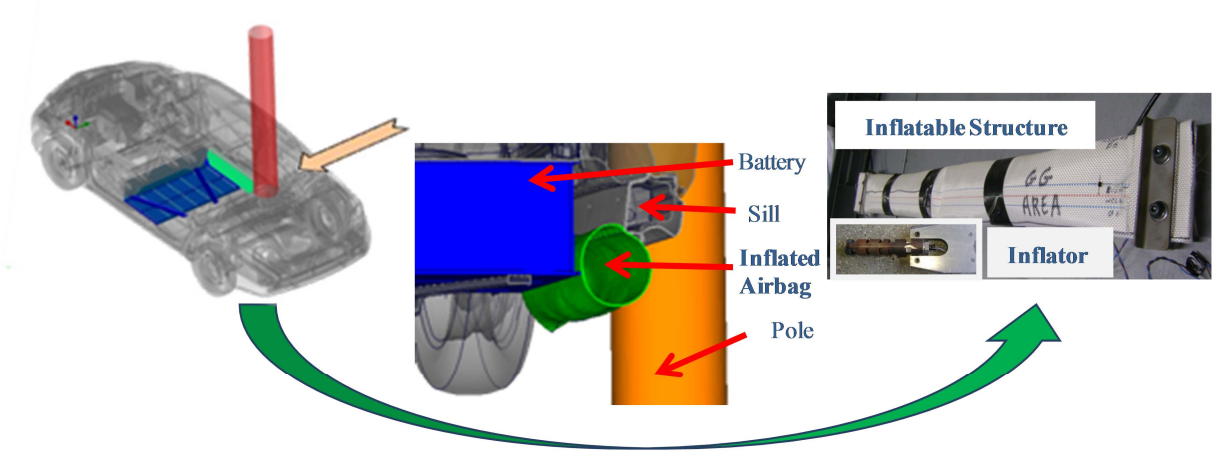

Figure 5. Active Protection concept

Such a structural airbag resembles a normal airbag from the point of view of its constituent components, i.e. mainly a fabric cushion, a pyrotechnic inflator and a wire harness to the standard airbag ECU, but differs greatly in the performance characteristics. The cushion consists of a highly reinforced fabric capable to withstand gas pressures more than 20-30 times that of a passenger airbag and also capable to resist mechanical aggressions from its surroundings.
This high pressure made the cushion becoming almost rigid and, compared to metal reinforcement, had the potential of a lower weight and a reduced packaging (both critical to EVs). It was placed in the free space between the battery pack and the sill, right in front of the lower part of the battery pack in order to take advantage of its rigid bottom plate.
The FE model of the battery pack including the FE model of the pouch cells made it possible to define the mechanical requirements for such a structural airbag.

Active Protection efficiency

With an added weight of 4 kg (2 kg for both sides of BP) compared to the unreinforced reference structure, the intrusion into the battery pack was reduced from 157 mm to 121 mm in the physical tests. This was a reduction of 23 % taking the unreinforced battery pack as reference. The reduction within the simulation loop was predicted with 28 % (157 mm to 116 mm). Compared to the passive reinforcement of the battery structure, the weight-specific intrusion reduction (intrusion reduction [%]/ added weight [kg]) of the active system was over four times higher (1.57 %/kg passive system to 7 %/kg active system).

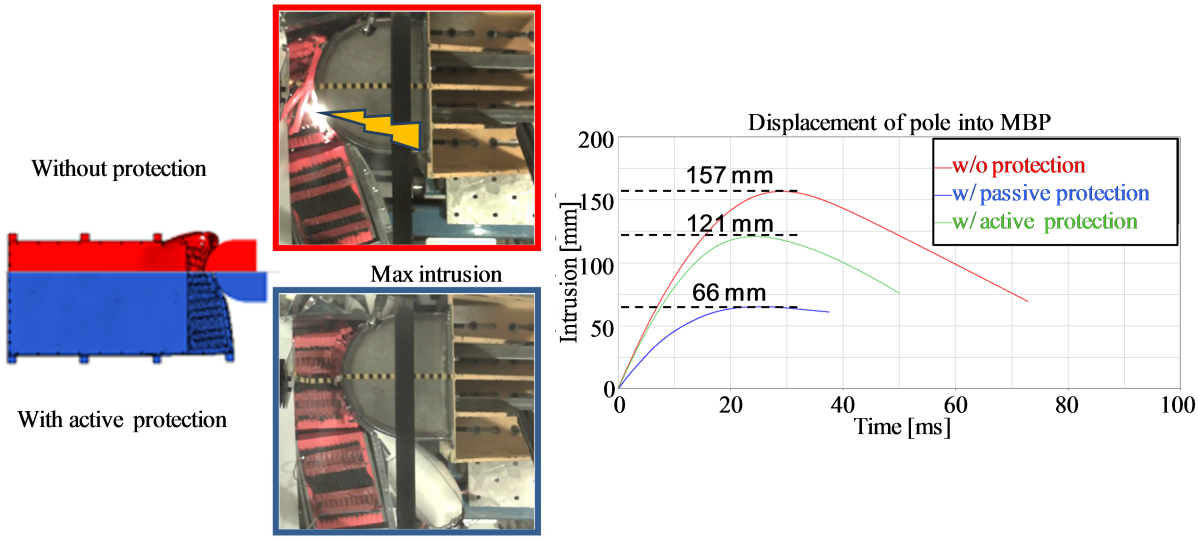

Figure 6. Effects of active structure (targeted load case: pole side impact at 50km/h)

CONCLUSIONS

The relevant modeling of cells, which could be elaborated through the approach presented, offered the opportunity to dimension and design the battery pack casing and the associated safety measures. It enabled to investigate the protection of the battery pack using an alternative system in means of an inflatable element. The investigation showed that the protection of the main battery pack by an active structure is possible (as presented for the worst load case, with the MBP as defined above). It successfully reduced the intrusion into the battery system. The additional mass of the active system was small compared with the mass of the passive reinforcement.

Smartly combining benefits of the active protection with a passive protection according to the protection requirements of the MBP, along with an optimization of MBP construction allows for a wider MBP and therefore an increase in EV's driving range with favorable weight balance (added weight by active structure, reduced weight of casing of MBP).

The used approach of identifying the cell loads, generating a cell simulation model and the afterwards design process can also be seen as guideline for future investigation concerning the crash safety of battery packs. Once generated, the cell model can be applied to various investigations (battery pack position, pack dimensions,..) as long as the cells experience the same type of mechanical loads the model was validated for. In the case the loads are different; the simulation model can be adapted to this by means of additional cell tests.

REFERENCES

[1] Michael Funcke, Sebastian Schäfer, Roland Wohlecker, Dominique Dufaut, David Sturk, Kyriakos Vavalidis „Evaluation report in active and passive protection solutions", www.ostlerproject.com/Downloads

[2] Elham Sahraei, Rich Hill, Tomasz Wierzbicki "Calibration and finite element simulation of pouch lithium-ion batteries for mechanical integrity", 201, 307– 321, Journal of Power Sources, 2011

[3] Hyung Yun Choi, Inhyeok Lee, June Soo Lee, Young Man Kim, Hyunjin Kim "A Study on Mechanical Characteristics of Lithium-Polymer Pouch Cell Battery for Electric Vehicle", Paper Number 13-0115, 23rd International Technical Conference on the Enhanced Safety of Vehicles (ESV), Seoul, Republic of Korea, May 27-30, 2013

[4] Lutz Eckstein, "Strukturentwurf von Kraftfahrzeugen", p. 183, Schriftenreihe Automobiltechnik, Germany, 2010

[5] LS-DYNA Manual, DYNA MORE, 2014

E-Vehicle Safety – Pyro Switch as High Voltage Circuit Breaker & Bypass

David, Sturk
Per, Gustafsson
Autoliv Development AB
Alf, Holgers
Håkan, Sundmark
Autoliv Sweden AB
Sweden
Christian, Cavell
Autoliv Germany
Germany
Francois Gaudinat
Etienne Dugast
Autoliv NCS
France

Paper Number 15-0163

ABSTRACT

An E-Vehicle (i.e. electrified vehicle such as EV and HEV) is often equipped with a traction battery with voltage of as high as 200 to 600 Volt dc. It is critical that such voltage shall not be put in circuiting contact with any person at any point – workshop, crash or post-crash rescue. NHTSA have defined testing procedures in FMVSS 305 so as to assure that a basic level of safe guard systems shall be utilized by conventional E-Vehicles. The paragraph S5.3 (b) demands that the traction battery shall present an external voltage <60 Volt dc after crash. This is commonly solved with relays and melting fuses which have their Pros and Cons. Relays/contactors have the benefit of being a reversible active component but are limited to operative currents and are prone to switching bounces and they are relatively heavy, large and expensive. A melting fuse is a passive component that can operate at extreme currents but is irreversible and their cutting speed is dependent on the magnitude of the fault-current.

In this paper Autoliv will present a methodology on how to disconnect a faulty battery unit rapidly (in milliseconds) regardless of the magnitude of the fault-current. This methodology can also be used to divide a traction battery down to minor units of <60 Volt dc or even bypass and disconnect a faulty battery module with maintained power electronics in order to retain mobility as well as adding the option of discharge the disconnected module so as to prevent stranded energy.

Autoliv has investigated how to use pyrotechnic switches for disruption of over-currents in a traction system with battery packs of about 300-400 Volt dc. Those tests, aiming at safe disconnection without lasting arcs, included static faulty-current tests and tests simulating an E-Vehicle traveling 50-70 km/h on a horizontal surface. Autoliv's Pyro Safety Switch (PSS) arrangement proved capable to safely disconnect both a complete battery pack (ranging from 300 to 400 Volt dc) and the intended battery module (30-60 Volt dc) in less than 0.5 milliseconds.

INTRODUCTION

While the number of E-Vehicles on our roads is steadily increasing, new safe guard systems are continuously being developed in order to extend their electric range in terms of higher energy density without compromising safety. Safe disconnection of high voltage battery in the event of an error is mandatory and conventionally relays and fuses are used to manage such safety issues. Continuous efforts to reduce component size and weight are challenged by

issues such as arcing and switching bounces as well as unintended division of the electric energy over relays and fuses in case of harmful over-currents. The latter may occur during exposure to high over-currents if relays experience electromagnetic repulsion or bad contacts.
In his article "Hochvolt-Relais von morgen: Sichere Minimalisten" product manager Thomas Merkel of Panasonic Electric Works Europe AG educate the reader on the potential consequences if the interaction between relays and fuses does not work properly. Mr. Merkel offers an illustration to clarify this interaction between relays and fuses in general; hence the lack of definite figures for Current respectively Time in Figure 1. In tests done by Autoliv on fuses the corresponding results to the yellow curve indicate that its delta time to completion of disconnection can vary from tens of milliseconds (at over-currents of several thousands of Amps) to seconds (at lower fault currents).

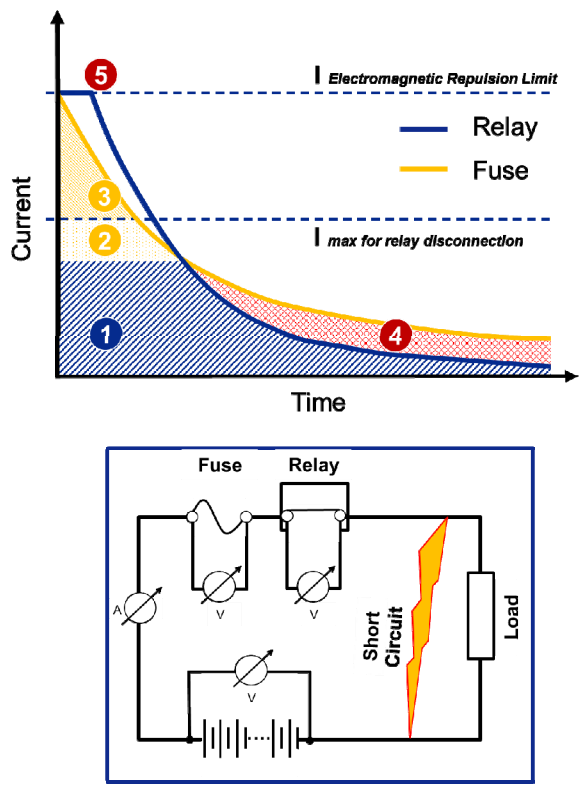

Figure 1. **a) A comparison of characteristics of conventional relays and fuses when circuit disconnect is demanded. b) Simplified representation of the High Voltage circuit. (Merkel, 2014).**

In Figure 1a the blue line represent the maximum current that a relay may carry whereas the yellow line represent the characteristics of a fuse and the condition at which it will disconnect the circuit. The curve of the fuse present the dependence between the magnitude of the over-current and the rate at which the current is reduced when the fuse performs its disconnection. Figure 1b illustrates a simplified representation of a High Voltage circuit related to Figure 1a. The five areas represent the following conditions (Merkel, 2014):

1. This is the area in which a relay can comply with electrical conditions and successfully act upon activation signal.
2. Although relays can operate in this area they are often designed not to disconnect the circuit because the fuse act faster than the relay and thereby protect the relay from potenially harmful exposure to over-currents.
3. Under these conditions the relay must stay closed. Instead, the fuse shall disconnect the circuit as it is faster than a relay at these over-currents. If the relay fail to stay firmly closed and do open, a difference in

potential will be established across the contacts of the relay and the electric energy required for disconnection by the fuse will not be sufficient. A risk of severe damage to electrical components in the circuit will be imminent.

4. In this region, the system is exposed to an unacceptably long-lasting faulty-current. The fault current is not high enough for the fuse to disconnect the circuit before the relay is damaged. The system must rapidly regulate down the power in order to avoid harming the relay.
5. Fault/over-currents above the Electromagnetic Repulsion limit cannot be safely handled by neither fuse nor relay. Electrical components in the circuit will be severely damaged.

Permanent damage to the electrical system and/or its safeguard components is commonly related to overheating that is induced by over-currents and/or arcing. The time to successfully complete a disconnection of a circuit that is experiencing an over-current must be minimized in order to assure that irreversible damage to electrical components in a high voltage system also is minimized.

In contrast to a fuse, the time to achieve a complete disconnection of a circuit by means of a pyrotechnic circuit breaker will not be dependent on the magnitude of the over-current. In general, Autoliv's series of pyrotechnic switches utilizes a miniature guillotine that is propelled by a pyrotechnic charge to achieve the force required to cut through a metallic conductor. The first generation of these PSS devices have been designed for disconnection of 12 Volt batteries in the event of a traffic accident (Autoliv, n.d.) and is widely used by automanufacturers. Later PSS versions address the issue of high voltage disconnection and a methodology for such an action is presented in this article.

In the tests presented in this article, the bypass and disconnection sequence was executed by one PSS that closes a circuit so as to establish the bypass path (i.e. *a PSS which is Normally Open* – ***PSS/NO***), and a second PSS that opens a circuit in order to disconnect the faulty unit (i.e. *a PSS which is Normally Closed* – ***PSS/NC***). In later versions those two types of PSS:s are combined into one unit. By the use of Autoliv's pyrotechnic switches this bypass and disconnection sequence offers an safe high voltage disconnection with minimized risk of arcing and an extraordinary short delta time to complete the disconnection of less than 0.5 ms. The pyrotechnic switch design assure that the delta time of bypass and disconnection is kept to a minimum. This is of most importance since it will provide that the heat generated by a fault current and its harmful effects on electrical components are also put at a minimum.

METHOD

The fundamental idea is to "redirect" the main current so as to bypass the "faulty battery unit(s)" before it is to be disconnected. At that point an extreme over-current will develop through the faulty battery unit and therefore rapid disconnection is of vital importance. Moreover, the load applied need to take into account the range of inductance that is experienced by an E-Vehicle traction system. Preparatory tests (conducted at inductance levels within a range from 0 to 154 µH) proved that when performing a direct cut off to a traction system or sub-units thereof, the higher the inductance is, the greater the propensity is of developing lasting arcs across the gap between the formerly connected conductors. Hence, the key tests (i.e. to measure the performance of the bypass and disconnection methodology) were those with the inductance above 100 µH.

The bypass of the faulty unit is the key of solving the issue with the risk of harmful arcing when cutting off an inductive circuit. A simplified explanation for this is that the circuit with inductive current is reluctant to change. This reluctance causes a harmful arc to develop between two formerly connected conductors at the moment of disconnection. In contrast to the type of "soft" arc that appear anytime when a circuit with no inductance (i.e. a capacitive circuit) is disconnected, an arc under influence of inductance will not be easily extinguished. By first establishing the bypass path, the influence on the faulty unit by the inductance from the

electric traction system will be greatly reduced. Thereafter, a rapid disconnection of the faulty unit can be achieved with minimum risk for harmful arcing.

This PSS arrangement was tested in two major setups – Complete High Voltage Disconnection and Partial High Voltage Disconnection. In the former test series, the tests were performed on a complete battery pack with test voltage ranging from 300 Volt dc up to 400 Volt dc where the arrangement replaced a Main Fuse. The latter test series were conducted on the same battery pack but the arrangement acted as a pack-internal bypass and disconnection device that allow a "faulty battery module" to be selectively disconnected while retaining operative conditions for the remaining traction system.

Complete High Voltage Disconnection

The diagram and photographs in Figure 2 present the test setup and the key equipment. In order to substitute a Main Fuse the PSS arrangement, i.e. a bypass switch (PSS/NO) and disconnection switch (PSS/NC), was located outside the battery pack. The intention with this test was to expose this "main fuse substitute" to an extreme condition of 5000 Amp of short circuit current carrying an inductance of 154 µH. A coil was used as static load and all power was supplied by the battery pack after a contactor (i.e. an ASEA EG315 that normally operate for steady three-phase current up to 690 Volt ac and present a very low resistance) had established the short circuit across the coil. In order to assure that the circuit carried 154 µH of inductance the short circuit was allowed to prolong for about 20 ms before the PSS/NO and PSS/NC arrangement was activated (i.e. time 0 ms). The bypass and disconnection sequence was performed in less than 0.5 ms. An additional 20 ms of data was acquired in order to visualize the relaxation of the system after the short circuit had been eliminated.

Three shunts (60 mV @ 400 Amp) measured currents as experienced by the battery pack (I_{Batt} Battery Current), by the bypass circuit (I_{BP} Bypass Current), and through the load (I_L Load Current). All data was acquired by use of a data acquisition unit with a sampling rate of 100 kHz.

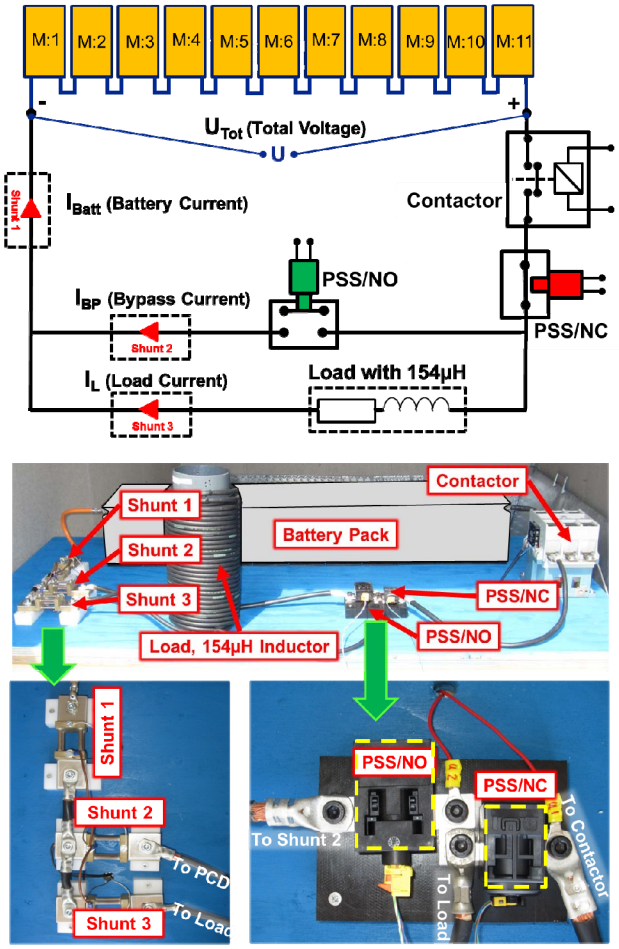

Figure 2. **Complete HV disconnection. Diagram on test setup, and picture of the physical test setup.**

Partial High Voltage Disconnection

In Figure 3 a diagram is presented where the PSS arrangement has been mounted inside the battery pack in order to allow the removal of a "faulty battery module" while retaining the main current flow through the neighboring battery modules. A Resistor-Inductor-Capacitor (i.e. RLC) load that provided a load representative for an electric car driving at steady state of 50-70 km/h on a horizontal surface regulated the main current to 25 Amp. The inductance of the system was 108 µH, which is a result of a capacitive impedance of 0.19 Ohm @300 Hz, inductive impedance of 3.4 Ohm, and a resistance of 4.5 Ohm of the RLC load.

The RLC load included a current converter with six silicon-controlled rectifiers (SCR) in bridge feeding the power from the complete battery power pack back to the national power grid. This power electronics had also a capacitor bank on the DC side to simulate the commutation capacitance in the inverter. Between the power grid and the current converter a three phase coil was located to simulate the induction in an automotive traction machine. This three phase coil also ensured that a smooth current was fed to the grid (dI/dt).

The instruments used to observe the wave forms were two Fluke® oscilloscopes of model 199C respectively 99B. Both of these were triggered by a step response, i.e. when a large change in voltage and current were evident in the circuit.

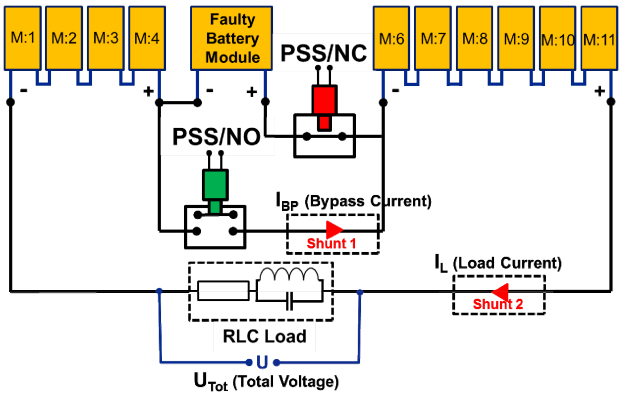

Figure 3. **Partial HV disconnection. Diagram on test setup, and picture of the physical test setup.**

RESULTS

In both test series – i.e. Complete HV Disconnection and Partial HV Disconnection – a battery pack (ranging from 300-400 Volt dc) was used together with a load that was designed to simulate an E-Vehicle electric traction system. Test results showed that breaking the high voltage circuit or isolating a faulty battery subunit, by the use of the PSS arrangement, was successfully achieved without harmful arcing or electrical fluctuations of a magnitude that may damage the surrounding electronics. As can be seen in Figure 4 and Figure 5, this action was performed in less than 0.5 ms and only minor current spikes (i.e. the integral of such a spike represent little electrical energy) and momentarily voltage variations were seen in the traction system. After a test the total battery voltage showed a reduction corresponding to the unit disconnected.

Complete High Voltage Disconnection

At the start of the Complete High Voltage Disconnection test the contactor was closed to create a hard short circuit across the poles of the battery pack. The inductance of the system (i.e. 154 µH) delayed the balancing current conditions, which are presented in Figure 3a (between approximately -10 ms to 0 ms), i.e. the plateau for *Battery Current*, *Load Current* and Total Voltage. Meanwhile the *Bypass Current* is zero since the bypass circuit is not yet connected. See Figure 4a.

Starting at the time of the connection of the bypass circuit (i.e. at 0 ms) and prolonging for 0.5 ms (i.e. throughout the bypass/disconnect delta time) the *Battery Current* experience an even higher extreme current than before, while the *Load Current* only experience very short current spikes at the point in time of disconnection (i.e. at 0.5 ms). See Figure 4b.

After the disconnection of the battery pack the inductive circuit relaxed. This is seen in Figure 4a as the *Bypass Current* (negative direction) and *Load Current* (positive direction) decreased.

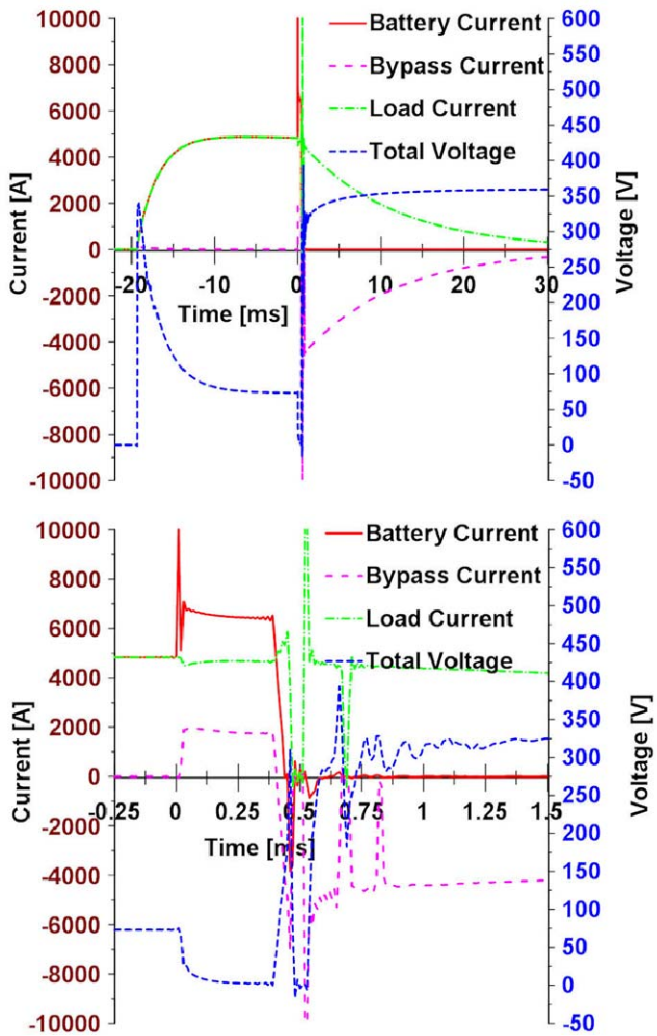

Figure 4. **Complete HV disconnection. a) Current flow and voltage change during test (range -20 to 30 ms). b) Current flow at time of disconnection (range -0.25 to 1.5 ms).**

Partial High Voltage Disconnection

The delta time for the process of active bypass and disconnection in the Partial HV Disconnection test series was about 0.35 ms. At the time of the activation of the bypass circuit (time 0 ms) a very rapid negative current spike was seen in the main circuit (see Figure 5a), while the battery module to be disconnected experienced an extreme short circuit that rushed to a peak of at above 3000 Amp just before the action of disconnection (see Figure 5b). At the time of disconnection the Load Current experienced one rapid positive spike followed by one rapid negative spike, while the short circuit current across the Bypass path was sharply terminated.

After the completed process of active bypass and disconnection in the Partial HV Disconnection test series the battery pack offered a total voltage equivalent to the original voltage minus the disconnected battery module (see Figure 5a)

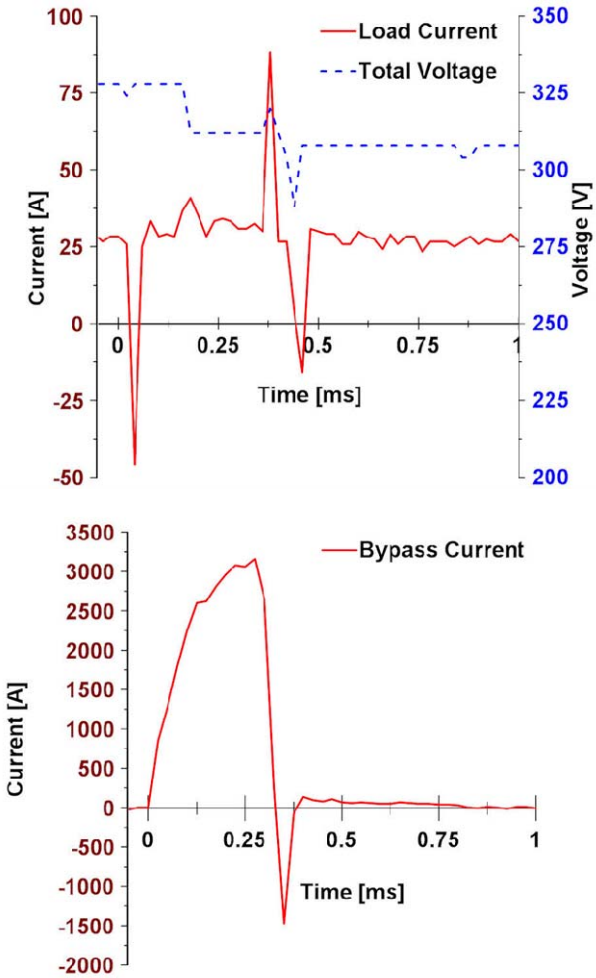

Figure 5. **Partial HV disconnection. a) Main current flow and total voltage change across the bypass and disconnect sequence. b) Short circuit current flow through the bypass path and the faulty module.**

DISCUSSION

The tests series presented in this report were performed on battery packs of ranging from 300 to 400 Volt dc and the disconnected unit was either the complete battery pack or a constituent battery module of the pack. The risk of generating a severe arc when cutting off a complete battery pack of 300-400 Volt dc or disconnecting subunits of such a battery pack, is greatly reduced by the presented methodology. However, this methodology demands a very short delta time between the connection of the bypass circuit and the disconnection of the battery unit. This short delta time is vital in order that the extreme short circuit, which instantaneously develops across the battery unit to be disconnected through the bypass circuit, shall not generate heat or other phenomena that are harmful to the battery system.

Autoliv achieved the required short delta time by using pyrotechnic switches (i.e. the PSS/NO and PSS/NC) which are available in Autoliv's product portfolio. A later version of PSS offers a single unit with those two functionalities combined. Furthermore, in order to deal with the risk of stranded energy of a disconnected battery unit an additional PSS/NO functionality can be incorporated in order to engage a Drain Unit after the sequence of bypass and disconnection has been completed (see Figure 6).

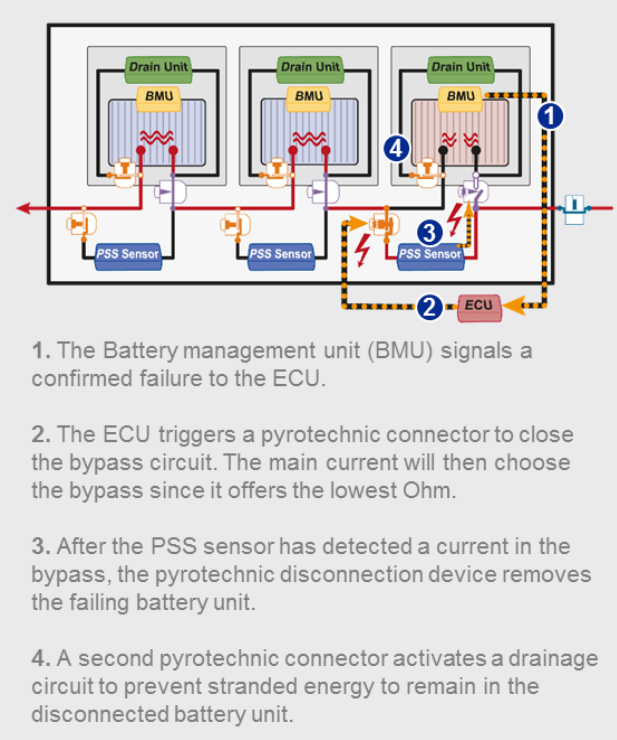

Figure 6. **Concept sketch with separated PSS/NO and PSS/NC units for clarity. In later PSS version, a single unit of combined functionalities of PSS/NO and PSS/NC offers a multiple connection/disconnection opportunity.**

The Complete HV Disconnection that is achieved with the methodology of Active Bypass & Disconnection can alternatively be achieved with a single 'one-stage' pyrotechnic switch that perform a disconnection of the HV battery but no bypass (i.e. a 'one stage' PSS/NC). Such a device must be very robustly designed to anticipate the extreme conditions of arcing that evolves within the device when carrying out a disconnection without first diverting the inductive current. This type of device is defined in Autoliv's product portfolio as PSS/NC High Power. However, it has not been subject to the test series presented in this paper as it is using a different methodology.

CONCLUSIONS

The key feature of the successful disconnection and bypass, seen in the tests presented, is the diversion of the electrical traction system's inductive influence away from a faulty battery pack or battery subunit, right before that unit is disconnected. This diversion of the influence of the inductance on the pyrotechnic circuit breaker prevent the formation of harmful arcs across the divided conductor.

When the bypass has been established it is crucial that the subsequent disconnection of the faulty battery unit (i.e. complete battery pack or a battery subunit) is performed extraordinary quick in order to minimize the effects of the short circuit current that is rushing between the "faulty unit" and the bypass circuit. Autoliv is capable of achieving this by using a pyrotechnic switch sequence with a delta time of less than 0.5 ms between bypass and disconnection. This extraordinary short delta time provides that the otherwise harmful effects of an extreme short circuit remain at a minimum, and therefore damage to the battery system as well as potential repair costs can be kept at a minimum.

Complete High Voltage Disconnection

Autoliv's PSS arrangement can offer an alternative to main fuses and, in contrast to a conventional fuse; it will perform a clean cut-off of the conductor at a speed that is independent of the magnitude of the fault current.

Partial High Voltage Disconnection

Autoliv's PSS arrangement can offer an alternative to relays/contactors when reversibility is less important than speed, physical weight and size as well as cost and the ability to act properly beyond current levels during the E-Vehicle's operational driving conditions. The risk of switching bounces is eliminated when using Autoliv's pyrotechnic switches.

Furthermore, when a faulty battery sub-unit is bypassed and disconnected properly, a "limp-home" ability can be offered since the battery power electronics are remained unharmed due to the extraordinary short delta time and the minimized effects of inherent current spikes during process of the bypass and disconnection.

General

The setup of Pyro Switches for High Voltage Circuit Breaking & Bypass not only prove to assist in solving the acceptance criteria of the FMVSS 305 for E-Vehicle crashes, but also offers a tool to achieve retained mobility after a faulty battery unit(s) have been disconnected. Additionally, by using the Autoliv's PSS arrangement the faulty battery unit(s) will be isolated from the rest of the traction system and thus will not experience further electric exposures that otherwise may cause more damage to such unit(s). Instead, a discharge unit may be connected in order to release stranded energy in a safe manner.

REFERENCES

Autoliv. (n.d.). Life saving in only a few milliseconds. Retrieved March 2015, from Autoliv Pyroswitch: http://www.pyroswitch.com

Merkel, T. (2014). Hochvolt-Relais von morgen: Sichere Minimalisten. Hanser Automotive - OEM Supplier - Elektro und zukunftsmobilität, 106-108. Retrieved March 2015, from https://www.panasonic-electric-works.com/cps/rde/xbcr/SID-13796B8A-54077247/pewnew/fb_x61_de_oemsupplier_201409.pdf?type=target

A PARTNERSHIP BETWEEN RENAULT AND FRENCH FIRST RESPONDERS TO ENSURE SAFE INTERVENTION ON CRASH OR FIRE-DAMAGED ELECTRICAL VEHICLES.

Claire, Petit Boulanger ; Jacques, Thomazo ; Bruno, Azmi
Renault SAS
France

Olivier, Labadie
Yvelines Firefighters Brigade
France

Bruno, Poutrain,
Paris Firefighters Brigade
France

Michel, Gentilleau
Vienne Firefighters Brigade
France

Hervé, Bazin
Laboratoire Central de la Préfecture de Police
France

Paper Number 15-0252

ABSTRACT

In order to ensure first Responder safety, Renault set up a collaborative approach to involve rescuers in our electrical vehicle conception. The breakthrough came from the integration of crash and fire deterioration from the earliest stages of vehicle development.
Collaboration with fire brigades revealed 5 key areas which were then dealt with: electrical vehicle identification; prevention of electrical risk during emergency intervention; the impact of Li Ion batteries on occupant extrication and fire; co-creation of decision-making tools (Emergency Response Guide or ERG, rescue cards); training sessions on electrical vehicles.
EV prototypes were provided to study how the 400V system affected fire brigade intervention. Extrication tests were led on the full range of Renault electrical vehicles to take into account the different locations of the 400V battery. Fire tests were carried out until total combustion of the 400V batteries was reached. Then, extinction tests in open and closed environments were conducted, led by French scientific laboratories. Temperatures, thermal radiation, and concentrations of flue gases effluents were measured in most of these tests.
A large number of electrical vehicles were donated to French and European fire brigades for extrication training and fire demonstration. Bespoke electrical vehicles were produced as training supports and offered to fire brigades.
Trainings are given for free to French rescuers all around the year by an engineer from Renault, expert in electrical vehicle interventions.Finally, Renault regularly participates in national working groups with fire brigades and contributes to the ISO initiative on ERG writing and templates.
This combination of actions and results removed doubts as to the safety of electrical vehicle 400V batteries in a deteriorated state; enabled the proposal of a modus operandi for fire brigade intervention; led to the modification of the architecture of the 400V battery casing and the vehicle itself to improve rescuer intervention; highlighted the need to standardize service plug location across the range of Renault electrical vehicles.

Thanks to this fruitful collaboration between Renault and French fire brigades, rescuers acquired knowledge and skills for intervention on Li Ion battery electrical vehicles.

INTRODUCTION

When launching the Renault Electric Vehicles (EV) programs, the overall safety of these vehicles along their life cycle was a major concern for the company, as it already was for Internal Combustion Engine vehicle (ICE). The safety was integrated in the technical specifications by a careful selection of Lithium ion batteries safety concepts: electric architecture, service disconnect switch (SD/SW) integration, mechanical structure, " Battery Management System " (BMS) protection strategy of the battery for a maximal safety level in all use cases. Many validation tests were led to guarantee the battery safety, including in abusive conditions such as: electrical abuse, thermal abuse, mechanical abuse and cell internal defect.
Renault's innovative way was to get involved, from the design of vehicles, first responders to study incindental situations of EV life cycle, such as road accidents and vehicles fires. Those sharing seemed particularly useful as it could raise relevant questions coming from fire brigades interventions habits and not yet identified by development teams.

GOALS

The five actions areas identified with firefighters to guarantee their safety and the victims one in emergency interventions were the need of :

- Efficiently identifying the vehicle as electric.
- Getting the vehicle safe easily
- Keeping low the Li-Ion battery effect on extrication and extinguishing situations
- Creating common standards to help first responders decision (Emergency Response Guides, and Rescue Cards)
- Training them free of charge by our EV experts

METHODS

The first step was to understand the difficulties of fire brigades during their interventions on crashed, burning, or immersed vehicles … During their intense exchanges, Renault and first responders drafted together the technical specifications of EV Emergency Response Guide to be sure to answer the real needs of the firefighters. To fill some chapters of this ERG and validate its EV safety level during rescuers future interventions, Renault conducted field testing together with fire brigades.

EV Identification and safety

Fire brigades expressed their need to be able to distinguish the EV from an ICE in case of emergency intervention.
Renault took into account this necessity with standard distinctive visual elements in its EV; special Headlights, lack of exhaust pipe, logos Z.E. lack of petrol filling flap, underhood orange wires and connectors, specific elements on the dashboard
The BMS is in charge of managing the battery functional and dysfonctional safety , this is achieved by controlling both temperature and voltage and ensuring they remain in between the defined functional tresholds. Furthermore, aiming to guarantee the best safety level for people, Renault recommends beforehand in any intervention of extrication, to isolate the electric 400V circuit of the battery from the vehicle by disconnecting the SD/SW.
A 2 steps cut-off mechanism ensures the lack of electric arc during the operation of service plug disconnexion.

First extrication tests on Electric Vehicles

Renault was willing to verify before the selling of its two first EV models (Kangoo Z.E. and Fluence Z.E.) if the 400V battery and wires could affect usual extrications technics. A prototype of each EV model was thus given to French fire brigades so that they could check the possibility of keeping their usual cutting techniques .

They concluded that Renault EV wedging could be done the same way as ICE, including by applying rams directly on the battery casing. Weight distributions are different between EV and ICE, because of the lack of internal combustion engine and the presence of 300kgs batteries under the vehicle for Kangoo Z.E. and in the trunk for Fluence Z.E. As a matter of fact, if it lies on the roof after a crash, the EV is in balance (figure 1). It requires more wedging elements than for ICE which tilts forwards, because of its engine weight. Rescuers confirmed that Kangoo Z.E. floor had no risk of downward movement when positioned on the roof, in spite of the weight of the underfloor battery. They also showed that it was possible to extricate a victim through the Fluence Z.E. rear window when on the roof, using rams for example, in spite of the weight of the battery in the trunk (figure 1).

All the techniques of intervention used usually for extrication have been tested and rescuers concluded that none of their manoeuvre was forbidden by the presence of the battery or electric wires in Renault EV, because none is located in cutting areas. These results were used to fill in Renault EV ERGs and Rescue Cards .

Figure 1 : a-Fluence Z.E. in balance on the roof ; b-poosible wedging on Kangoo Z.E. battery ; c- no downward movement of Kangoo Z.E. on the roof ; d-possible exit of victims from Fluence Z.E. on the roof despite battery located in the trunk.

Electric Vehicles first tests of fire in closed environment

The aim of these tests was to answer the questions of fire brigades about EV (with Li-Ion batteries) behavior when involved in a fire. These first fire tests were organized by Renault and performed in the Centre National de Prevention et Protection (CNPP), in partnership with fire brigades.

They included bruning a Fluence Z.E. and a Kangoo Z.E. (with batteries at 100% charge level) in closed environment (16m x 19m x 2.9m) by placing them on an aluminum pan of 150 x 100 x16 cms filled with 150 l of alcohol, to ensure at least 15 mn to fire exposure.

After ignition started, each EV was left until total combustion (body and battery), without any external intervention. These tests led to the following conclusions: the kinetics of the fire of Fluence Z.E. and Kangoo Z.E. is similar to ICE fire. Without any extinguishing, the Li-Ion battery has a total combustion duration of 1 hour without any explosion. The EV close neighbooring temperature tops 900°C during the burning of the car and decreases to 350°C during the combustion of the battery. 5m away, the maximal temperature does not overtake 350°C (figure 2).

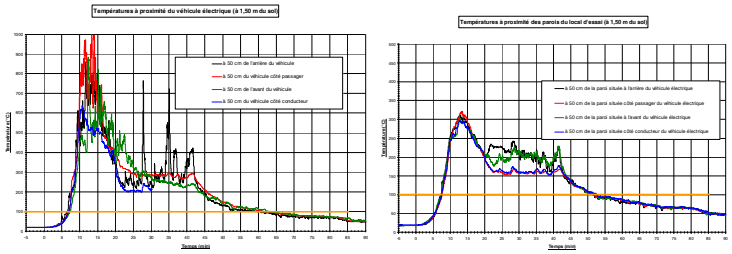

Figure 2: EV close neighbooring temperature and at 5 meters distance

Firefighters were able to conclude that this Renault EV fire behavior was similar to ICE fires they have experience with. Nevertheless, it was deemed necessary to perform comparative fire tests on EV and ICE to confirm these observations with quantified data.

Comparative tests of EV and ICE fires in closed environment

The purpose of this second test was to have comparative data between EV and ICE fire behaviour. These tests were performed by the "Institut National de l'Environnement Industriel et des Risques" (INERIS) on a conventional Fluence and a Fluence Z.E. . The only difference between these two cars is the presence of a Li-Ion battery instead of a diesel fuel tank. The Li-Ion battery of Fluence Z.E. was charged up to 100 % capacity and the diesel tank of the Fluence full (50L of fuel). The ignition was started into the passenger compartment from the driver seat with a gas burner.

As described in the first tests, there was no evidence of projections nor explosion resulting from the battery fire. The fire maximal thermal power and the total energy released are lower for the EV than for ICE: respectively 4.7MW against 6.1 MW, and 8 500 MJ against 10 000 MJ. The toxic effects during the combustion of the EV and the ICE were also compared.

Total quantities of CO2, CO, HCl, hydrocarbons, NO, NO2, HCN emitted during the combustion of EV are close or lower than those of the ICE (table 1).

Table 1: Pollutants measurements [1]

Emitted gas (g)	ICE	EV
CO_2	722 637	618 487
CO	15 732	11 700
HCl	2 139	1 933
NO	740	770
NO_2	410	349
HCN	178	148
HF	813	1472

Significant quantity of HF was emitted during combustion of both the EV and the ICE: a first peak of HF emission 14 min after the beginning of the test was observed in both cases. It results from the combustion of air conditioning fluid (figure 3).

A second wave of HF emission is observed in the case of the EV, linked to the presence of fluorinated salts in the Li-Ion battery. The associated kinetic is relatively slow and the instantaneous flow rates remain much lower than those from the the air conditioning liquid combustion. Moreover, it is interesting to notice that the overall amount of emitted HF from the battery is relativeley low compared to the potential content. Indeed, except the part linked to the A/C liquid combustion, assuming all the HF emitted from the vehicle comes from the battery, this is approximately 1050g of HF. Compared to about 5050g potentially contained into the battery, it is roughly only 20% of effective emission. This can be explained by the high affinity of HF for common metals present all over the vehicle frame (iron, steel, aluminum,...) thus it will react with apparent metallic surfaces and therefore will be less

present in gaseous emissions. The total quantity of HF remains superior to the ICE, without preventing fire brigades from applying their usual intervention procedures [1]. During later intervention testing of Fluence Z.E. fire, a HF detector positionned on the first fireman shoulder never measured concentration exceeding the tolerated threshold in intervention.

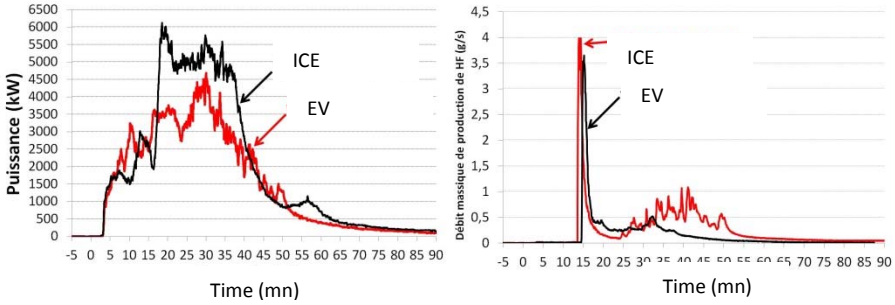

Figure 3: comparison of released energy and HF emission during the EV and the ICE combustion.

First EV extinguishing tests by fire brigades.

Prior to the selling of its two first EV models, Renault gave the fire brigades 2 Fluence Z.E. to perform outdoor fire and extinguishing tests. Firefighters wanted to reproduce the fire context of the most common vehicle fire situation : vandalism ignition, throwing a flammable object on the rear seats. As the objective was ensure the Li-Ion battery would catch fire, firefighters waited for 30 mn from the fire beginning and until launching the extinguishing intervention. At this moment, they could visually confirm the Li-Ion battery combustion, thanks to flames behind the vehicle. The firefighters extinguishing strategy was similar to ICE one: start from the front of the car, get rid of engine compartment fire, then move to the body and the peripherals (tires). Fire brigades *finally* focused on the Li-Ion battery extinguishing by spraying water on its casing for cooling . It was an ineffective attempt because the fire started again after every stop of water spraying, this until battery total combustion (~ 1h). Following this extinguishing failing attempt, a reflection was led to define the best strategy to stop the Li-Ion battery fire.The second test of Fluence Z.E. fire and extinguishing was set up by flooding the battery from firefighters hose, directly into the battery cooling system. This second attempt appeared to be particularly effective because the complete and definitive extinguishing of the Li-Ion battery was achieved within 5min.

The following recommendation was thus proposed: the extinguishing of a Li-Ion battery is possible and effective only by filling it with common water in the aim to flood it.

As Kangoo Z.E. didn't provide direct access to the Li-Ion battery (whereas Fluence Z.E. did) , the question of how to flood the battery remained. Several tests of fire and extinguishing of Kangoo Z.E. were thus performed in partnership with fire brigades and the "Laboratoire Central de la Prefecture de Police" (LCPP) to make sure that it was also possible to fill in the Li-Ion battery of this EV with water.

As the *main* objective was to be sure that the Kangoo ZE Li-Ion battery would *catch* fire during the test, firefighters filled the passenger compartment of wood pieces , and added some also on the ground underneath the battery. This set up was chosen to ensure a sufficient heat capacity to trigger the battery combustion. In every fire test, the Kangoo Z.E.battery, located under the vehicle, caught fire approximately half an hour after the beginning of vehicle fire. With the intense heat of the fire, it appeared that the Li-Ion battery aluminum casing melted in different points, allowing direct injection of water inside the battery, consequently the complete and definitive extinguishing was achieved in approximately 15 mn after the beginning of its combustion. [2]

The third Renault EV, ZOE, took experience from these fire tests results and integrated an innovative technical solution for allowing a fast and effective extinguishing of its Li-Ion battery: the "fireman access". It is a thermal fuse part based on plastic, located on the body of the vehicle, under the the rear passenger seat cushioning, which will melt because of the fire heat and therefore provide to firefighters a direct access to the vents of the Li-Ion battery (figure 4).

Figure 4: Fireman Access on ZOE before, during and after the fire test.

This worldwide innovation, allows efficient Li-Ion battery fire extinguishing within one minute, by flooding it with the fire nozzle. This shows a typical example of OEM taking in account the fire brigades needs. Since these tests took place, Renault integrated an additional requirement for this specific access dedicated to firefighters in the specifications of development of all its embedded Li-ion batteries. This "fireman access" presents a double interest: a direct and easy access for fire nozzle, and a direct view on the battery flames which makes easier the hole localisation , even for a first responder unaware of its existence. This improvement of rescuers intervention efficiency and safety was confirmed during others fire tests realized on ZOE in partnership with fire brigades and LCPP according to the same protocol as for Kangoo Z.E. (wood pieces inside the passenger compartment and under the vehicle). [2]. After usual extinguishing of the EV body, its Li-Ion battery was quickly and definitely extinguished by flooding it within one minute.

Simulation test of fire coming from inside the Li-Ion battery.

When it has been decided to add a "fireman access" in the passenger compartment of ZOE, the engineering team worried about a possible side effect in the highly improbable case of Li-Ion battery thermal runaway. Indeed, if a fire departure occurred inside the battery, would there be a life threatening risk (toxic gazs and smokes or flames) for the car passengers? To answer this difficult question and make sure that the "fireman access" would not decrease the safety level of the vehicle, a simulation test of fire coming from inside the Li-Ion battery was conducted, by overcharging a cell in the battery, considering this was the worst case possible of battery malfunction. This test was led once again in partnership with fire brigades and LCPP [3]. The heat increase of the overcharged cell was observed only after 1:30 hour of charging, and was associated with emission of smokes observed only outside of the vehicle (figure 6a). This phenomenon was observed during the heat propagation from cell to cell during 90 mn. During the same period, the heavily instrumented vehicle cabin (thermosensors, gas sensors & cameras) could not see any evidence of smoke nor flame presence inside the car. The LCPP and the fire brigades suggested to stop the test at this moment, concluding that if such a situation would occurred in the reality on EV with passengers blocked inside the car, rescuers would have enough time to extricate them .

After this test, the good behaviour of the "fireman access" *part* has been proved in spite of a skin temperature measured at 200°C (Figure 5 b and c).

Figure 5 : a – external smokes during heat increase distribution in nearby cells of Li-Ion battery ; b &c - Fireman Access after heat increase distribution in nearby cells of Li-Ion battery.

The conclusion of this test is that there is no increase of toxic risk or fire in the passenger compartment due to the presence of the fireman access.

CONCLUSIONS

All these tests contributed to improve knowledge on Renault EV safety when submitted to abuse situations such as road accidents and fire. Thanks to the intrinsic safety *level* of Li-Ion batteries on EV Renault and their BMS, as well

as to all the tests described in this paper, there is no particular risk found associated to EV for people (rescuers and car occupants). All the EV fire and extinguishing tests conducted in partenrship with fire brigades, that is 16 since 2011, guaranteeing a good reproducibility of the behavior of the Renault EV and their batteries (kinetics, intensity). Water was found an effective extinguishing agent for Renault EV battery Li-Ion. It is nevertheless necessary that the first responders are informed about the recommendations given by Renault. These knowledge, shared during the tests with some fire brigades experts, were thus *widely* distributed *to* fire brigades, by publishing on-line documents such as Emergency Response Guides (ERG) [4] [5] [6]) and Rescue Cards [7 [8] [9].

At the same time, trainings on Renault EV intervention are given free of charge in French fire brigades *by* a Renault expert, also volunteer fireman. A partnership French Renault / fire brigade was also set up to propose these trainings in the fire brigades of other countries wishing to benefit from it.

These actions and the results obtained allowed to provide answers to the fire brigades questions on EV safety when involved in abuse situations. Operating procedures have been adjusted by fire brigade. Renault found how to modify the battery casing architecture and the vehicle itself to improve first reponders interventions, and integrated the necessity of homogenizing the location of its SD/SW in spite of the associated stresses *on* mechanical and electrical architecture.

These works have been made possible thanks to a close partnership between French fire brigades and Renault EV engineering teams. Each part has been able to deepen its knowledge, to make sure Renault EV safety level is at least equivalent to ICE one. Fire brigades were able to adapt their methods of intervention and Renault learned how to integrate into its specifications the particular needs of first responders.

REFERENCES

[1] Rapport d'Etude INERIS, « Essais d'incendie de véhicules et de batteries » 17/11/2011 DRA-11-123008-09671A

[2] Rapport d'étude LCPP « Étude de l'impact de feux de véhicules électriques (RENAULT) sur les intervenants des services de secours » 20 janvier 2012

[3] Rapport d'étude LCPP n°13/11747, « Évaluation du comportement de la trappe thermo-fusible sur la propagation d'effluents gazeux dans l'habitacle d'un véhicule de type ZOE (RENAULT) en cas d'emballement thermique de sa batterie de traction

[4] Emergency Response Guide Fluence Z.E. Renault - http://www.infotech.renault.com/fo/accueil.action

[5] Emergency Response Guide Kangoo Z.E. Renault - http://www.infotech.renault.com/fo/accueil.action

[6] Emergency Response Guide ZOE Renault - http://www.infotech.renault.com/fo/accueil.action

[7] Rescue Sheet Fluence Z.E. Renault - http://www.infotech.renault.com/fo/accueil.action

[8] Rescue Sheet Kangoo Z.E. Renault - http://www.infotech.renault.com/fo/accueil.action

[9] Rescue Sheet ZOE Renault - http://www.infotech.renault.com/fo/accueil.action

RECOMMENDATIONS FOR SAFE HANDLING OF ELECTRIC VEHICLES AFTER SEVERE ROAD TRAFFIC ACCIDENTS

Marcus Wisch
Julian Ott
Federal Highway Research Institute (BASt), Germany
Robert Thomson
Chalmers University, Sweden
Michael Abert
Fraunhofer Institute for Chemical Technology ICT, Germany

Paper Number 15-0361

ABSTRACT

The EVERSAFE project addressed many safety issues for electric vehicles including the crash and post-crash safety. The project reviewed the market shares of full electric and hybrid vehicles, latest road traffic accident data involving severely damaged electric vehicles in Europe, and identified critical scenarios that may be particular for electric vehicles. Also, recent results from international research on the safety of electric vehicles were included in this paper such as results from performed experimental abuse cell and vehicle crash tests (incl. non-standardized tests with the Mitsubishi i-MiEV and the BMW i3), from discussions in the UN IG REESS and the GTR EVS as well as guidelines (handling procedures) for fire brigades from Germany, Sweden and the United States of America. Potential hazards that might arise from damaged electric vehicles after severe traffic accidents are an emerging issue for modern vehicles and were summarized from the perspective of different national approaches and discussed from the practical view of fire fighters. Recent rescue guidelines were reviewed and used as the basis for a newly developed rescue procedure. The paper gives recommendations in particular towards fire fighters, but also to vehicle manufacturers and first-aiders.

INTRODUCTION

This paper is based on work performed in the EVERSAFE project which, among other research topics, dealt with the crash and post-crash safety of electric vehicles (EVs) aiming to provide safety requirements and research needs for these (Wisch, et al., 2014). The project ran from 2012-2014 and was a collaborative project in the ERA-NET Electromobility+ programme.

EVs can be categorized into first (1GEV) and into second generation electric vehicles (2GEV), respectively. While 1GEV were defined as being solutions of electric vehicles based on existing chassis, vehicle geometries and established materials; 2GEV were defined as being developed and fabricated specifically by the car manufacturers and suppliers to best fit the users' demands of electric vehicles considering new vehicle construction concepts (including mass compensation measures regarding heavier battery weights), safety technologies and functionalities.

Motor vehicles with partial or full electric drivetrains are a small but growing component of the European vehicle fleet. An analysis of the current stock (end of year 2013) for different vehicle segments with electric drivetrains was performed based on figures for Germany (from the German Federal Motor Transport Authority) and Sweden (Trafikanalys, 2014). In both countries these vehicle types represent less than 1% of the vehicle fleet. Even in countries where government incentives are available, like Norway, the EV type is increasing faster but still is at only 1% of total vehicles (Statistics Norway, 2014). In terms of vehicle segments, in Germany around 81% of all registered passenger cars classified as battery (full) electric vehicles (BEV), range extender electric vehicles (REEV), fuel cell electric vehicles (FCEV) and plug-in hybrids have been assigned to the segments "mini" (56.7%), "small vehicle" (18.7%) and "compact class" (24.6%). The remaining share of around 19% contains larger vehicles. Due to this bias towards smaller vehicle sizes the target vehicles for investigating safety issues in EVERSAFE (and in this paper) were superminis and small family cars.

Accident Data

The penetration of electric vehicles in the vehicle fleet is still low and this is reflected in the number of available analyses of electric vehicle crashes based on national data sources such as police reports. The most relevant report describing electric vehicle crash risks was that provided by Daimler (Justen & Schöneburg, 2011). Although electric vehicles could not be directly analyzed, they used conventional vehicles as a surrogate and identified deformation maps that could identify the most risky areas for battery placement in real crashes which were compared to deformation from standard crash tests. Also, given that electric vehicles will tend to operate in

a similar manner in the road system, the accident configurations most commonly observed should also be relevant for the near future.

Marschner and Liers also discussed potential road traffic accidents involving electric vehicles based on assumptions of similarity to existing vehicles types (Marschner & Liers, 2013). For that reason, a GIDAS (German In-Depth Accident Study) analysis was carried out focusing on microcars and similar. More than 22,000 accidents were used to identify all vehicles with usage patterns close to future electric vehicles. Afterwards, numerous parameters of anticipated electric vehicles and conventional M1 vehicles were compared from which safety requirements have been derived. To characterize the expected accident scenario of urban electric vehicles, typical collision constellations, collision parameters and injury mechanisms were analyzed. Even though the analyzed vehicles were mostly small and compact cars, a significant mass difference for future urban cars was foreseen. Since the majority of the electric vehicles will be used in urban areas, it was concluded that there will be a change in the future accident occurrence. In general, lower accident severities were expected including less crashes in the longitudinal direction but with an increase in crashes at junctions while crossing and turning conflicts result in a higher proportion of side crashes. The severity of such an accident is influenced greatly by the vehicle mass and speed of the striking vehicle but the proportion of crashes with heavier vehicles was expected to remain similar to today's situation with conventional passenger cars.

The Swedish Project "Räddningskedjan- EV Safe Rescue" reviewed 165 crashes involving hybrid vehicles based on the accident data from NASS-CDS database, the majority being the Toyota Prius and followed by Honda Civic Hybrid (Vinnova, 2014). The accident investigation team identified the primary impact direction and damage location. Of 110 hybrid vehicles with identified impact directions, 65% had a frontal impact followed by 20% with rear impacts. The car front and rear were also the two most frequently damaged areas (Vinnova, 2014), which accounted for 61% and 18% of identified damaged locations. In these 165 cases there were no fire accidents reported directly after the crash.

Lithium-ion Batteries and Potential Hazards after Crash Loads

Current Lithium-ion (Li-ion) batteries are highly developed, well balanced chemical systems. These batteries are comprised of two highly lithiated contrary charged electrodes commonly separated by an olefinic separator and filled with flammable organic solvents. The formation of a Solid Electrolyte Interface (SEI) during the first cycling of a Li-ion battery after assembly is an essential step for the function of the battery. SEI is composed of stable compounds like Li_2CO_3 and meta-stable compounds like e.g. $(CH_2OCO_2Li)_2$. The SEI becomes unstable when the cell temperature rises above 70 °C – 100 °C with an exothermic decomposition according to Equations (1-2):

$$(CH_2OCO_2Li)_2 \rightarrow Li_2CO_3 + C_2H_4 + CO_2 + \tfrac{1}{2} O_2 \quad \text{(Eq.1)}$$
$$2\,Li + (CH_2OCO_2Li)_2 \rightarrow 2\,Li_2CO_3 + C_2H_4 \quad \text{(Eq.2)}$$

These reactions lead to the formation of ethene (C_2H_4) and carbon dioxide (CO_2). As a result, Li-ion batteries are very damageable by elevated temperatures. For example, an internal or external short circuit will raise the temperature inside the cell. An internal short circuit could arise when an external metallic part intrudes into the cell or by direct contact of battery electrodes after excessive compression of the separator. These examples may occur as a result of a car crash. Particles may also be introduced inside the cell during manufacturing process and cause an internal short circuit. Thermal and/or mechanical impact leads to the destruction of the SEI. After SEI decomposition, lithium reacts with organic electrolytes. Depending on the organic carbonates used as electrolyte components, different gaseous unsaturated hydrocarbons according to the reactions above are generated: ethene (C_2H_4), propene (C_3H_6), ethane (C_2H_6) and/or propane (C_3H_8). All these compounds are flammable and may form an explosive mixture depending on its concentration. An additional gas, hydrogen fluoride (HF), may also be produced due to reactions involving the conducting salts within the battery. Li-ion batteries can be provoked by internal or external heat sources and produce different gases that can be combustible or poisonous. The source of the heat can be fires surrounding the battery or internal short circuits of the battery cells caused by mechanical damage. High temperatures at one cell may affect adjacent cells and cause a chain reaction. With the organic solvent the conducting salt, $LiPF_6$, is also emitted and reacts in contact with water/air moisture according to Equations (3-4):

$$LiPF_6 + 4\,H_2O \rightarrow LiF\,(s) + H_3PO_4\,(l) + 5\,HF\,(g)\uparrow \quad \text{(Eq. 3)}$$
$$PF_5 + H_2O \rightarrow POF_3 + 2\,HF\,(g)\uparrow \quad \text{(Eq. 4)}$$

If a thermal runaway occurs a large number of different kinds of chemicals are generated. Combustion reactions evolve mainly the gases CO, CO_2 from organic materials, NO_x, HF as well as low molecular weight organic acids, aldehydes, ketones etc.

Crash Safety by Regulation

Electric vehicles shall fulfill all crash safety requirements as for conventional vehicles. Thus the current prevailing homologation tests regarding crash safety are applicable to electric vehicles as well. Depending on the market, different homologation tests are required for new vehicles to be type approved. It is necessary to address potential safety risks of EVs while in use and after a crash event, including electrical shocks associated with the high voltage (HV) circuits of EVs and potential hazards associated with Li-ion batteries and/or other rechargeable energy storage systems (REESS) (UNECE, 2012). In principal, the tests shall address safety considerations regarding the HV electrical safety, safety of electrical components, and REESS whereby there shall be no evidence of electrolyte leakage, fire, or explosion.

In Europe, all new vehicles should pass crash tests as specified by the United Nations Economic Commission for Europe (UNECE). With respect to complete vehicle crash tests, required tests include UN-R94 for frontal crash, UN-R95 for side crash, UN-R12 for steering mechanisms, and UN-R32 for rear end crash. For new vehicles to be sold in USA, they need to pass crash tests specified by the Federal Motor Vehicle Safety Standards (FMVSS). With respect to complete vehicle crash tests, they should pass FMVSS 208 (frontal crash, rollover, side crash), FMVSS 214 (side crash), and FMVSS 301 (rear end crash). The homologation tests in other regions such as in China, Japan, Australia and Canada are similar to those devised by UNECE and FMVSS.

Due to the introduction of HV system and traction battery system in electric vehicles, extra demands were raised concerning high voltage safety and battery safety in crash accidents. In Europe (and especially the 1958 agreement affiliated countries), UN-R100 sets requirements for the electric powered vehicles (classes M and N) and their REESS. In UN-R100, specific requirements on the REESS performance are defined concerning vibration, thermal shock and cycling, mechanical impact, fire resistance, external short circuit protection, overcharge/discharge protection, over-temperature protection and emissions. The date of entry into force of its latest series of amendments was 15 July 2013. Basic post-crash requirements regarding the safety of electric vehicles have also been added to UN-R94 and UN-R95 (e.g. regarding the releasing of electrolyte). In USA, FMVSS 305 specifies performance requirements that specify the: allowable electrolyte spillage, retention of propulsion batteries, and electrical isolation of the chassis from the high-voltage system during the crash event. This regulation is used in conjunction with FMVSS 208 (frontal rigid barrier crash tests), FMVSS 214 (side impact), and FMVSS 301 (rear, rigid barrier and deformable barrier impact tests).

Besides these crash regulations another Global Technical Regulation (GTR) is under development which addresses the safety of EVs. The Executive Committee of the 1998 Agreement (AC.3) gave, in November 2011, its general support to a joint proposal by the United States of America, Japan and the European Union to establish two working groups to address the safety and environmental issues associated with electric vehicles (EVs). That proposal (ECE/TRANS/WP.29/2012/36 and its Corr.1) was submitted to the World Forum for Harmonization of Vehicle Regulations (WP.29) at its March 2012 session for further consideration and formal adoption. The WP29 Committee has adopted this proposal with China as one of the co-sponsors together with the United States, Japan, and European Union (UNECE, 2012). The purpose of this regulation is to avoid human harm that may occur from the electric power train. The crash and post-crash phase are addressed by measures for the protection against electrical shock; REESS crashworthiness, including the limitation of electrolyte leakage, physical battery retention, and the maintenance of essential safety performance; and REESS safety assessment and stabilization procedures (UNECE, 2014). Major results from the GTR EVS are expected in 1-2 years.

METHODS AND DATA SOURCES

Abuse Cell Tests

To study the performance of batteries under crash type loading a set of experimental abuse tests on cell level were conducted in the EVERSAFE project aiming to understand the deformation tolerance and potential thermal and gas generated by batteries (Wisch, et al., 2014). Nail penetration is part of the standard tests being conducted on cells. In EVERSAFE two different nail penetration test setups were conducted using pouch cells. Test setup 1 used a nail (rounded plastic punch) that had penetrations limited by the fixture back plate and did not fully penetrate the cell as specified in the standard procedures while test setup 2 had a nail penetrator according to the SAE J2464 standard (tapered conductive metallic nail) to promote internal short circuits that passed through a hole in the back plate allowing full penetration. The first case test can be considered more of a localized crush test. Another abuse test, a shear test, cleanly sliced the cells with metallic knives. Again, two different test configurations were applied. On the one hand a support plate for the pouch cell was used (test setup 3) and on the other hand the pouch cell had no support structure at the cut edge (test setup 4).

Non-standardized Vehicle Crash Tests

To study the performance of electric vehicles under crash type loading, and in particular their HV batteries, as well as and to evaluate the current protection levels of EVs and safe handling procedures for rescue services, two crash tests were conducted. Since both vehicles to be tested were already cars in serial production on the market

and successfully passed regulation and consumer program (Euro NCAP) tests, non-standardized crash test configurations have been developed to study other realistic impact conditions that are challenging for the HV battery system and which allowed studying existing and updated safe handling procedures for rescue services.

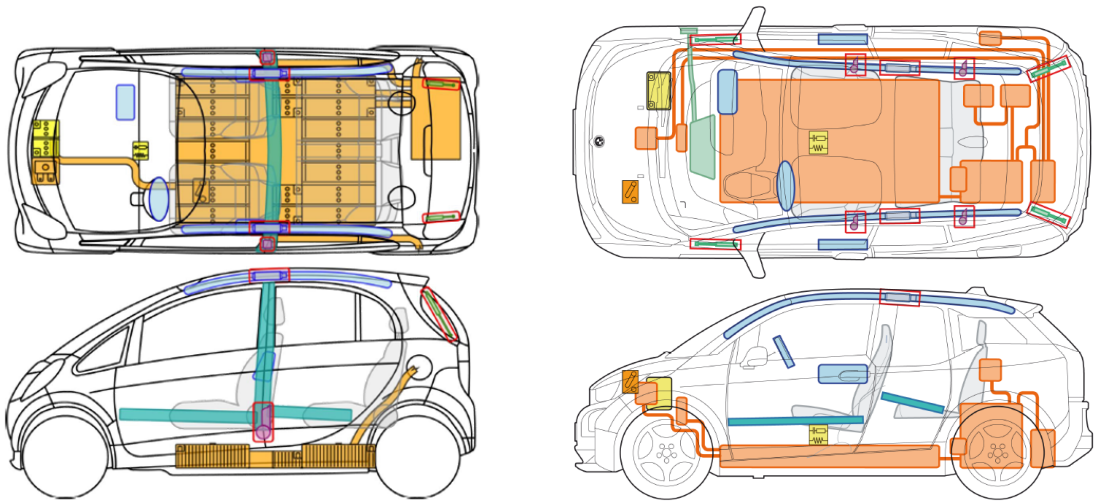

Figure 1: Left: schematic Mitsubishi i-MiEV (source: Rescue data sheet Mitsubishi) and Right: schematic BMW i3 (source: Rescue data sheet BMW)

Non-standardized Vehicle Crash Test #1 – Mitsubishi i-MiEV

As a first vehicle under test, the Mitsubishi i-MiEV (1GEV) was chosen representing a full electric vehicle with a Li-ion battery (330 V, 88 Li-ion cells, 16 kWh) that is located beneath both seat rows (see Figure 1) and two charging devices in the rear, a service-disconnect device beneath the driver seat and power electronics in the rear. As the test configuration, a 90 degree side pole impact was chosen whereby the i-MiEV was stationary (but not braked and with activated HV system) and a moving crash barrier (trolley) carried a rigid pole at its front (total mass ~2 t) approaching with 35 km/h, see Figure 2.

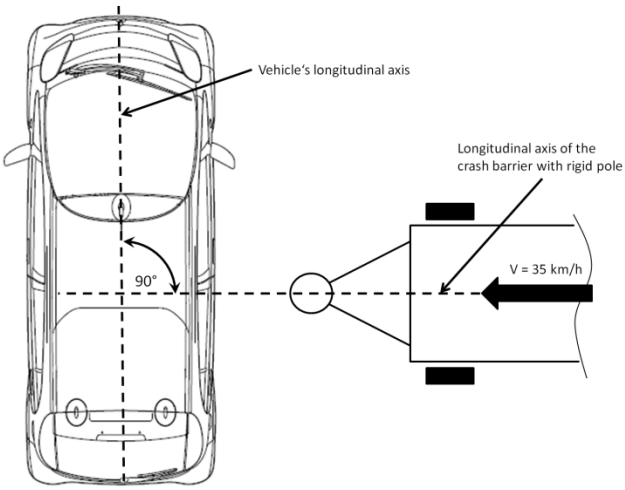

Figure 2: Scheme of test configuration side pole impact Mitsubishi i-MiEV

Non-standardized Vehicle Crash Test #2 – BMW i3

The second vehicle tested, the BMW i3 (2GEV), was chosen representing a full electric vehicle with a Li-ion battery (380 V, 96 Li-ion cells, 21.6 kWh thereof 18.8 kWh usable) that is located beneath both seat rows, see Figure 1. Further, it has one charging device in the rear, a service-disconnect device (executed as 12 V cutting line) in the car's front part and power electronics in the rear. Another peculiarity of the BMW i3 is that carbon fiber reinforced plastic (CFK) is primarily used as chassis material. However, the material used for front and rear crash structures are steel and aluminum. A crash configuration that represents both a frontal and a rear-end crash, as might occur in a traffic jam situation, was selected see Figure 3. A stationary, braked truck (weight ~10 t) was placed 2 m in front of the stationary BMW i3 test vehicle. The HV system was active and in driving readiness mode (with gear in neutral). A crash trolley fitted with a deformable barrier (total mass ~2 t) crashed then into the rear of the test vehicle BMW i3. All vehicles were centered along a common longitudinal axis. The trolley had a speed of 80 km/h. This test configuration exceeded standard crash requirements due to the fact that multiple impacts to the same vehicle were conducted.

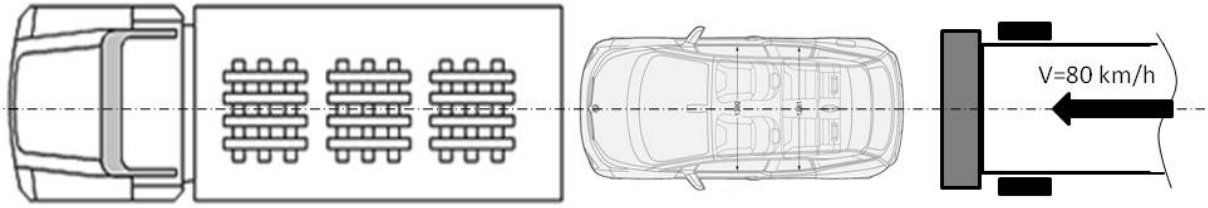

Figure 3: Scheme of test configuration front and rear-end crash with BMW i3

Rescue Procedures / Guidelines, Rescue Data Sheets and Technical Solutions

Rescue procedures vary within and between countries depending on the national, regional, and local organization of rescue services (Wisch, et al., 2014). Regardless of the location, firefighting and rescue services share common themes and technologies but there are local requirements that prohibit rigorous definition of rescue procedures. Due to the diversity of vehicles, occupants, and road conditions that will define a rescue operation, it is desirable that rescue personnel have a fundamental training that they can adapt to all possible conditions that they may encounter during their working career.

A study was performed to obtain an overview of existing rescue guidelines in Germany with special focus on information regarding the dealing with crashed electric vehicles (Wisch, et al., 2014). The information gained from the document "Accident Assistance & Recovery vehicles with high voltage systems" (German Association of the Automotive Industry (VDA), 2013) was considered to be most current and applicable. Other guidelines, as published by professional associations, do not focus sufficiently on the complete picture which is seen at a crash scene nor focused already on Li-ion battery technologies, but on organizational (mostly educational) aspects such as qualification levels or protection clothes.

Rescue data sheets have been developed to provide most important vehicle information for rescue teams in a clear and standardized way as well as in shortest time to ensure best rescue conditions for injured occupants. In Germany, the ADAC (General German Automobile Association) appealed in 2009 to the vehicle manufacturers to provide rescue data sheets for all new cars and to position them under the sun visor to provide information about cutting and pressure points, airbag zones and the location of the battery (Deutscher Feuerwehrverband e.V. (DFV), 2009). In addition to these data, rescue data sheets now include information regarding type of drive and the location of high-voltage components. Meanwhile several associations from the automobile sector and firefighting/rescue as well as vehicle manufacturers themselves and governmental entities promote the usage of these sheets in Europe. However, a legal obligation to carry a rescue card currently does not exist. The International Organization for Standardization (ISO) is developing a standard for rescue sheets (ISO, 2014). To ensure the availability of a rescue data sheet, Mercedes-Benz has introduced to the inside of the gas cap and on the opposite b-pillar QR codes that enables emergency services to access the individual sheet with a smartphone or tablet (Daimler AG, 2013).

In Germany in 2013, the Federal Ministry of Transport has set the basis to retrieve vehicle-related information directly from the database of the Federal Motor Transport Authority on software solutions on a tablet or laptop (Joint press release from von VDA, VDIK, ADAC, DAT and BMVBS, 2013). Two software solutions similar in functionality, the SilverDAT® - FRS (DAT group, 2013) from DAT (Deutsche Automobil Treuhand GmbH), and the Crash Recovery System® (Moditech Rescue Solutions BV, 2014) from Moditech Rescue Solutions use this option in the form of a license number query. Thus, it is possible to obtain directly by means of the license plate number at the accident scene information about the type of vehicle or drive and the access to the vehicle-related, digitized rescue data sheet.

In the United States, the National Fire Protection Association conducts diverse research on the handling of crashed electric vehicles and offers safety trainings as well as produces comprehensive material to be studied by firefighters. One of the basic documents, the Electric Vehicle Emergency Field Guide, provides an intuitive, quick reference guide, covering all current makes and models of hybrid and electric passenger cars drawn from manufacturer Emergency Response Guides (NFPA, 2012). Regarding the approach to a crashed vehicle, this document refers to always assume that the vehicle is some type of hybrid, electric or alternative fueled until proven otherwise.

The emergency call (eCall) is a system that in the event of a car accident automatically informs the locally responsible Public Safety Answering Point (PSAP). Technically, often the triggering of the airbag sensors initiates this automatic emergency call over the mobile network to the nearest PSAP. In addition to the position of the crashed car, vehicle-related data is transmitted, which are thus available to the emergency services even during the travel to the scene (German Federal Ministry of Transport and Digital Infrastructure, 2014). “The EC proposals for legislative acts foresaw that eCall would be seamlessly functioning throughout Europe by end of

2015. As the adoption procedure of these legislative acts by the European Parliament and the Council is still ongoing, the deadlines for implementation will most likely be the end of 2017 or early 2018." (European Commission - Digital Agenda for Europe - A Europe 2020 Initiative, 2014)

RESULTS

In general the tested pouch cells in the EVERSAFE project were quite resistant to the abuse. Only 1 of 19 cell tests resulted in thermal events. One cell was provoked by an overloading of the cell, after an external short circuit before testing and showed no negative effect on cell integrity. Shear tests gave comparable good results with no significant thermal activity (under 30°C) but with some toxic substance release. Even after the cells had been cut, there was a stable voltage developed by the cell. The lack of reaction in these tests could confirm that a clean cut of the cell will not lead to a failure of the separator and thus no direct contact appears between the cathode and anode. Results of nail penetration tests differ according to different types of nail (test setup 1 with rounded plastic punch and test setup 2 with thin metallic nail). None of the test setup 2 nail tests produced any significant cell swelling although there were traces of toxic substances. Temperatures did not exceed 60 °C. However, test setup 1 nail penetration tests produced some cell swelling and thermal activity was observed where temperatures up to 300 °C were recorded. The nail used at test setup 1 was made of plastic and could expand during the test, resulting in a local compression of the cell compared to the full nail penetration of the cell at test setup 2. The comparison of these tests shows that a clean penetration with a thin metallic, electrical conducting nail didn't lead to a reaction of the cell, whereas an intrusion with a wider object leads to a local compression and an internal short-circuit which deems to be more realistic in road traffic accidents. A special area of concern was also the reproducibility and the robustness of these tests since it could be shown that the results of cell tests might strongly differ already due to small differences of the test conditions and test scenarios applied. Pouch cells were also tested for external short circuit and overcharge of cells. External short circuit of cells has led to a tremendous evolution of gas inside the pouch cell, resulting in an inflating of the pouch like a balloon, but did not lead to bursting. After the temperature decreases, swelling was reduced and the pouch returned to its original flat profile but with wrinkles. Even a pouch cell rigidly held to the fixture by covering with non-flammable material has shown no bursting after inflating due to external short circuit. A consecutive overcharge with 5 V led to a thermal runaway with fire. It has to be pointed out that these tests should be referred to as extreme and demonstrate the high safety level of the device under test.

The crash tests with the two electric vehicles (Mitsubishi i-MiEV and BMW i3) produced no significant battery reactions (no new or unexpected risks such as electrical hazards, chemical reactions, thermal events, release of toxic substances battery, fire or explosion) and vehicle damage was as expected for current vehicle safety levels. Figure 4 shows the BMW i3 detached from the ground shortly after crashing into the rear of the truck indicating the high crash severity. Full test reports are provided in the EVERSAFE Deliverable 3.1 (Wisch, et al., 2014). Thus, both test vehicles exhibited high levels of safety in non-standardized, but realistic experimental configurations which were shown by:

- Good mechanical protection of the battery system.
- High-voltage system disconnected automatically to safe condition.
- Shut-down times of the HV systems much quicker (< 2s) than required by crash regulations (< 60s).
- No incidents (no undue temperature increase, no release of toxic / flammable gases or liquids).
- Intact cabin; a few bruised HV wirings and small deformations to the outer battery casing but without negative consequences.
- Newer chassis materials can produce stiff structures that increase the vehicle accelerations but can provide easier access to injured occupants as the doors may not bind due to distortions of the structure.

Figure 4: BMW i3 and crash trolley have fully left the contact to the ground at ~494 ms after the first impact

The main battery requirement from vehicle safety regulations was that the high-voltage outside the HV battery should drop down quickly (below 60 V) in a crash and this situation was fulfilled. As example, Figure 5 shows the HV network shut-off of the Mitsubishi i-MiEV after crash. There was no evidence of any danger after both crash tests that could be hazardous to occupants or rescue teams, neither with regard to electrical, thermal, nor chemical hazards. However, it could not be shown which effects further handling of this crashed vehicle might have (e.g., due to pulling, cutting or distorting the vehicle) during recovery operations.

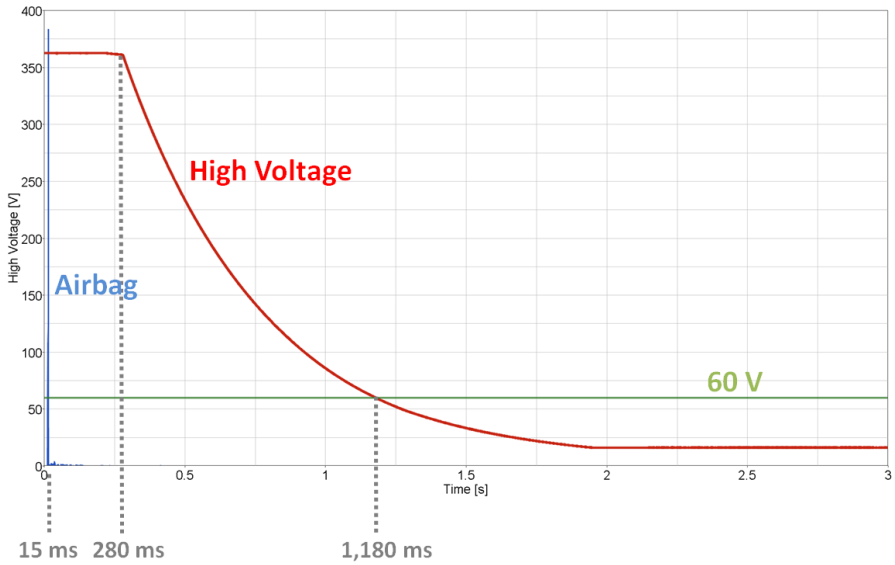

Figure 5: Airbag ignition and high-voltage network shut-off of the Mitsubishi i-MiEV after side pole impact

The severity of the full scale crash tests was chosen to be more challenging than required by the UN regulations or Euro NCAP tests, respectively. This decision was made because both test vehicles (Mitsubishi i-MiEV and BMW i3) have already successfully passed regulation and Euro NCAP crash tests and thus demonstrate a certain level of crash safety even with their new drive trains. The particular test configurations have been selected to reflect worst case, but realistic scenarios where potential hazards might occur.

Potential hazards originated from the high-voltage battery in severe crashes due to mechanical loading or fire close by during a crash are electrical shock risks, thermal events, chemical reactions and release of emissions of flammable, ignitable and/or toxic battery substances as well as fire or explosion. The main substances that can be expected from a Li-ion cell and their potential consequences are presented in Table 1.

Table 1: Table of critical emitted gases

Substance	Chemical formula	Health Risk	Toxic Concentration/ exposure time	Flammable
Hydrogen	H_2	No		Yes
Carbon monoxide	CO	Yes	6,400 ppm / 30 minutes	No
Carbon dioxide	CO_2	No	30,000 ppm	No
Methane	CH_4	No		Yes
Hydrogen fluoride	HF	Yes	50-250 ppm / 5 minutes	No
Phosphor pentafluoride	PF_5	Yes	3 ppm / 8 hours	No
Electrolyte fumes	$LiPF_6$	unknown		Yes

Portable multi-gas detectors are diffusiometers by default and are appropriated to detect critical emitted gases at a crash scene. Specialized rescue vehicles have addition measurement devices with active intake (integrated pump). In general, the multi-gas detectors allow directly measuring CO, H_2S and O_2. Further the available Ex-sensor (explosion sensor) only measures combustible gases and hereby only measures exactly, when calibrated on these substances (often methane (CH_4) and nonane (C_9H_{20})). However, gases such as H_2 can be calculated qualitatively using the explosion limit. As identified for Germany, in case of volunteer fire brigades a multi-gas detector is equipped on a vehicle specialized for measurements with a standardized configuration of the sensors and would be called subsequent to the initial vehicle arriving at the scene, whereas in case of a professional fire department this multi-gas detector is carried as standard in a vehicle of the first squad team.

A non-representative survey for available multi-gas detectors in Germany was performed in 2014 (Wisch, et al., 2014). Results have been summarized in Table 2. Although no longer commercially available the MSA “Solaris”

is still in use. There are other suppliers of portable gas detectors, but the companies MSA Auer and Dräger have largely prevailed in the fire service in Germany as standard.

Table 2: Typical multi-gas detectors used by German firefighters

Gas detector class	Label
1-5	Dräger "X-am® 5000"
	MSA Auer "ALTAIR 5X"
1-4	Dräger "X-am® 2500"
	Honeywell/ Compur Monitors "Impact (Pro)"
	MSA Auer "ALTAIR 4X"

To determine unknown liquids, a litmus paper test is standard for both volunteer and professional fire brigades. The same is true for thermal imaging cameras. In contrast, only specialized vehicles (e.g. the ABC-explorer) are typically equipped with short-time measurement tubules and need to be called subsequently by the incident commander. Water is still the standard extinguishing agent. However, additives are also used such as fire fighting foams which increase the impact of smothering a fire and cooling. Electrical measurements will be performed in most cases with a voltage tester that is present in the appropriate standardized toolbox.

An extended personal protective equipment (PPE) includes a chemical splash suit is available in several types ranging from part to full body protection in contrast to the standard PPE which contains of heat and (shortly) flame resistant jacket and trousers, helmet, leather boots (security class S3), respirator mask, special harness (incl. abseiling eyelet and hatchet).

Recommendations for Rescue Teams

In order to support rescue services when approaching road traffic accident scenes involving severely damaged electric and/or hybrid vehicles, a procedure for handling these vehicles with Li-ion traction batteries has been developed considering best practices and realistic resources. Inputs for the proposed rescue guideline (in the flow chart format of Figure 6) have come from several sources:

- Review of existing handling procedures for firefighters in particular from Germany and Sweden.
- Exchange of information and experiences with local firefighters around the crash tests conducted.
- Discussions within the EVERSAFE consortium and external experts.
- Survey regarding gas measurement devices available at German fire departments.

The flow chart in Figure 6 is divided into three columns identified with color. The middle, light blue column represents the decision path; the left, green column gives explanations and advice for the decision path; while the right, red column gives advice for measurement devices or special personal protection equipment. In addition to the explanations, information or user warnings are provided, partly by color or pictograms.

In addition to the measures for vehicle drivetrain identification, securing and deactivation of electric vehicles and the technical possibilities of monitoring the work site, the patient's health condition plays a decisive role in the flow chart. This results in a quick assessment of the accident and selection of the three approved types of rescue "Gentle rescue", "Fast rescue" and "Immediate rescue" as made use of in Germany. This approach uses procedures familiar for accidents involving conventional vehicles and reduces additional training requirements. The monitoring of the patient and the applied measurement technology must continue following the initial patient assessment and needs to follow the procedures identified in the flowchart until the patient is rescued from the vehicle. The ‘immediate rescue’ is the fastest possible rescue, tolerating a possible further deterioration of the patient from immediate danger or due to medical conditions. ‘Fast rescue’ is the fastest possible rescue of the patient with respect to time, tactical and medical aspects. In order to minimize the travel time to the hospital, transport is to be aimed at the ‘fast rescue’ time window of 20 to 30 minutes. ‘Gentle rescue’ is a rescue, in which the time aspect moves into the background because the diagnosed injury is not sensitive to time and the time window for medical consultation may in some cases be even greater than that of ‘fast recovery’) (Vereinigung zur Förderung des deutschen Brandschutzes e.V., November 2011).

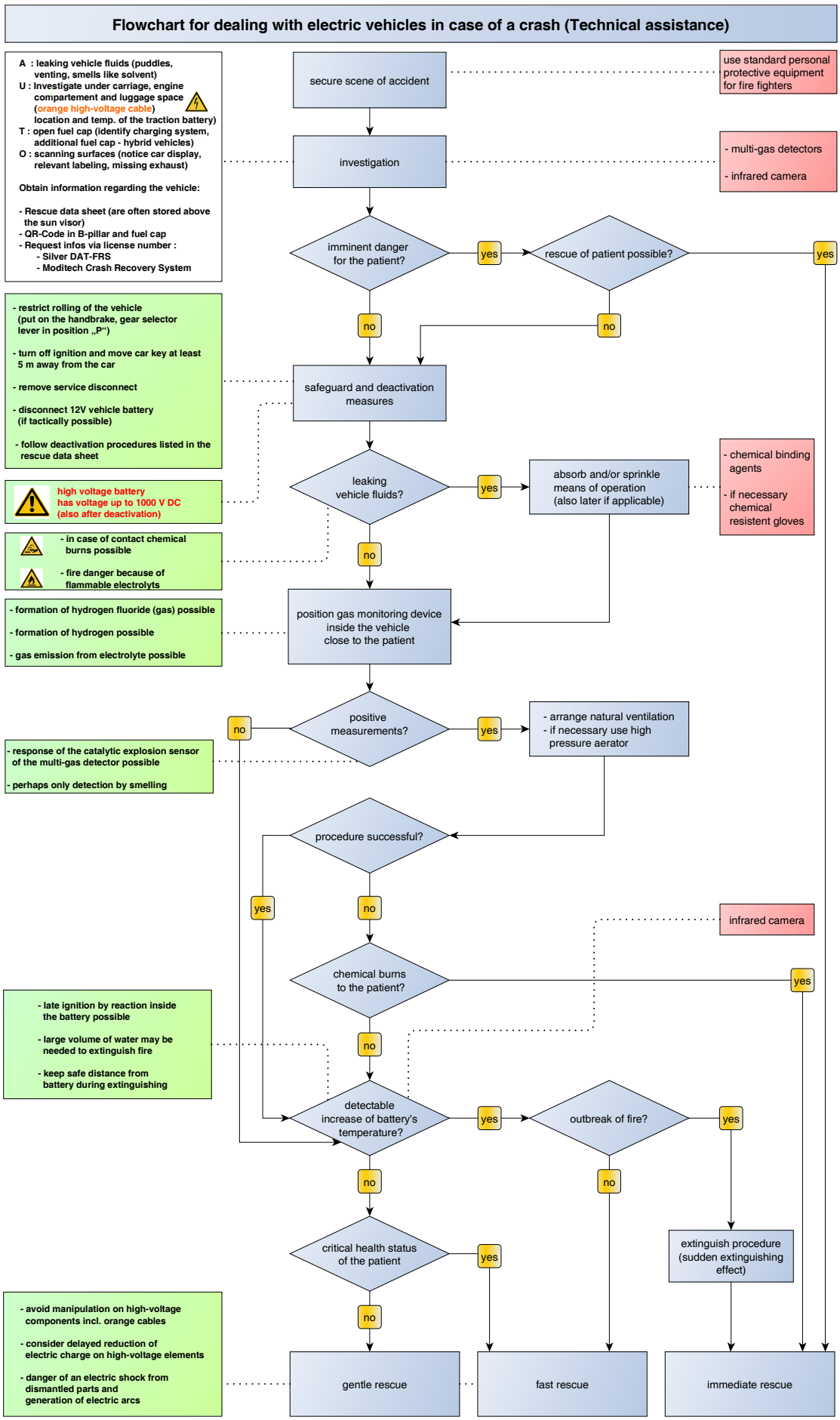

Figure 6: Updated rescue guideline

A summary of the features of the new handling procedure (see Figure 6) is provided below:

- Flow chart layout similar to best practices documentation but specialized for crashed vehicles with electric drive. The flowchart is focused on Li-ion battery technologies and not fuel cell drives.
- Clarity by three-column principle and color highlighting
- Flow chart can be used properly printed in an A4 format for use on scene
- Clear depiction that flammable, irritant and corrosive materials may be released by the HV battery and proposals for how to deal with them. For example, the explicit naming of the possible development of hydrogen fluoride (HF) could not be found in literature reviews of handling procedures.
- Procedure was optimized to maintain existing standard procedures used by (German) firefighters regarding their activities based on the patients' health states ("Gentle rescue", "Fast rescue" and "Immediate rescue") and if possible, to return rapidly to these three approved types of rescue
- Inclusion of relevant indicators for possible hazards (monitoring electrical and chemical conditions as well as temperature)
- Common measures to disable the HV system as replacement if specific rescue data sheet is not at hand.

With regard to the potential dangers that may arise due to a highly damaged electric vehicle, further recommendations and advice are provided below to complement the proposed updated rescue guidelines.

With focus on chemical hazards and fire:

- Chemical hazards exist and must be considered.
- The carbonates dimethyl carbonate (DMC), diethyl carbonate (DEC), ethylene carbonate (EC) and propylene carbonate (PC) are typical chemical substances used as electrolyte (also in mixed forms) in high-voltage traction batteries that possibly being released in case of mechanical damage to the HV battery or a cell. Therefore, these substances should be monitored using the gas detectors.
    - If released, then check the patient's condition (see also Figure 6).
    - In case patient should react to these carbonates (e.g. noticeable by sore throat or cough) cancel 'gentle rescue' and change to 'immediate rescue'
- Depending on the organic carbonates used as electrolyte components (see previous bullet point) and temperatures around 110 °C, different gaseous unsaturated hydrocarbons may be generated due to battery decomposition: ethene (C_2H_4), propene (C_3H_6), ethane (C_2H_6) and/or propane (C_3H_8). All these compounds are flammable and may form an explosive mixture depending on its concentration. A spark may ignite flammable gases or gas mixture.
- Hydrogen fluoride (HF) is difficult to measure on site (also costly due to required specialized gas detectors), therefore measurement of combustible gases is a suitable indicator (see previous bullet points) and is proposed by means of standard multi-gas detectors
- Multi-gas detectors should continuously measure the accident scene instead of using short-time measurement tubules which only provide a value per initiated measurement.
- Released substances are problematic in the case of Li-ion batteries because these would indicate opened (compromised) battery cells and packs which could increase the risk for gas development and resulting fire hazard.
    - The coolant may also be hazardous (not investigated here)
    - In case of Ni-MH traction batteries, alkaline solutions (pH 14) are used as electrolyte which leads to a risk of skin burns (not investigated here)

With focus on electrical hazards:

- Electrical hazards play a minor role due to multiple safety measures implemented by the vehicle manufacturers (no electrical hazards reported in the field known to date). However, in case of a severely damaged traction battery, extreme caution is appropriate.
- Difficulties at the scene:
    - The voltage tester or similar equipment / measurements must be used and assessed only by authorized personnel (electrically instructed person).
    - Difficult to determine measurement points on the vehicle as this is not described in rescue data sheets.
    - Possibly poor accessibility
- *Important to note:* Car manufacturers have not harmonized their recommendations with regards to the mandatory or voluntary usage of high-voltage gloves for rescue services during the de-activation process of the electric vehicle's high-voltage system. Some rescue data sheets (e.g. from Nissan or from Citroen) dictate wearing high-voltage gloves. Since no electrical issues in case of crashed electric vehicles were known from the field and any research project, and even the highly-challenging crash tests conducted in EVERSAFE did not lead to any safety issues, it is recommended that the use of HV

gloves is only warranted in case of a severely damaged traction battery and availability of specialized personnel. Latest news from the media need to be considered on this topic.

With focus on explosion:

- The risk of an explosion of the HV battery is very low.
- Ignition only occurs for high concentrations of chemical degraded products and only at high temperatures.

Monitoring the temperature change (in particular the increase of the temperature over time) of the Li-ion traction battery is probably the safest indicator for potential hazards in case of damaged electric vehicles.

- Due to available resources (in most cases only a thermal imaging camera is available) accurate measurement of the vehicle temperature is not possible and only a large increase of the temperature inside the battery is measurable from outside. The battery is often well insulated and might be difficult to be accessed for temperature measurements. Environmental influences such as high winds may exacerbate the measurement.
- If a traction battery is located below the passenger compartment, it is recommended to measure underneath the vehicle with a thermal imaging camera.
- As the temperature rises, the off gassing is amplified, which results in an increased concentration of carbonates.

Further general recommendations and advice for safe handling of EVs:

- Firefighters can approach the electric vehicle with standard PPE as approved for approaching conventional vehicles after crash. In case of any hazard (e.g. release of combustible gases) additional protection measures should be considered (e.g. wearing the respirator mask or the chemical protective clothing).
- The United States (NFPA) recommends the approach to always assume that it could be an alternatively powered vehicle (NFPA, 2012).
- The location of a vehicle's rescue data sheet may be changed and is recommended to be behind the driver's sun visor due to the severity of the crash sustained.

After the development of the new rescue guidelines, possibilities and proposals for further information and consolidation on knowledge regarding the handling of highly damaged electric vehicles involved in a crash include:

- Information and experiences with electric vehicles (and other alternatively powered vehicles) should be part of the basic training for firefighters
- Careful review of reports such as the VDA document (German Association of the Automotive Industry (VDA), 2013), from firefighting associations, research projects, service providers such as Dekra, articles in the magazine "Fire protection", etc.
- Create experience exchange forums (possibly on the Internet or in conferences)
- Firefighters are recommended to continuously browse through rescue data sheets
- Monitor current vehicle propulsion technologies and market shares

Technical solutions promising to provide important information about the vehicle in crash:

- Automatic Emergency Call (eCall) should include drivetrain information
- Query by vehicle's license number using the Crash Recovery System® of the Moditech Rescue Solutions or SilverDAT® - FRS
- QR-Codes applied to the vehicle

Finally, it should not be forgotten to ask the driver, when possible, about the type of drive and that all senses should be used in a careful manner when dealing with a crashed electric vehicle:

- Smell (e.g. released gases)
- Hear (e.g. opening of battery's safety relief valves)
- Feel (e.g. temperature increase)
- See (e.g. disrupted traction battery)

Recommendations for Vehicle Manufacturers

Vehicle manufacturers are requested to update rescue data sheets with information about chemical substances used in HV battery and possible reactions, to grant firefighters fast and simple access to (different) locations where the HV system can be shut down manually and to provide convenient, harmonized storage (positioning and attachment) for rescue data sheets inside the vehicle. Further, harmonization processes shall be reinforced with other manufacturers, automotive associations and governmental entities, e.g., to agree or not agree on the

mandatory usage of high-voltage gloves for rescue teams. Vehicle manufacturers should also promote eCall to their customers and provide as much useful information as possible within the emergency message. Finally, the communication with rescue team associations and fire brigades shall be continued and expanded.

Recommendations for First-Aiders

Based on the current results from crash tests and field experiences, persons arriving the crash scene first do not need to have specific concerns about their own safety when approaching a crashed electric vehicle in order to apply first aid to occupants. However, common sense should be applied all the times and news about this topic in media should be monitored. It is also recommended to inform other people close by about the presence of an electric vehicle if identified, including professional emergency workers. For first-aiders it is strongly prohibited to touch or modify any HV related vehicle components which are e.g. marked by an orange color or by figures.

DISCUSSION

In general and to the current state of the art technology, the batteries of electrically propelled mass production cars of the M1 category are well protected on standardized tests (e.g. according to UN-ECE R 94/95, Euro NCAP etc.) and even beyond. Nevertheless, in very severe crashes or unfortunate circumstances, the battery can be damaged severely causing hazards. Simulations in the EVERSAFE project and electric vehicle crash results showed that some current cell abuse tests, e.g. SAE J2464, might not be representative of what may happen in a vehicle crash as the intruding object would probably be wider as a thin nail.

Fuel sources for vehicles are becoming more individualized to the vehicle type and manufacturer. Additionally, the diversity of fuel types for vehicles sharing the same platform can lead to different rescue operations for vehicles with identical appearances. It is in regards to this point that electric vehicles impose new, and currently undefined, training needs for firefighters. Manufacturers can offer internal combustion, hybrid, or fully electric variants of the same vehicle model. Each has specific features that influence the rescue procedures. The documented rescue training materials for Swedish and German firefighters were summarized and compared in (Wisch, et al., 2014). Information provided is based on basic instructions that is under constant review and not every document is covered. Interviews with fire fighters were also conducted to capture the formal and informal knowledge of electric vehicles. A general outline of rescue operations for crashes involving electric vehicles was identified to facilitate the analysis. A general approach to rescue operations can be considered as:

1) Information on the way to the scene
2) Appraisal of the vehicle on the scene, identification of vehicle
3) Securing/stabilizing the vehicle
4) Fire control
5) Chemical hazard control
6) Shut-down electrical systems (to cut the vehicle)
7) Occupant extraction
8) Post crash issues

The review of Swedish and German rescue procedures and training materials indicate that there are many similarities that can be exploited when adapting existing methods for new vehicle technologies. The main point to be aware of is that the basic structure for approaching and acting at a accident scene are similar between countries and that the only issues that need to be addressed are related to the battery and its connections to the electric drivetrain. From the testing and simulation activities in the EVERSAFE project, there does not seem to be significant differences between EV and conventional vehicles in terms of fire and occupant extraction procedures.

The crash tests have also been used as training for firefighters. In particular, existing and alternative post-crash guidelines were considered and checked for their viability under realistic conditions. Different portable multi-gas detectors have been utilized to identify combustible gases (diffusion devices MSA Auer Altair 4X and devices with active intake MSA Auer Altair 5X and MSA Auer Sirius PID). Since hydrogen fluoride (HF) is the worst case result of possible chemical reactions, a special gas detector (Dräger X-am 5100 with HF/HCL sensor) was rented to directly measure HF (which did not emerge). Due to the high acquisition costs (around 1,500€) and maintenance costs of such a specialized gas detector it was considered to be not economical to propose the purchase for general application by rescue services. This conclusion was strengthened by consideration of the difficulties to measure under real conditions (e.g. wind) and the order of emergence of combustible gases due to a damage of the HV battery which can be detected with usual multi-gas detectors.

Following the crash test of the BMW i3, the work of the fire brigade was analyzed and discovered the following:

- Finding the rescue datasheet proved difficult, as this was thrown by the impact from the original position behind the sun visor in the back seat area and was discovered only in the further course of the training by the fire department. The firefighters were then able to act purposefully.
- The orange color of the 12 V rescue disconnect point and the resulting suspected high voltage danger were misleading so that the deactivation measures were carried out with high voltage gloves. Since the pulling of the plug required a detailed manipulation and took too long, the decision was taken to cut all connecting wires. However, it has to be noted that an adaptation of the color of the rescue disconnecting point was already provided at the time by BMW.
- Subsequent to the firefighter training performed at the BMW i3 crash test, the firefighters indicated that it is of high importance for them to recognize early in time the presence of an alternatively propelled vehicle. Therefore, the firefighters considered it advisable to consistently mark electric vehicles, e.g., similar to the license plate marking used in Norway (Balzter, 2013).

The training also confirmed the theoretical assumption that many firefighters are not yet adapted to the dangers of electric cars. Further, flowcharts of the procedure for accidents involving electric vehicles are largely unknown in the fire service. There is little distinction in the use of measures between conventional and electric vehicles.

There are some common actions observed in the rescue guidelines that need to be developed into rescue service education programs or better information is needed for rescue workers. The main points of interest are:

- How can EVs be readily identified at a crash or rescue scene? It is desirable that the vehicle identifies itself by eCall information or are there standardized identifications visible on the vehicle itself?
- How can a high-voltage system disconnect be confirmed? There is no visible indicator on the vehicle exterior that readily shows the high voltage circuit has been disconnected. This information can remove one step (Item 6) in the rescue process.
- Can there be a requirement (such as a UNECE regulation) that requires the HV system to disconnect when the 12V is disconnected? As rescue services routinely disconnect the 12 V system to eliminate pyrotechnical safety systems from inadvertently deploying, this interlock would also eliminate one step (Item 6) in the rescue process.
- How are batteries affected during extreme manipulation of the vehicle during occupant extrication? For example, the extension of the car from two winch points involves tension and bending loads on the vehicle floor, particularly if any of the pillars have been cut. This may induce internal deformation in the battery that may not have arose in the original crash, or accentuate existing damage in the battery caused prior to the extrication procedure.

In addition to the need to address the issues raised above, there is a lack of standardized or legislated procedures outlining the towing and storage of electric vehicles after a crash. Vehicle manufacturers develop their own product recommendations but there should be universal procedures to eliminate the risk of mistreatment of an EV due to a diversity of handling procedures.

The need for firefighters and other rescue workers to use specific protective equipment for EVs needs further investigation. Rescue operations should not require high voltage electrical repairs or investigation by individuals without appropriate training. It is desirable that standard protective equipment is sufficient and the vehicle systems are designed to ensure electrical isolation from rescue workers under foreseeable rescue operations.

One additional issue that requires further investigation is the influence of battery aging. Li-ion batteries are still a new technology with few years of service and thus experience with older batteries is lacking. There is a need to monitor EVs and identify if batteries and their structures exhibit degradation in their mechanical tolerance to failure.

The battery protection was achieved by very stiff protective structures using new materials as carbon fiber reinforced carbon (especially in 2GEV). This may lead to less overall vehicle deformations and higher acceleration loadings for occupants during crashes and thus increases the risk for severe, internal injuries. With regard to future user patterns, it has to be noted that other vehicle categories than the often discussed passenger vehicles (M1) will enter the markets. Especially in urban areas, smaller electric vehicles such as quadricycles and microcars are alternatives. Many of these small electric vehicles will be certified as vehicles of categories L6e or L7e which do not have to fulfill any legal crash requirements in Europe by now. This may result in less performing vehicle crash structures and other safety issues as tests of Euro NCAP have shown in 2014 (Euro NCAP, 2014). However, it has to be noted that most of the full-electrified small vehicles will run on low voltage networks that reduce the electrical hazards but depending on the cell chemistry thermal and chemical potential hazards may remain existent.

One final point regarding the risks from traction batteries is the influence of state of charge (SOC). The energy content of the battery is a function of its SOC. If a battery with a high SOC is disconnected from the external cables, the battery still has the potential to react internally and the safest condition would be to discharge or neutralize the battery immediately after the crash event. The former action is not feasible without developing extreme heat and electric shock hazards and there are no published methods yet to safely neutralize a fully charged battery. This is an area for new investigations.

REFERENCES

Balzter, S. (2013). Förderung von Elektromobilität: In Norwegen ist für Elektroautos sogar der Strom gratis. *Frankfurter Allgemeine*.

Daimler AG. (2013). Neue Mercedes-Benz Initiative: QR-Code kann Leben retten. http://www.daimler.com/dccom/0-5-7153-49-1601547-1-0-0-0-0-0-0-0-0-0-0-0-0-0-0.html.

DAT group. (2013). SilverDAT® - FRS Fire rescue brigade data sheet system. http://www.dat.de/en/offers/information-services/silverdatr-frs-fire-brigade-rescue-data-sheet-system.html.

Deutscher Feuerwehrverband e.V. (DFV). (2009). Rettungskarte soll Feuerwehr bei Unfällen helfen / Deutscher Feuerwehrverband begrüßt ADAC-Initiative für mehr Informationen. Press Portal - URL: http://www.presseportal.de/pm/50093/1404957/rettungskarte-soll-feuerwehr-bei-unfaellen-helfen-deutscher-feuerwehrverband-begruesst-adac.

Euro NCAP. (2014). *2014 Safety of Quadricycles*. http://www.euroncap.com/en/vehicle-safety/safety-campaigns/2014-quadricycles-tests/

European Commission - Digital Agenda for Europe - A Europe 2020 Initiative. (2014). eCall: Time saved = lives saved. http://ec.europa.eu/digital-agenda/en/ecall-time-saved-lives-saved.

German Association of the Automotive Industry (VDA). (2013). *Accident Assistance and Recovery of Vehicles with High-voltage Systems - Frequently asked questions.* Berlin.

German Federal Ministry of Transport and Digital Infrastructure. (2014). eCall für mehr Sicherheit im Straßenverkehr. http://www.bmvi.de/SharedDocs/DE/Artikel/LA/ecall-fuer-mehr-sicherheit-im-strassenverkehr.html.

ISO. (2014). *Road vehicles - Information for first and second responders - Rescue sheet for passenger cars and light commercial vehicles.* ISO/TC 22/SC 36: ISO 17840-1.

Joint press release from von VDA, VDIK, ADAC, DAT and BMVBS. (2013). Schnellere Hilfe mit dem digitalen Rettungsdatenblatt. http://www.dat.de/aktuell/news/schnellere-hilfe-mit-dem-digitalen-rettungsdatenblatt-156.html.

Justen, R., & Schöneburg, R. (2011). Crash Safety Of Hybrid- And Battery Electric Vehicles. *22nd ESV Conference.* Washington D.C.

Marschner, M., & Liers, H. (2013). Untersuchung des potentiellen Unfallgeschehens eineszukünftigen urbanen Elektrofahrzeuges auf Basis von Realunfalldaten. *9. VDI-Tagung mit Fachausstellung Fahrzeugsicherheit 2.0 - Wie viel passive Sicherheit benötigen zukünftige Fahrzeuggenerationen?* Berlin.

Moditech Rescue Solutions BV. (2014). The Mobile Vehicle Information System For Rescue Workers. http://www.moditech.com/en.

NFPA. (2012). *Electric Vehicle Emergency Field Guide - Classroom Edition.* Electric Vehicle Safety Training of the Naitonal Fire Protection Association (NFPA).

Statistics Norway. (2014). *Registered Vehicles*. URL: www.ssb.no/

Trafikanalys. (2014). URL: www.trafikanalys.se

UNECE. (2012). *Terms of Reference of the Informal Working Group on Electric Vehicle Safety.* ECE/TRANS/WP.29/2012/121, Paragraphs 1-6.

UNECE. (2014). *EVS GTR Draft protocol ver.4 (EVS-06-14e Rev.1.doc).* https://www2.unece.org/wiki/display/trans/EVS+6th+session.

Vereinigung zur Förderung des deutschen Brandschutzes e.V. (November 2011). *Merkblatt: Technisch-medizinische Rettung nach Verkehrsunfällen.*

Vinnova. (2014). *Räddningskedjan (E-Vehicle Safe Rescue).* www.vinnova.se/sv/Resultat/Projekt/Effekta/Raddningskedjan-Utformning-av-raddningstjanststrategi-baserad-pa-E-fordons-riskfaktorer/

Wisch, M., Ott, J., Thomson, R., Léost, Y., Abert, M., & Yao, J. (2014). *EVERSAFE - Deliverable 3.1 Recommendations and Guidelines for Battery Crash Safety and Post-Crash Safe Handling*. www.eversafe-project.eu, EC FP7 ERA-Net Electromobility+.

EVALUATION ON MEASUREMENT PROCEDURE FOR POST-CRASH HYDROGEN CONCENTRATION

Yohsuke Tamura
Hiroyuki Mitsuishi
Japan Automobile Research Institute
Japan

Paper Number 15-0047

ABSTRACT

To examine the measurement method for post-crash hydrogen or helium concentrations in the cabins and other enclosed spaces of vehicles which is provided in the UN Global Technical Regulation on hydrogen fuel cell vehicles (HFCV-gtr), the present study investigated 1) wind velocity conditions not affecting the hydrogen concentrations in the cabin, 2) the effect of the impact absorber of a moving deformable barrier, and 3) the feasibility of substituting the hydrogen concentration measurement with helium gas. The results indicated that the HFCV-gtr measurement method posed problems in its accuracy and reliability because hydrogen concentrations in the cabin varied under the influence of a 0.1 m/s wind and in the presence of an impact absorber in contact with the test vehicle. Furthermore it was found that although HFCV-gtr defines a permissible hydrogen concentration of 4vol% to be equivalent with a permissible helium concentration of 3vol%, this equivalence could not be verified. Consequently it is necessary to replace the HFCV-gtr measurement method for in-cabin hydrogen concentrations with a simpler method immune to external disturbances.

INTRODUCTION

Currently the UN Global Technical Regulation on hydrogen fuel cell vehicles (HFCV-gtr)[1] regulates the hydrogen leakage of HFCVs and the hydrogen concentrations in enclosed spaces such as the cabin and the trunk room, after a crash test. HFCV-gtr permits a maximum hydrogen leakage of 118 NL/min and a maximum hydrogen concentration of 4vol%; in addition, HFCV-gtr allows the use of helium gas in place of hydrogen gas for ensuring the safety of crash tests. The maximum permissible helium leakage is set at 88.5 NL/min (= permissible hydrogen leakage flow rate x 0.75), and the maximum permissible helium concentration set at 3vol% (= permissible hydrogen concentration of 4vol% x 0.75) in view of the leakage-related properties of the two gases[2]. Nevertheless, in case hydrogen does not start leaking from the fuel system within 5 sec since the closure of the main stop valve after the crash, HFCV-gtr allows the omission of the hydrogen concentration measurement.

Unlike the gasoline vehicles and compressed natural gas vehicles that are required to measure only their fuel leakage flow rates after a crash test, HFCVs are required to measure both fuel leakage flow rate and hydrogen concentration, thus subjected to more complex measurement procedures.

Regarding the HFCV-gtr measurement methods for post-crash hydrogen and helium concentrations, there was a study on their possible replacement with the measurement of oxygen concentrations[2]. In another study, a crash test was performed with hydrogen sensors installed inside the test vehicle[3,4]. On the other hand, the present authors in their previous study investigated hydrogen concentrations in the vehicle underbody and the cabin with varied leakage locations, directions, flow rates and flow velocities (nozzle diameters) on the assumption that a side window pane is broken open in a side crash[5]. It was found that when hydrogen gas was leaked from the underbody, hydrogen rose along the side doors and infiltrated into the cabin from the lower side of the open window. This finding suggested that the presence of winds or a moving deformable barrier in the infiltration route of hydrogen

might affect the hydrogen concentrations in the cabin; also that for the cases where more complex hydrogen infiltration routes and more open windows are involved, it would be necessary to verify the validity of substituting hydrogen gas with helium gas, two types of gases with different diffusion coefficients.
Additionally the present study evaluated the hydrogen and helium concentration measurement methods by investigating , (1) wind velocities not affecting the hydrogen concentrations ,(2) the effects of moving deformable barriers (MDB), and (3) the reliability of the helium substitution test.

DESCRIPTION OF EXAMINATIONS

Test vehicles: A 2,000cc gasoline vehicle (mini-van, sized L4,630 x W1,695 x H1,710mm, interior size of L2,775 x W1,505 x H1,350mm) was employed as the test vehicle, which was collided with a 950 kg carriage serving as MDB at a crash speed of 55 km/h according to the Japan New Car Assessment Program test method. Figure 1 shows the post-crash view of the test vehicle and the MDB both of which came to a stop with the MDB impact absorber (honey-comb structure made of aluminum) in contact with the crashed side door of the test vehicle. The lateral center window of the test vehicle had broken open as a result of the crash.

Figure1. Test vehicle and side impact MDB after side crash test

Because the post-crash measurement method of HFCV-gtr requires the measurement of hydrogen or helium concentrations and leakage, the crashed test vehicle was transported to the explosion resistance fire test cell of the Japan Automobile Research Institute in order to conduct an experiment in a safe, windless condition. The effect of the MDB was examined after placing a simulated impact absorber in contact with the test vehicle as shown in Figure 2.

Figure2. Simulated side impact MDB

Leakage conditions: Hydrogen (or helium) was leaked upward from the nozzles located at the center of the vehicle's underbody and at the center of the cabin floor, with the flow rate regulated by a mass flow controller. Only one (upward) nozzle direction was applied because previous studies[4,5] had found that hydrogen concentration distribution and the maximum concentration did not differ significantly between upward and downward nozzle directions when the hydrogen flow rate was about 2,000 LN/min.

In light of the fact that the fuel systems of HFCVs have pipes of a 1/4-inch (approx. 4 mm) inner diameter, nozzles of three different diameters (i.e., 1, 2, 4 mm) were applied. Considering the fact that HFCV-gtr permits a maximum hydrogen leakage of 118 NL/min, three different flow rates were applied--118 NL/min, 69 NL/min (a half), and 35 NL/min (a quarter). Two different leakage durations were applied--800 sec during which hydrogen concentrations were known to become constant inside the vehicle and 30 sec during which the hydrogen gas (estimated 59L) remaining in the piping after the closure of the main stop valve would be completely released at the maximum permissible hydrogen leakage of 118 NL/min for vehicle crash tests. To examine the effect of winds, an explosion-proof fan 600 mm in diameter was placed 5m away from the vehicle side.

Figure 3 shows the hydrogen concentration measurement positions in the cabin. Hydrogen and helium concentrations were measured using thermal conductivity hydrogen sensors (New Cosmos Electric Co., Ltd. XP-314).

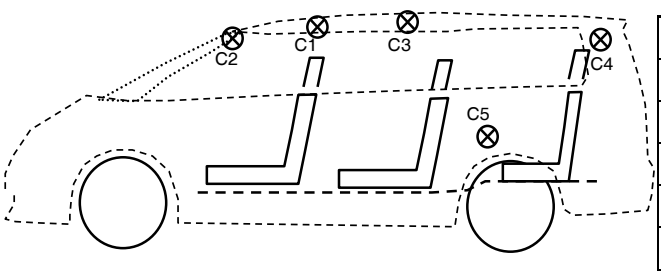

Position	Hydrogen concentration measurement position
C1	50mm below the roof above the driver's seat
C2	Near the mirror
C3	The center of the vehicle roof
C4	50mm below the roof at cargo compartment center
C5	50 mm above the floor at rear seat

Figure3. Hydrogen concentration measurement positions in the cabin

RESULTS AND DISCUSSION

Effect of winds on in-cabin hydrogen concentrations: The effect of winds blown from a side of the test vehicle was investigated concerning hydrogen concentrations in the cabin. Hydrogen was leaked from the vehicle underbody center or the cabin floor center continuously at a flow rate of 118 NL/min when a wind of 0.1 m/s was applied from a side direction. Figure 4 shows the hydrogen concentrations measured under the above conditions. The wind blowing was started 600 sec after the crash in Figure 4(a), and 300 sec after in Figure 4(b).

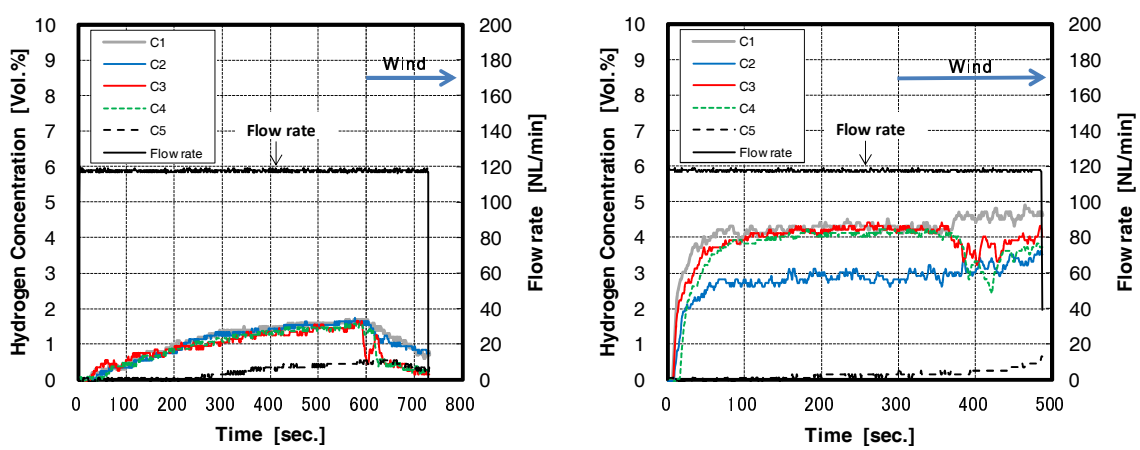

(a) Leakage point: Center of vehicle underbody ***(b) Leakage point:Center of cabin floor***

Figure4. Hydrogen concentrations in time sequence
(Wind velocity: 0.1 m/s and upward, Nozzle diameter: 4 mm, Flow rate: 118 NL/min)

In both figures, in-cabin hydrogen concentrations were affected when winds were blown. Due to measurement accuracy limitations, the effect of winds below 0.1 m/s could not be examined in the present study. According to the Beaufort scale of wind force[5], a wind velocity of 0.1 m/s corresponds to a Beaufort number of 0 and is rated as "Calm". In other words, 0.1 m/s represents practically a windless state. Accordingly it can be considered problematic to conduct a measurement, verification or reproduction test on hydrogen concentrations in an outdoor testing facility where natural winds easily exceed 0.1 m/s. Similarly, it should be necessary to consider the effect of winds even in an indoor testing facility in warm seasons when the air conditioning is in operation. For example, the wind velocity around a test vehicle in the indoor crash test facility of the Japan Automobile Research Institute in summer (July) is an average of 0.5 m/s and a maximum of 3 m/s. Accordingly it is necessary to take account of wind factors even in an indoor testing sites.

Effect of the MDB impact absorber: The effect of the presence or the absence of an MDB impact absorber was examined in relation to in-cabin hydrogen concentrations. Figures 5, 6 and 7 show the hydrogen concentrations in time sequence measured under varied test conditions concerning the nozzle location (vehicle underbody center), nozzle diameters (1, 2, 4mm), flow rates (118 NL/min continuously), and the impact absorber's condition (present in contact with the vehicle side door, removal from the crash site).

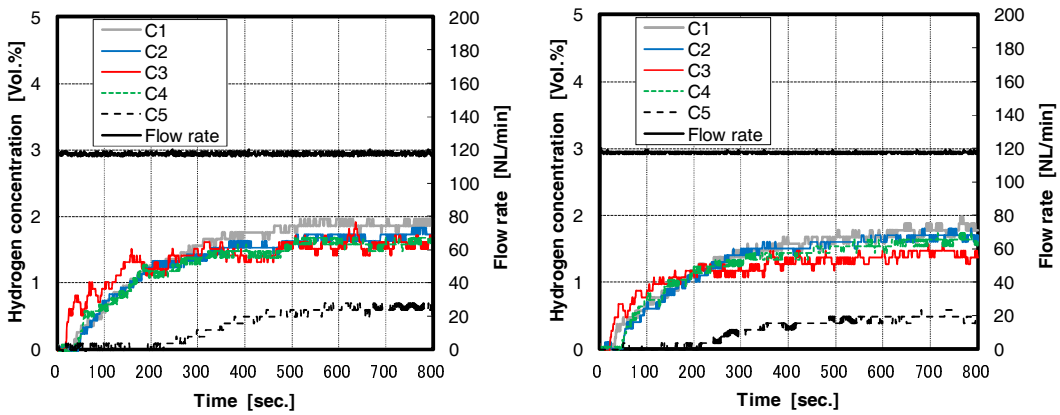

(a) Impact absorber contact case *(b) No impact absorber case*

Figure5. Hydrogen concentrations in time sequence (Leak point: center of vehicle underbody, Leak direction: upward, Nozzle diameter: 4 mm, Flow rate: 118 NL/min)

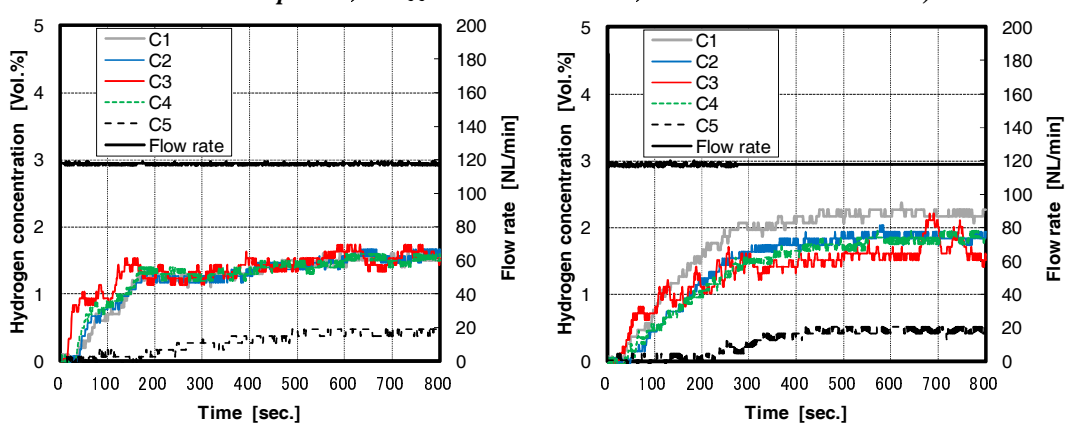

(a) Impact absorber contact case *(b) No impact absorber case*

Figure6. Hydrogen concentrations in time sequence (Leak position: center of vehicle underbody, Direction: upward, Nozzle diameter: 2mm, Flow rate: 118 NL/min)

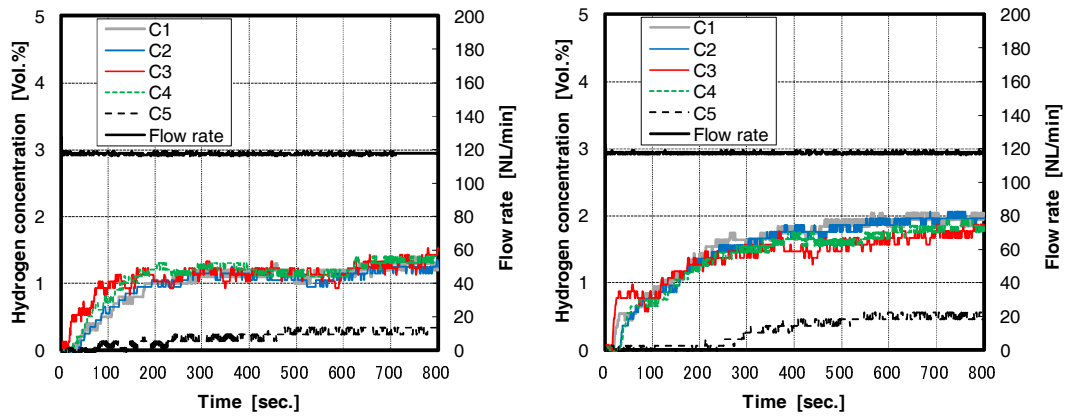

(a) Impact absorbing contact case *(b) No impact absorber case*

Figure7. Hydrogen concentrations in time sequence (Leak position: center of vehicle underbody, Direction: upward, Nozzle diameter: 1mm, Flow rate: 118 NL/min)

Comparison between an impact absorber in contact with the side door and the absence of an impact absorber at the crash site indicated differences in in-cabin hydrogen concentrations. Tables 2 and 3 show the comparison results in terms of maximum hydrogen concentrations under varied test conditions.

Table2. Maximum hydrogen concentrations when in contact with impact absorber [vol%]

Leak position	Direction	Nozzle Dia. [mm]	Flow rate [NL/min.]	Door	Wind	Leak time [sec.]	C1	C2	C3	C4	C5	Max (Position)
Underbody center	Upper	4	118	Close	No	800	2.0	1.8	1.9	1.7	0.7	2.0(C1)
		2					1.6	1.7	1.7	1.6	0.5	1.7(C2,C3)
		1					1.4	1.3	1.5	1.4	0.3	1.5(C3)
		4	69				1.4	1.3	1.5	1.2	0.5	1.5(C3)
			35				0.9	0.7	1.0	0.8	0.3	1.0(C3)
			118			30	0.5	0.3	0.7	0.4	0.1	0.7(C3)

Table3.
Maximum hydrogen concentrations with only test vehicle (No impact absorber case) [vol%]

Leak position	Direction	Nozzle Dia. [mm]	Flow rate [NL/min.]	Door	Wind	Leak time [sec.]	C1	C2	C3	C4	C5	Max (Position)
Underbody center	Upper	4	118	Close	No	800	2.0	1.8	1.6	1.7	0.6	2.0 (C1)
		2					2.4	2.0	2.2	2.0	0.5	2.4(C1)
		1					2.0	2.1	1.9	1.9	0.6	2.1(C2)
		4	69				1.3	1.3	1.3	1.2	0.5	1.3(C1,C2,C3)
			35				0.9	0.9	0.9	0.9	0.3	0.9(C1,C2,C3,C4)
			118			30	0.5	0.4	0.7	0.5	0.1	0.7(C3)

As indicated in Tables 2 and 3, the maximum hydrogen concentrations varied among the measurement positions, thus confirming the effect of impact absorbers on maximum hydrogen concentrations. The explanation of this effect is that as leaked hydrogen ascended along the doors and infiltrates into the cabin from an open window[4,5], the presence of the impact absorber in a hydrogen dispersion route affected the hydrogen infiltration into the cabin.

For the above reason, it should be difficult to accurately evaluate the diffusion behavior of hydrogen gas leaking from an HFCV in the presence of an MDB or a fixed barrier each equipped with an impact absorber.

Due to the HFCV-gtr requirement to measure in-cabin hydrogen concentrations immediately after a crash test, it should be necessary to remove the MDB near or in contact with the test vehicle to a sufficiently distant place so that the in-cabin hydrogen concentrations will not be affected.

Helium substitution test procedure: If the test condition of a 118 NL/min permissible hydrogen leakage is substituted with helium, the permissible helium leakage is 88.5 NL/min by applying a He/H_2 permissible leakage ratio of 0.75 (= 88.5/118). Based on the observation that gas concentrations in an enclosed space are in proportion to the gas leakage flow rate, HFCV-gtr[1] gives the following Equation **(1)** for the calculation of permissible helium concentration X_{He} conducive to a permissible hydrogen concentration of 4vol%.

$$X_{He} = 4vol\%\ H_2 \times 0.75 = 3vol\% \qquad \textbf{(1)}$$

To verify if Eq.(1) is reliable under various test conditions, the present study investigated the He/H_2 ratios in the cabin under identical test conditions between hydrogen leakage at 118 NL/min and a helium leakage at 88.5 NL/min. Figures 8, 9 and 10 show the results of this test. Because the concentration values measured at the C5 position near the cabin floor proved exceptionally low, the concentrations only at C1 through C4 are shown in the following three figures.

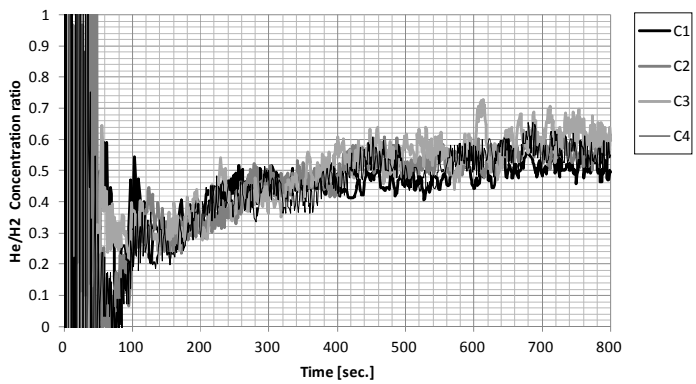

Figure8. He/H_2 concentration ratios
(Leakage point: center of vehicle underbody, Nozzle direction: upward, Nozzle diameter: 4 mm, Hydrogen flow rate: 118 NL/min, Helium flow rate: 88.5 NL/min)

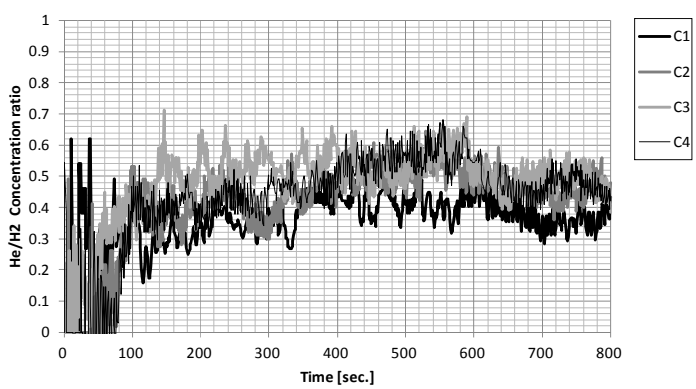

Figure9. He/H_2 concentration ratios
(Leakage point: center of vehicle underbody, Nozzle direction: upward, Nozzle diameter: 1 mm, Hydrogen flow rate: 118 NL/min, Helium flow rate: 88.5 NL/min)

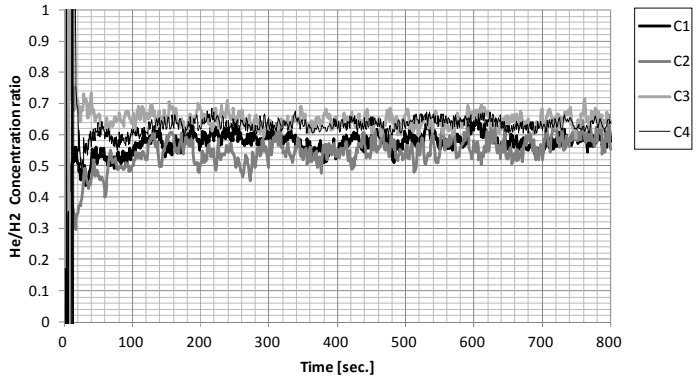

Figure10. He/H_2 Concentration ratios
(Leakage point: center of cabin floor, Nozzle direction: upward, Nozzle diameter: 4mm, Hydrogen flow rate: 118 NL/min, Helium flow rate: 88.5 NL/min)

The results indicated that the He/H_2 concentration ratio varied in the early phase of the test but gradually stabilized in the following phase onward. Nevertheless the ratio, instead of stabilizing at 0.75, varied according to leakage locations and nozzle diameters. The primary cause of this discrepancy was attributed to the fact that the aforementioned Equation (1) does not take account of differences in the diffusion behaviors of hydrogen and helium. Therefore, since no correspondence was found between a permissible hydrogen concentration of 4vol% and a permissible helium concentration of 3vol%, the validity of the helium substitution measurement method provided in HFCV-gtr was considered questionable.

CONCLUSIONS

To examine the measurement method for post-crash hydrogen concentrations provided in HFCV-gtr, the present study investigated 1) wind velocity conditions not affecting the hydrogen concentrations in the cabin, 2) the effect of the impact absorber of a moving deformable barrier, and 3) the feasibility of substituting the hydrogen concentration measurement with helium concentration measurement. As the results indicated that hydrogen concentrations in the cabin were affected by the presence of a 0.1 m/s wind in the testing facility and an impact absorber in contact with the test vehicle, the HFCV-gtr measurement method is considered to pose some problems in its accuracy and reliability. In addition, since the correspondence between a permissible hydrogen concentration of 4vol% and a permissible helium concentration of 3vol% assumed in HFCV-gtr could not be confirmed, the existing helium substitution measurement method was also considered questionable. Consequently it is necessary to replace the HFCV-gtr measurement method for in-cabin hydrogen concentrations with a simpler method immune to external disturbances.

Finally, the present study was carried out as part of the “technology development project for hydrogen production, transport and storage systems” commissioned by New Energy and Industrial Technology Development Organization (NEDO), a national research and development agency of Japan.

REFERENCES

[1] Global Technical Regulation (gtr) on hydrogen and fuel cell vehicles
[2] Isaac W. Ekotoa, Erik G. Merilob, Daniel E. Dedricka, Mark A. Groetheb, Performance-based testing for hydrogen leakage into passenger vehicle compartments, International Journal of Hydrogen Energy, Volume 36, Issue 16, 10169–10178, 2011

[3] Barbara Hennessey, James J Reuther, Jeffery S John, Paul E Shawcross, Gregory Kimmel, Post-crash fuel leakage and fire safety experiments for hydrogen vehicles, 22nd Enhanced Safety of Vehicle Conference, Paper Number 11-0439,2011

[4] Yohsuke Tamura, Noriaki Ohtsuka, Masayuki Takeuchi and Hiroyuki Mitsuishi, Determining hydrogen concentration in a vehicle after a collision test, Conference Proceedings on Fires in Vehicles (FIVE) 2012, SP Technical Research Institute of Sweden, September 27-28, 213-222, 2012

[5] Yohsuke Tamura, Masayuki Takeuchi and Kenji Sato, Effectiveness of a blower in reducing the hazard of hydrogen leaking from a hydrogen-fueled vehicle, International Journal of Hydrogen Energy, Volume 39, Issue 35, 20339–20349, 2014

ID#: 15-0326
Title: Failure Analysis of Compressed Natural Gas Containers for Automotive Use
Session: Advanced Fuels Crash Safety

Barbara Hennessey NHTSA, Nathanael Greene NASA, Darren Cone NASA, Tommy Yoder NASA, Daniel Wentzel NASA, David McColskey NIST

ABSTRACT

In 2009, the National Highway Traffic Safety Administration's (NHTSA's) Office of Defects Investigation made site visits to two different companies that utilized compressed natural gas (CNG) to fuel their vehicle fleets. The purpose of these site visits was to obtain information concerning two independent incidents where high pressure CNG fuel containers on fleet vehicles ruptured during or shortly after refueling. These containers were represented as conforming to industry standard ANSI/NGV2 [1], and were still within their 15 year manufacturer recommended service life (although they had experienced several years of on-road use). Further, the newer model containers were self-certified by the manufacturer as compliant with Federal Motor Vehicle Safety Standard (FMVSS) 304 [2].
After the container ruptures occurred, each of the companies, for reasons of safety, retired the sister vehicles in their fleets. The decommissioning of these fleets offered an opportunity to NHTSA to obtain some of the retired CNG containers, which experienced similar service conditions to those that ruptured during refueling, and to subject them to both nondestructive (NDE) and destructive evaluation (DE) to document in-service wear, damage and residual life.
To this end, NHTSA entered into an Interagency Agreement with the National Aeronautics and Space Administration (NASA) White Sands Test Facility (WSTF), to conduct the evaluation of the used containers and compare them to unused containers of similar design. NASA has been performing test and evaluation of composite pressure vessels, similar to those designed for automotive use, since 1978. The objective of the evaluation is to gain valuable insight into the construction and deterioration elements that could suggest potential improvements in the existing standards. Destructive and nondestructive evaluation of the aged and new containers is on-going. This paper presents the results of the evaluation to date and potential future steps in the program.

INTRODUCTION

In 2009, the National Highway Traffic Safety Administration (NHTSA's) Office of Defects Investigation made site visits to two different companies that utilized compressed natural gas (CNG) to fuel their vehicle fleets. The purpose of these site visits was to obtain information concerning two independent incidents where high pressure CNG fuel containers on-board fleet vehicles ruptured shortly after refueling. After the container ruptures occurred, each of the companies, for reasons of safety, retired the sister vehicles in their fleets. The decommissioning of these fleets offered an opportunity to NHTSA to obtain retired CNG containers which experienced similar service conditions to those that ruptured during refueling, and to subject them to both nondestructive (NDE) and destructive evaluation (DE) to document in-service wear, damage and residual life. To this end, NHTSA entered into an Interagency Agreement with the NASA/WSTF, to conduct the evaluation of the used containers and compare them to unused containers of similar design.
NHTSA had sister containers from each of the retired fleets shipped to NASA/WSTF for evaluation. The shipments included twenty-three Brunswick Type-4 CNG containers from one fleet and thirty-six Lucas Aerospace Type-2 containers from the other. The "Type" designation refers to the construction of the container. Type-1 containers are all metal – e.g., aluminum alloy or steel. Type-2 containers have a load bearing metal liner that is reinforced with composite (glass, aramid, carbon fiber or combinations thereof) hoop wrap around the parallel length of the container. Type-3 containers are fully wrapped by composite fiber and have a thin metal liner with most of the stress on the composite wrap. Type-4 containers have a non-metallic liner fully wrapped with composite fiber, which provides all of the container strength. The Brunswick containers were manufactured in 1994, and certified to ANSI/NGV2 for 15 years. The Lucas containers were manufactured in 1998 and certified for 15 years to ANSI/NGV2. They were also self-certified as compliant with FMVSS 304, which went into effect in 1995.
Federal Motor Vehicle Safety Standard 304*, Compressed Natural Gas Fuel Container Integrity*, is based on a subset of recommendations in the industry standard NGV2, and specifies performance and labeling requirements for the integrity of CNG motor vehicle fuel containers. Specifically, FMVSS 304 requires that non-welded containers (such as those evaluated in this study) do not leak or rupture in a hydrostatic burst test, when held at not less than 2.25 times the service pressure (SP) for 10 seconds. Containers must

also undergo a hydraulic pressure cycling test without leakage, and are subjected to bonfire tests per FMVSS 304. They must be labeled with information specified in the standard, and the label must remain affixed and legible for the manufacturer's recommended service life of the container. The FMVSS 304 labeling requirements are shown in Figure 1.

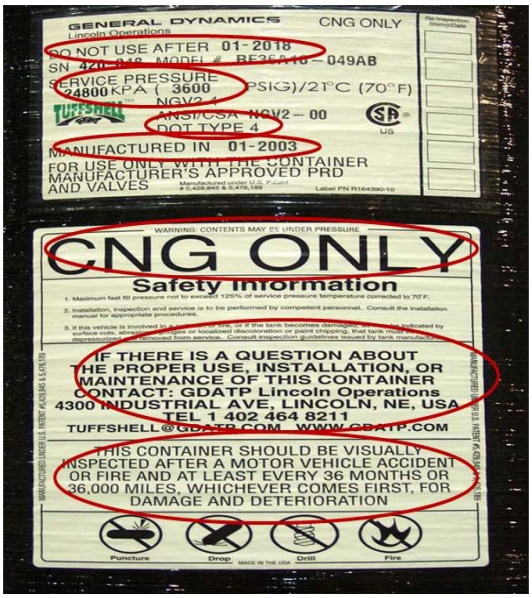

Figure 1. Labeling Requirements in FMVSS 304, CNG Fuel Container integrity

PURPOSE

The purpose of this effort is to document in-service wear, damage and residual life in CNG containers that have seen real world service, through nondestructive and destructive evaluation techniques. New containers are certified to the strength (i.e., burst) and durability (i.e., cycling) test requirements in standards and regulations such as ANSI/NGV2 and FMVSS 304, but (in this study) we seek additional data about the effects of the real world service environment on container life. While this study may not determine the root cause of the failures that occurred in the aforementioned two fleet vehicles, internal/external examination and residual strength tests may reveal weaknesses that can be addressed through improved tests, periodic inspection, and/or installation guidelines.

Synopsis of the CNG Container Failures

On June 9, 2008 a Type-2 Lucas Aerospace CNG container in a 1998 dedicated CNG Ford E350 van ruptured shorty after refueling at a Philadelphia Gas Works facility. The vehicle was equipped with three 3,000 psi rated containers that had a manufacturer recommended service life of 15 years and were manufactured in March 1998. Two 14" x 34" containers were mounted transversely in the rear of the vehicle. The third 12"x72" container, which ruptured, was mounted alongside the driveshaft inside the frame rail on the driver's side. The glass fiber overwrap failure was the result of stress corrosion cracking caused by an unidentified corrosive agent between the overwrap and the steel liner [3,4]. Over-pressurization of the steel liner during fueling also may have contributed to the failure. This may have been caused by a failure to close condition of the tank mounted solenoid valve and/or an improperly set relief valve on the fueling station [5]. Figure 2 shows the failed container.

Figure 2. Failed Type-2 Lucas Aerospace Container (portions of overwrap and steel liner missing)

On March 16, 2009 two Brunswick Type-4 containers ruptured during refueling of a laundry truck (i.e., conversion step van) in Pasadena CA. For the 3,000 psi rated containers, the manufacturer stated that the service life is 15 years and these containers were manufactured in 1994. They would have been at the end of their manufacturer recommended service life in October 2009. One of the containers was mounted vertically inside the back of the van onto a rubber padded steel ring with the shut off valve, pressure relief device (PRD), and piping exposed under the vehicle. The second ruptured container was mounted longitudinally under the vehicle, unshielded, and with its valve end dome directly beneath the vertical container [5]. The containers ruptured sequentially. The order and exact cause of rupture is unknown. Possible scenarios are that either the horizontal or vertical container failed first, due respectively to possible road damage or damage caused by the vertical mounting. The second container failed from fragmentation caused by the first rupture. Figure 3 shows some of the damage to the vehicle.

Figure3. Step Van Damaged by Type-4 Container Ruptures on Driver's side

Program Plan Overview/Status

The objective of the test program is to employ destructive and nondestructive evaluations on intact containers removed from service, and new containers. The goal is to ascertain if there are gaps in codes, standards and regulations which could be addressed to improve safety performance of future container designs.

The Test Plan consists of the following major components shown in Table 1.

Table 1.
Overview of Phased Evaluation of Type-2 and Type-4 CNG Containers

	Test Plan Phase	Status
1.1	Type-4 Nondestructive Service Evaluation	Complete
1.2	Type-4 Destructive Evaluation	Complete*
1.3	Type-4 Mechanical Sectioning and Materials Analysis	Complete
1.4	Type-2 Nondestructive Service Evaluation	Underway
1.5	Type-2 Destructive Evaluation	Planned

*One additional pneumatic burst test of an aged Type-4 container will be conducted in 2015

Type-4 Test Articles
Twenty-three Type-4 containers were removed from service and shipped to WSTF for testing. The WSTF numbers assigned to the containers for testing are WSTF# 11-45269 through 11-45291. These control numbers provide traceability to historic records and to each test that is performed. The containers were individually packaged in cardboard boxes for shipment from California. Once received at NASA/WSTF the containers were locked inside controlled access facilities.

Type-4 Containers - Nondestructive Service Evaluation Methods
Each of the containers was subjected to the following nondestructive examination techniques, the results of which are documented in individual data packages.

- Shipping containers, packing materials, and all accessible exterior surfaces were inspected in the as-received condition. Digital photographs of the container, packaging arrangement, and exposed surfaces were taken.
- An as-packed coordinate system was registered to the exposed features on the test article, enabling subsequent registration with a fully-exposed-article grid coordinate system to be referenced and remain consistent throughout the examination.
- Once the CNG containers were removed from the shipping containers, visual inspections of the remaining exterior surfaces were completed and documented through a combination of near and far field photography. Visual indications were recorded and documented per the manufacturer's criteria.
- Physical dimensions such as weight, length, and circumference at several distances from the top dead center (TDC) reference boss (A-end or valve end boss), were measured and recorded.
- A detailed visual inspection damage log and high magnification photography, recorded damage indications mapped to the coordinate system on the exterior upper dome (A-end), hoop region and lower dome (B-end plug) of each container.
- Prior to internal inspection, the break-away torque of the manual valve and plugs were measured.
- Internal visual inspection and boroscopic images recorded presence of contaminants (e.g., compressor oil), bubbles, voids, staining, and other indications on the container interior.
- Radiographic images of the interior documented internal interfaces such as boss-to-liner and liner-to-overwrap.
- Flash thermography was used to reveal infrared transfer of heat into wall surface fiber layers, useful for identifying subsurface areas of delamination.
- Laser shearography was used to detect non-visible internal flaws (two containers only).
- Samples of interior and exterior contaminants and foreign debris were collected, analyzed, and archived (twenty-three samples of each collected and archived, 2 analyzed).
- Samples of residual gas in containers that arrived with valve closed were collected and analyzed (three containers only).

Type-4 Containers - Nondestructive Evaluation Results
Appendix A provides an inventory of the Type-4 containers and a summary of the NDE results. The following general observations were made.

- Some damage was observed on several shipping containers, including mechanical damage and oil contamination.
- Inconsistent and/or variable debris buildup was observed on test article exteriors.
- Some labels were missing, illegible, or obscured by container mounting straps in service.
- Some labels were wrinkled in such a way to imply containers were shifting within vehicle mounts during service.
- Paint transfer was observed on numerous test articles. Primers, paints, or other "incidental contact" chemicals not addressed in testing may not be compatible with container overwrap materials.
- Break-away torque of the pressure fittings on containers varied from below 5 ft-lb to 170 ft-lb, with oil on the outside of some containers which was chemically similar to oil found on the inside, possibly indicating a chemical/flammability hazard.
- The largest average container circumference was near the dome regions. The smallest circumference was near the center of the container length.
- No provisions for proper torque of the pressure fittings (wrench flats) are available. Over torque may cause damage to boss-to-liner or boss-to-overwrap interface.
- Mechanical damage was present up to Level 2 per CGA Pamphlet C-6.4-2007 and Level 2b per OEM technical inspection manual. Level 1 damage does not require repair. Level 2 damage requires the manufacturer's recommendation in writing for disposition or repair of the container. Level 3 damage requires the container to be condemned.
- Rubber hose mounting ring and adhesive material was observed on containers that were mounted vertically in vehicles which may not be compatible with overwrap.
- Vertical dome mounting configuration was not addressed by the container manufacturer, which recommends horizontal strap mounting with guidance on strap locations. There may be potential for direct dome mounting to damage the structural composite.
- Circumferential witness marks were unevenly spaced from boss to boss with a variation in witness mark width. This provides evidence of shifting during service. Torque and pre-load specifications on container straps should preclude structural damage and limit lateral translation.
- Oil was observed on the interior and exterior of the test articles, internally as much as half a gallon of compressor oil was measured in a container used in the horizontal mounting configuration.
- Liner visual indications such as blistering were observed in the dome regions of almost all test articles. Significance of blistering, whether from manufacture or use, is unknown.
- Evidence of severe liner separation from overwrap and boss was observed in one container via computed radiography.
- Laser shearography data was of little value and excessively noisy due to as-received surface condition of containers. The "Tuffshell" sacrificial glass layer distorts data in the hoop transition and dome regions. Application of a dulling developer solution improved readings slightly.
- Thermography data was of little value. The overall composite wall thickness and sacrificial glass layer distorts heat transfer characteristics. The addition of impact protection in hoop transition and dome regions confounded useful data from the load bearing surface underneath.
- Three containers with closed valves had 1 – 5 psi residual gaseous contents composed of approximately 94% air, 3.5% ethane, 1.5% propane, 0.6% butane and a trace amount of methane.
- Exterior contaminants consisted of kaolin (clay), aliphatic hydrocarbon (oil), and silicon dioxide (sand) – all expected road contaminants.
- Interior contaminants were a two phase oil residue/paste consisting of aliphatic hydrocarbon and polypropylene glycol, white crystalline carboxylic acid and cellulose acetate butyrate.

Type-4 Containers - Destructive Evaluation Methods
Seven of the twenty-three containers that were examined nondestructively were selected for destructive evaluation under this test plan. The NDE served as the basis for selection of six test vessels to undergo

hydraulic cycling and burst, based on the test methods in certification standards. One container was selected for pneumatic burst testing, as pneumatic burst was the failure mode in the delivery vehicles. For comparison, two new vessels of similar design were also selected for hydraulic burst testing. Unfortunately the new containers are not the exact configuration of the service containers, but they do share many of the same features of construction and materials, giving them some limited value as reference test articles. A comparison of the containers is provided in Table 2.

Table 2.
Typical Dimensions of Type-4 Service and New Containers

Description	Service Containers	New Containers
Manufacturer	Brunswick Composites (now Lincoln)	Lincoln Composites
Mfgr Part Number	RA30A16-055AB	240172-030
Service Pressure (SP)	3000 psig	3600 psig
Standard	NGV2-4	ANSI/CSA NGV2
Volume	124 L	54 L
Length (typical)	55 in.	35 in.
Weight	114 lb	65 lb
Diameter (typical)	16 in.	13.8 in.
Shell Construction	Glass/C/epoxy hybrid with TuffShell®[a] protective shoulder	Glass/C/epoxy hybrid with TuffShell protective shoulder
Liner Material	HDPE	HDPE
Resin	Epoxy	Epoxy
Fiber Reinforcement	Carbon and glass fiber hybrid	Carbon and glass fiber hybrid

[a] TuffShell® is a registered trademark of General Dynamics Armament and Technical Products, Inc., Charlotte, North Carolina.

Selection of the containers for cycling and burst testing sought to provide data representative from as broad a sample of container use-conditions as possible. Therefore, containers selected were as follows in Table 3.

Table 3.
Type-4 Container Cycling and Burst Tests

Hydraulic Cycling and Burst
New Test Articles: WSTF ID #12-45898 WSTF ID #12-45894 - Previously pressure cycled : (15,000 cycles to 1.25*SP) Service Test Articles (Unconstrained during Testing) Vertically-Mounted: WSTF ID#11-45272 Horizontally-Mounted: WSTF ID# 11-45276 Service Test Articles (Constrained in OEM Mounting Straps): Vertically-Mounted: WSTF ID#11-45278 Horizontally-Mounted: WSTF ID# 11-45273 Service Test Articles (Unconstrained, Tuffshell Removed from Dome): Vertically-Mounted: WSTF ID#11-45281

Horizontally-Mounted: WSTF ID#11-45282
Pneumatic Burst (Nitrogen Fill Gas)
Service Test Article (Unconstrained during Testing) Vertically-Mounted WSTF ID#11-45269

Pressure data, volumetric response, dome response, strain response (sixteen strain gauges) and high speed video was collected for each of the tests and archived in data packages.

Hydraulic testing on eight containers consisted of seven pressure cycles, each with a dwell time of sixty seconds, and then ramp at <50 psi/sec to burst. These pressurization rates are in family with existing limits. Cycle 1 had a dwell pressure of 1000 psi and was performed as an instrumentation check-out cycle. Cycles 2, 4 and 6 were to service pressure, and cycles 3, 5, and 7 were to 1.25 times service pressure.

Type-4 Containers - Destructive Evaluation Results

Observations and results of hydraulic cycling and burst tests are as follows:

- All Type-4 service test containers demonstrated repeatable response during cycling.
- Strain response was consistent in each respective gage location across the population of containers tested.
- Compressive/negative strain was observed in the transition regions.
- Volumetric change (mass of water put into the container) remained consistent.
- Containers grew axially (0.5 – 0.75 inches) between ambient and full fill pressure.
- Radial growth was minimal to 1.25 SP
- No significant difference in response was observed between unconstrained vs. constrained pressurization test conditions (OEM-supplied mounts were installed on constrained containers per OEM guidelines and in locations consistent with "witness marks" on service containers.)
- All containers exceeded minimum allowable burst pressure of 2.25 SP.
- No significant difference in response was observed between the new test container and the sister new container that had been previously cycled 15,000 times to 1.25 SP.
- All containers demonstrated the same failure mode. Split/rupture in the cylindrical section of the container. This was a different failure mode from that observed in the field.

Table 4 shows the burst pressures for each container.

Table 4.
Hydraulic Burst Test Results

WSTF ID	Burst Pressure (psi)	Service Pressure (psi)	Ratio Burst to Service Pressure
11-45898	12015	3600	3.34
11-45894	12521	3600	3.48
11-45272	8511	3000	2.84
11-45276	8166	3000	2.72
11-45278	8553	3000	2.85
11-45273	8246	3000	2.75
11-45281	8395	3000	2.80
11-45282	8358	3000	2.79

Observations and results of the pneumatic burst test are as follows:

- The final burst pressure was 7904 psi. Ratio of burst to service pressure (3000 psi) was 2.63.
- Rupture pressure was approximately 500 psi lower than the average hydraulic burst pressure of other test articles. This may be a temperature effect (adiabatic compression). One or more additional pneumatic burst tests for comparison are desirable.

- The failure mode resulted in total destruction of the container.
- Apparent rupture initiation location was in the mid-hoop region, similar to the hydraulic burst tests. Again, this was a different failure mode from that observed in the field.
- Rupture spiraled axially simultaneously toward both A and B-Ends.
- B-End remnants were found 220 feet from "ground zero".

Type-4 Containers - Mechanical Sectioning and Materials Analysis Methods
NASA/WSTF entered into an agreement with the Materials Science and Engineering Laboratory of the National Institute of Standards and Technology (NIST) to conduct complementary evaluation of mechanical and physical properties of coupon samples that were sectioned from the composite overwrap layer of two of the service containers (WSTF #11-45284 and 11-45290). Sections were examined microscopically for voids, porosity, matrix and ply cracking, and delamination. Specimens were tested for tensile and fatigue strength.

Type-4 Containers – Mechanical Sectioning and Materials Analysis Results
- There was significant void percentage throughout the dome/body transition region and body region of the container.
- Multiple cracks and ply delamination were found throughout the transition region.
- Ultimate tensile strength of straight-sided specimens had little data scatter.
- Fatigue of specimens at normal operating strains for 20,000 cycles had no effect on specimen residual strength.
- The Glass Transition Temperature (Tg) of samples compared to historical reference data increased with container use and age. This result may indicate an increase in brittleness.

Type-2 Test Articles
Thirty-six Type-2 containers were removed from service at Philadelphia Gas Works and shipped to WSTF for testing. In addition to these containers, WSTF maintains an inventory of thirty-one Pressed Steel Type-2 containers, which have seen real world service, and are available for comparative testing in this program. All containers are locked inside controlled access storage in the original shipping configuration. These containers are banded to pallets.

Type-2 Containers – Nondestructive Evaluation Methods
The nondestructive evaluation of the Lucas Aerospace and Pressed Steel containers employs the same techniques as those used for the Type-4 containers. Including the Pressed Steel containers in the evaluation provides a good representation from an additional vendor. These evaluations are scheduled to be completed in July 2015.

Type-2 Containers - Destructive Evaluation
In general, the destructive evaluation will follow the test plan developed for the Type-4 containers. However, since there are major differences in construction and failure modes between the two container designs, some modifications are planned, and others may develop over the course of the nondestructive evaluation.
For example, unlike the plastic liner of the Type-4 container, we believe the steel liner of the Type-2 container would be capable of withstanding at least 50% of the design burst pressure. Therefore, it is planned to conduct burst tests on containers, as received, and with the composite overwrap removed, to determine residual strength in the liner alone. These evaluations are scheduled to be completed in July 2015.

CONCLUSIONS AND RECOMMENDATIONS

NDE revealed mechanical damage and chemical exposure, which could be reduced through improved installation considerations. This damage was evidenced by missing and wrinkled labels, debris buildup, and "witness marks" left by container straps that indicated shifting during service, which may induce surface damage or stress on container valves and fittings. A large amount of compressor oil and other contaminants were drained from the interior of some containers. The effects of these contaminants on the container interior are unknown and could be assessed in further research. CGA Pamphlet C6.4 Level 2+ damage was observed on the exterior of two of the containers. It is not known whether this damage could have been detected in a periodic inspection with the container in situ, but CGA inspection requires the manufacturer's recommendation in writing for repair or disposal for Level 2 damage. No inspection records for the Type-4 containers were available. Labeling should remain on

the containers for life, in order to provide safety and tracking information like manufacturer contact information, service pressure rating, and end of life date for the containers.

The new and used Type-4 containers all exceeded the minimum hydrostatic burst strength requirement in FMVSS 304 of 2.25*SP. The container that was pneumatically burst exceeded the minimum burst strength as well, although at a lower margin. Running additional pneumatic burst tests of a Type-4 container would help to determine whether this result is consistent.

Microscopic inspection of composite coupon sections revealed voids, cracks, and ply delamination. Additional evaluation of new and used construction materials could provide insight into the relationship between physical and mechanical properties of samples and container performance and to provide comparison of what typical void and micro-cracking of unused containers looks like.

REFERENCES

[1] ANSI NGV2 (1992) Basic Requirements for Compressed Natural Gas Vehicle (NGV) Fuel Containers

[2] 49 CFR Part 571, FMVSS 304, Compressed Natural Gas Container Integrity, Effective Date March 27, 1995

[3] Brown, C., (2008) Metallurgical Evaluation of a Compressed Natural Gas Tank Cylinder Liner From PGW #3436, Report No. 0809-25278, Stork Technimet, Inc.

[4] Stenmark, N., (2008) Failure Analysis of a Composite Wrap on a Compressed Natural Gas Tank from PGW #3436, Report No. 0810-25584, Stork Technimet, Inc.

[5] Horne, D., (2010) CNG Cylinder Safety Issues & Opportunities, Natural Gas Vehicle Technologies Forum, October 12, 2010, Clean Vehicle Education Foundation

Appendix A

Table A1: NDE Summary of Service Containers (Horizontally Mounted

WSTF ID	S/N	Breakaway Torque Manual Valve (ft/lb)	Breakaway Torque Plug (ft/lb)	Weight [2] (lb)	Visual Inspection Internal Oil Present	Visual Inspection Internal Blister/wrinkle Indications	Visual Inspection External (# of indications) General [4]	Visual Inspection External (# of indications) CGA Level 1	Visual Inspection External (# of indications) CGA Level 2	Chemical Sampling External	Chemical Sampling Internal	Gas Sampling	Radiography A-End	Radiography Hoop	Radiography B-End
11-45271	43-3	105	< 5	118.7	Pooling	YES	6	3	1	Archived	Archived	N/A	Boss fitting delamination	Deformed Liner	Boss fitting delamination
11-45273	35-191	105	< 5	118.2	Trace	YES	4	5	0	Archived	Archived	N/A	Boss fitting delamination	No anomalies observed	Boss fitting delamination
11-45274	35-190	110	< 5	119.2	Trace	YES	7	4	0	Archived	Archived	N/A	Boss fitting delamination	No anomalies observed	Boss fitting delamination
11-45276	35-106	90	< 5	118.9	Pooling	YES	2	3	0	Archived	Archived	N/A	Boss fitting delamination	No anomalies observed	Boss fitting delamination
11-45277	35-107	105	< 5	120	Pooling	YES	5	6	0	Archived	Archived	N/A	No anomalies observed	No anomalies observed	No anomalies observed
11-45279	35-079	105	< 5	119.5	Pooling	YES	1	8	1	Archived	Archived	N/A	Boss fitting delamination	No anomalies observed	Boss fitting delamination
11-45280	35-078	105	< 5	119.7	Pooling	YES	3	4	0	Archived	Archived	N/A	Boss fitting delamination	No anomalies observed	Boss fitting delamination
11-45282	35-109	110	< 5	119.5	Trace	NO	2	6	0	Archived	Archived	N/A	Boss fitting delamination	No anomalies observed	Boss fitting delamination
11-45283	35-111 [1]	N/A	N/A	120.0	Pooling	YES	6	5	0	LWO# 726585	LWO# 726475	N/A	No anomalies observed	No anomalies observed	No anomalies observed
11-45285	35-042	40	< 5	118.7	Trace	YES	3	6	3	Archived	Archived	N/A	Boss fitting delamination	No anomalies observed	Boss fitting delamination
11-45286	35-039	100	< 5	117.7	Trace	YES	2	3	0	Archived	Archived	N/A	Boss fitting delamination	No anomalies observed	Boss fitting delamination
11-45289	35-123	130	< 5	121.2 [3]	Pooling	YES	3	1	1	Archived	Archived	Archived (~5 psig)	Boss fitting delamination	No anomalies observed	No anomalies observed
11-45290	35-121	115	< 5	121.4 [3]	Pooling	YES	3	0	0	Archived	Archived	Archived (~5 psig)	Boss fitting delamination	No anomalies observed	No anomalies observed

Notes:

1 Label detached and found loose within shipping container
2 Weight obtained after removal of boss fittings, includes residual oil
3 Weight includes closed boss fittings and residual gas contents
4 General indications, not assigned a classification level per CGA inspection criteria

Table A2: NDE Summary of Service Containers (Vertically Mounted)

WSTF ID	S/N	Breakaway Torque		Weight [2]	Visual Inspection					Chemical Sampling			Radiography		
		Manual Valve	Plug		Internal		External (# of indications)			External	Internal	Gas Sampling	A-End	Hoop	B-End
		(ft/lb)	(ft/lb)	(lb)	Oil Present	Blister/wrinkle Indications	General [4]	CGA Level 1	CGA Level 2						
11-45269	35-119	20	< 5	119.0	NO	YES	4	7	1	Archived	Archived	N/A	Boss fitting delamination	No anomalies observed	Boss fitting delamination
11-45270	43-2	110	< 5	117.8	NO	YES	4	6	0	Archived	Archived	N/A	Boss fitting delamination	No anomalies observed	Boss fitting delamination
11-45272	35-189	120	170	117.1	Trace	YES	2	7	0	Archived	Archived	N/A	Boss fitting delamination	No anomalies observed	Boss fitting delamination
11-45275	35-041	110	< 5	117.8	NO	YES	7	8	0	Archived	Archived	N/A	Boss fitting delamination	No anomalies observed	Boss fitting delamination
11-45278	35-074	100	< 5	120.1 [3]	NO	YES	2	7	0	Archived	Archived	Archived (~1 psig)	No anomalies observed	No anomalies observed	No anomalies observed
11-45281	35-108	105	170	117.6	Trace	YES	2	6	0	Archived	Archived	N/A	Boss fitting delamination	No anomalies observed	Boss fitting delamination
11-45284	35-040	120	160	117.8	Trace	YES	2	7	1	Archived	Archived	N/A	Boss fitting delamination	No anomalies observed	Boss fitting delamination
11-45287	35-122	105	< 5	118.1	Trace	YES	3	6	1	Archived	Archived	N/A	No anomalies observed	No anomalies observed	No anomalies observed
11-45288	35-120	115	< 5	118.9	Trace	YES	3	8	2	Archived	Archived	N/A	No anomalies observed	No anomalies observed	No anomalies observed
11-45291	35-038	N/A	N/A	117.4	Trace	YES	2	11	1	LWO# 726585	LWO# 726475	N/A	Boss fitting delamination	No anomalies observed	No anomalies observed

Notes:

1 Label detached and found loose within shipping container
2 Weight obtained after removal of boss fittings, includes residual oil
3 Weight includes closed boss fittings and residual gas contents
4 General indications, not assigned a classification level per CGA inspection criteria

GENERAL VIRTUAL TESTING METHODOLOGY FOR TYPE IV CNG TANKS

Ralf Matheis
Helmi Murnisya
Forschungsgesellschaft Kraftfahrwesen mbH Aachen
Germany

Roberto Puppini
Centro Ricerche Fiat S.C.p.A.
Italy

Paper Number 15-0405

ABSTRACT

The project MATISSE funded by European Commission's 7th Framework Programme (FP7) aims to make a significant step forward in the capability of the automotive industry to model, predict and optimise the crash behaviour of mass produced fibre reinforced polymers (FRP) with the focus set on components for alternatively powered vehicles (APV). One of the project's main research goals is the development of a general virtual testing methodology (VTM) for the development of APV driven by compressed natural gas (CNG) equipped with composite FRP tanks of Type IV.
Due to the increasing legislative demands on the emission of future vehicles, the development of APVs that are in this regard superior to conventional internal-combustion engines (ICE) driven by petrol or diesel fuel is currently in the centre of attention of the automotive industry. Here, the usage of ICE with CNG supply offers advantages in comparison to other concepts, since it requires only moderate modifications of the conventional drive train. Because of the high mechanical demands on the required high-pressure storage tanks and the need for lightweight structures, which also contributes to the emission reduction, the usage of material of high specific material properties is required. Especially the full composite tanks of the Type IV show a high potential in this regard. Since these high-pressure storage components form a significant safety hazard, the accurate analysis of the mechanical demands during relevant crash load cases is of great importance. For the proper and optimal integration of the tanks into the vehicle during the APV design and development process at industrial level, moreover the predictability of the material and component behaviour using the finite element method (FEM) is indispensable.
Within the MATISSE project a new overall approach for the crash analysis of CNG tanks is proposed. This paper describes the main aspects of this VTM:
First, a FRP material modelling approach for wet wound CNG tanks, that makes use of the so-called "reverse FEM" as well as of novel physically based material models that are fed with calculative as well as literature based material values and are validated on three point bending tests of wound tubes was defined.
Then, the derived material models for glass and carbon fibre were subsequently used for the modelling of FEM tank models, whereby different steps of optimisation of on the one hand the accuracy and on the other hand the simulation time were conducted.
In a next step, different relevant load cases on a full vehicle model of a compact car equipped with a CNG tank where simulated and analysed. The detected highest mechanical demands were thereupon transferred to a component test programme on a tank-subsystem that depicts the loads obtained by the tanks. Here again, the FEM model of the tank is used to find the appropriate boundary conditions.
The developed test programme was subsequently conducted on a series of physical tanks and the simulation approach and thus the VTM was validated on the results.

INTRODUCTION

Increasing energy costs, limitation of crude oil resources as well as constantly intensifying emission targets (especially w.r.t. CO_2) are a pivotal driver for current automotive research and development [1]. In this regard alternatively powered vehicles (APV) with drive-trains that differ from conventional internal-combustion engines (ICE) supplied with petrol or diesel fuel show high potential for energy economical and environmentally friendly propulsion [2]. On the other hand lightweight structures are a fundamental requirement in order to achieve a low demand of energy and to compensate possible higher structural masses of alternatively powered drive-trains [3].
An alternatively powered drive-train that is on the one hand cost efficient since it requires comparatively minor design changes to conventional vehicles (primarily ignition and valve-train system) and on the other hand has a perspective to evoke low CO_2 emissions, is an ICE operated with compressed natural gas (CNG) [4], [5]. This energy source requires high-pressure storage tanks that have to withstand the high mechanical

demands of internal pressures of 200 bars to 250 bars. In order to achieve energy storage that is simultaneously light and safe, pressure vessels of the Type IV that are entirely made of fibre reinforced polymers (FRP) are currently state of the art [6].
For the proper and optimal integration of the tanks into the vehicle during the APV design and development process at industrial level, moreover the predictability of the material and component behaviour using the finite element method (FEM) is indispensable [7]. Besides analyses of the passenger and partner safety of the vehicle, the simulation of the component loading behaviour and subsequent analysis of the material stresses and damage allows an optimisation of components concerning weight. Especially FRP laminates offer a potential for optimisation as well as numerous influence parameters [8].
One of the major advantages of FEM simulations is that, once a model validated on test results is established, analyses for different scenarios or design changes can be carried out virtually. This can reduce the development expenses as well as development cycles drastically. However, approval tests are obligatory for the final vehicle or respectively component [9].

MOTIVATION

Although virtual methods like FEM analyses have become an integral part of the automotive industry, they still lack in broad acceptance concerning their reliability. Especially, when it comes to unconventional materials like FRP, the development is characterised by conventional component tests. With regard to CNG tanks, the InGAS project identified the following open issues:

- No crash simulation models are available for such complex composite structures
- No standardised test procedures are available
- No validated methods are available to transfer the test results to the crash situation in a vehicle [10]

In order to overcome these issues and to make a step forward in the capability of the automotive industry to model, predict and optimise the crash behaviour of vehicles equipped with Type IV tanks, a virtual testing methodology (VTM) was developed within the project MATISSE funded by European Commission's 7th Framework Programme. As a demonstrator a belly mounted CNG tank consisting of a combined carbon fibre reinforced polymer (CFRP) and glass fibre reinforced polymer (GFRP) wet wound structure with a polyamide (PA) liner and aluminium bosses was used. However, the feasibility of the approach was also verified for a neck mounted design.

The physical tanks used as reference within the VTM are produced and provided by the MATISSE partner Xperion Energy & Environment GmbH and are approved for vehicle application.

All simulations within the VTM are carried out using the explicit FEM solver LS-DYNA which is provided by the MATISSE partner DYNAmore Nordic AB.

VTM APPROACH

The here presented VTM approach aims to achieve an adequate level of prediction of the failure behaviour of composite high-pressure storage tanks (HST) under crash loading conditions, both at component and vehicle level. This general VTM involves four main steps:

- Identification of relevant (full vehicle) crash scenarios.
- Their numerical simulation through FEM codes.
- Analysis of results obtained from these simulations and extraction of the envelope of crash loading conditions of interest insisting on HST.
- Definition of simplified/reduced test set-ups capable of generating, on the isolated HST, loading conditions that are equivalent and/or representative of the ones that are seen by the composite tank within the vehicle during full car crashes of interest (the above mentioned envelope), so that corresponding physical test-rigs

can be designed in detail and subsequently built for experimental testing campaigns on the composite tanks.

The general VTM is illustrated in Figure 1.

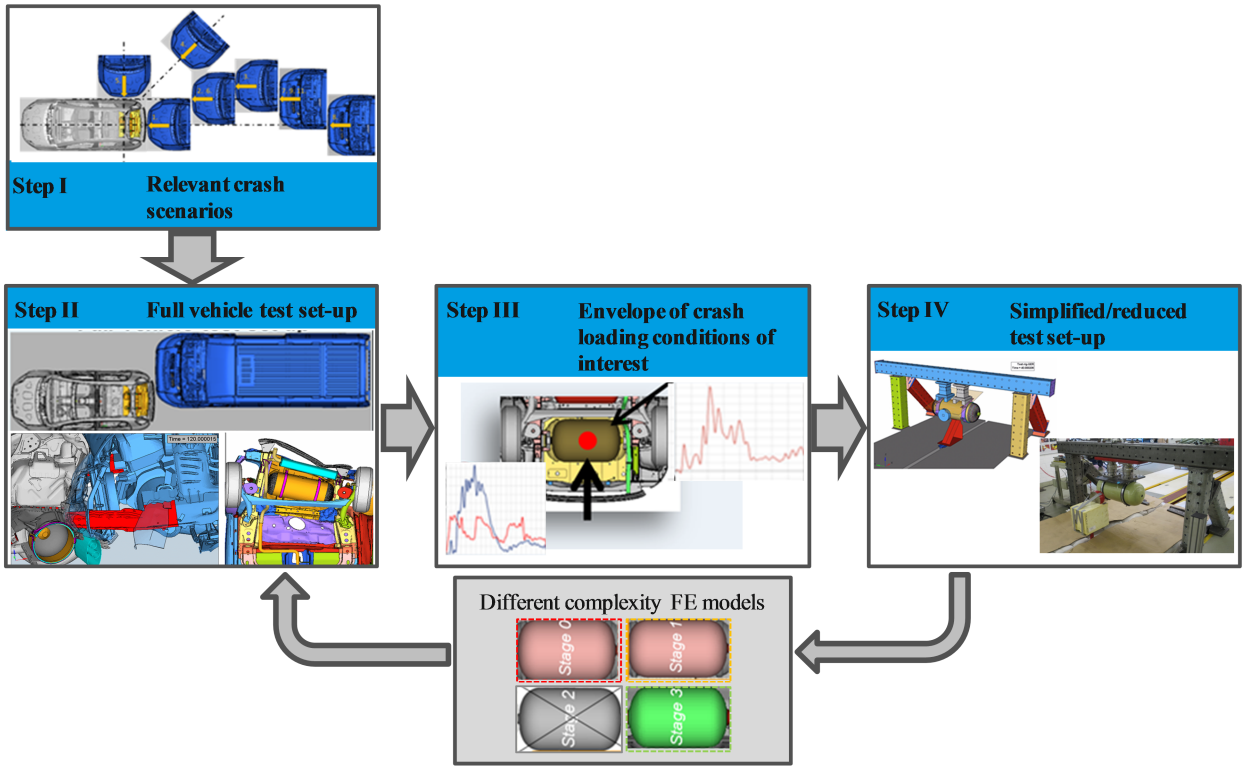

Figure1. Schematic diagram of the VTM

SIMULATION TOOLS

In order to successfully pass through these steps, a special focus has to be set on the CNG tank model, which is considered to be the key element of the methodology. The model is based on geometry and material information for the components liner and bosses as well as the winding and material information for the CFRP and GFRP winding layers. In order to achieve the highest precision of results but on the other hand to allow an efficient course of the project, here four different stages of modelling complexity are applied in the steps of the VTM. For the validation of the material model a so-called reverse FEM approach is applied.

Reverse FEM Approach

Based on the applied wet winding production process used to manufacture Type IV CNG tanks, a rather unconvential simulation approach has to be carried out, since the process does not allow the production of flat or ring shaped specimens for standardised quasi-static tests (for general data acquisition as it is usually done for FRP materials). In order to use a material structure that is windable and comparable to the investigated tanks, several tubes with different layer set-ups are tested in a quasi-static three point bending (3PB) test, with two circular lateral constraints and a cylindrical central indenter with a constant velocity of 1 mm/s. The material model for the simulation is defined using calculated literature or assumed values and then calibrated on the test results of the 3PB and checked for plausibility on virtual quasi-static coupon tests (that consider tensile, compression and shear loading). Furthermore, the delamination failure criteria are virtually validated by the simulation of an end notch flexure (ENF) test and a double cantilever beam (DCB) test. In order to achieve robust modelling different laminate set-ups are tested in the 3PB. The MATISSE modelling approach is presented in Figure 2.

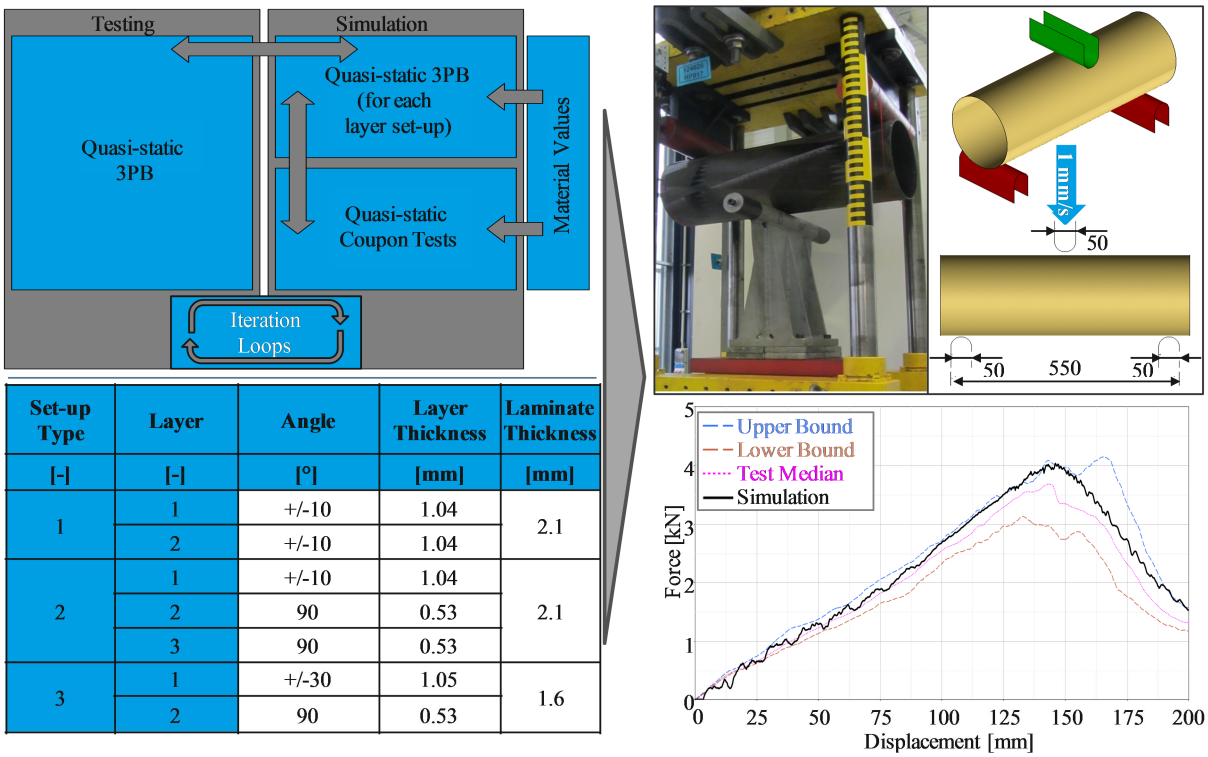

Set-up Type	Layer	Angle	Layer Thickness	Laminate Thickness
[-]	[-]	[°]	[mm]	[mm]
1	1	+/-10	1.04	2.1
	2	+/-10	1.04	
2	1	+/-10	1.04	2.1
	2	90	0.53	
	3	90	0.53	
3	1	+/-30	1.05	1.6
	2	90	0.53	

Figure2. Reverse FEM approach

Stage 0 tank model

Stage 0 defines a rough CNG tank model that has the geometry of the tank to be analysed but is meshed rather coarse with shell elements (average size of 10 mm) and assumes only elastic and isotropic material behaviour, without any failure criteria for the composite layers. The bosses are modelled as solid elements with elastic and isotropic material properties, too. However, the mechanical properties of the composite part of the vessel are correspondent to the in-fibre properties of the materials applied (average Young's modulus and density). The stage 0 derives from the past FP7 project InGAS and is applied in order to evaluate the crash conditions in a very early stage of the project since it does not require in-depth information of the materials and the winding set-up (see Figure 3).

Stage 1 tank model

For a more sophisticated evaluation of the crash behaviour the stage 1 model is applied. The model is provided with the geometry and winding information of the tank to be analysed and uses a much finer shell mesh of 3 mm with layer definition applied to different integration points. The shell mesh is used in order to allow time efficient modelling and calculation. However, the section of the wound areas of the tank show thicknesses up to 22.5 mm and thus exceeding the limitations of the shell theory. Furthermore, it is modelled with a special composite material model (*MAT_58) that considers material moduli and strength values for the fibre and transversal direction as well as for shear. The liner is considered to be elastic and the bosses are modelled as rigid. All material values are based on either literature research or calculations (see Figure 3).

Stage 2 tank model

The stage 2 represents the most complex tank model of the VTM and is used for the second loop of step IV. It uses the same component geometry and winding information as stage 1 but is meshed with several layers of thick shell elements with layer definition applied to different integration points. It uses a novel continuum damage model (*MAT_262). The model considers material moduli and strength values for the fibre and transversal direction as well as for shear and material damage mechanisms that are physically based and consider fracture toughness values.

Furthermore, the structural failure due to delamination is adressed using cohesive elements between the thick shell elements that consider different failure modes (see Figure 3).

Stage 3 tank model

Stage 3 is a predictive composite model suitable for the use within full car crash FE simulations and applied in a third loop of step 1 and respectively step IV of the VTM . It is based on the Stage 2 but comprises a set of simplifications such as coarsening, layer clustering and numerically more efficient elements. It derives from a number of simplification and subsequent simulation loops within step IV that are evaluated in comparison to the Stage 2 simulation results. After each measure of simplification the simulation results are compared and the accuracy and efficiency of the measure is evaluated. If the related gain in efficiency is considered to be worth the loss in accuracy a simplification measure is kept. If not, the measure is withdrawn and another measure is applied (see Figure 3).

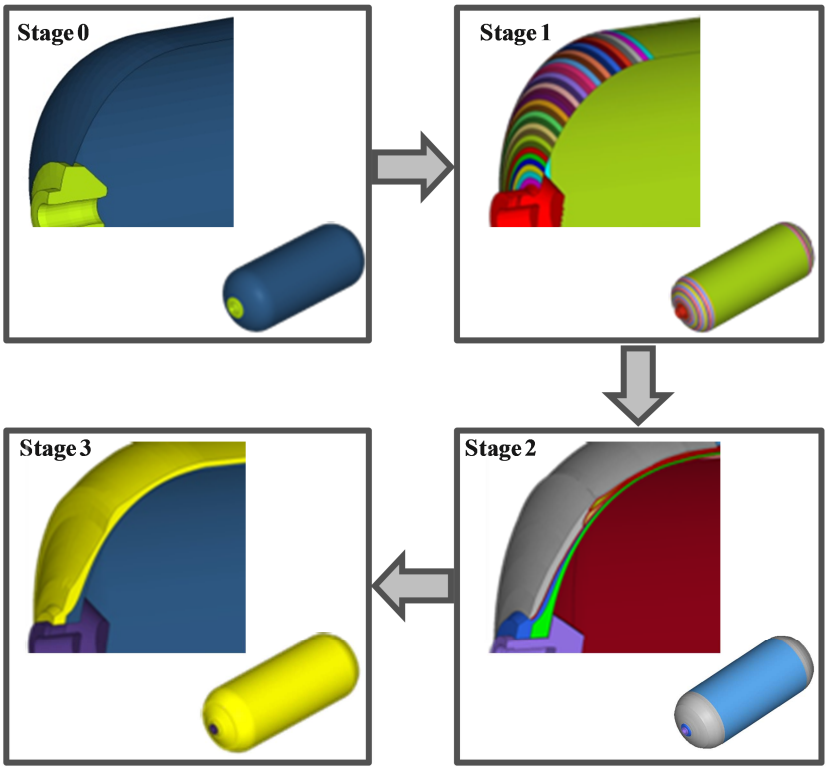

Figure3. Stages of CNG tank model

STEPS OF THE VTM

In the following the different steps of the VTM are described in detail and their application within the MATISSE project is presented.

Step 1: Identification of Relevant Crash Scenarios

The identification of the crash scenarios is not primarily based on statistical relevance since the focus of the VTM is not set on the most likely load cases but on crash scenarios that are relevant w.r.t. the potential to induce damages on the composite CNG tanks. For this concern numerous crash situations are proposed and evaluated by crash experts concerning their severity but also w.r.t. to probability.
More precisely, for the here described reference case eleven full car-to-car collisions involving a B-class vehicle equipped with an unpressurised CNG tank system and two different types of opponents (bullet vehicles) were chosen. As relevant bullet vehicles a B-class car and a van were considered. The target car is always assumed to be

stationary with released brakes. For the target car three different types of muffler locations/lay-outs were considered. The eleven load cases are as follows:

Target car without muffler between the tank and the rear crossbeam; bullet: B-class car impacting at 55 km/h
1. Rear impact, “full overlap”
2. Rear impact, “50% overlap”
3. Rear impact, “25% overlap”
4. Side impact, from the right side, “oblique”
5. Side impact, from the right side, “perpendicular”

Target car with muffler between the tank and the rear crossbeam; bullet: B-class car and van impacting at 55 km/h
6. Rear impact by car , “50% overlap”
7. Rear impact by van, “50% overlap”
8. Rear impact by van, “full overlap”

Target car with muffler between the tank and the rear crossbeam but with reduced distance w.r.t. tank; bullet: van impacting at 55 km/h
9. Rear impact by van, “50% overlap”
10. Rear impact by van, “full overlap”

Target car with muffler with reduced distance to tank; bullet: van impacting at 80 km/h
11. Rear impact by van, “50% overlap”

In this step of the VTM neither simulations nor physical tests are applied. However, the choice of relevant load cases forms the basis for the fully virtual step 2.

Step 2: Numerical Simulation of Relevant Crash Scenarios

Subsequently in the second step of the VTM all the considered collision scenarios are simulated and the results are evaluated concerning their severity. This includes the stresses and strains of the tank structure but also general endangerments of these components due to impacts on sharp or rigid components as well as the loading in the valve area.

In the reference case the simulation was carried out in LS-DYNA using existing models for the B-class car and the van. The model of the impacted vehicle is equipped with a tank model as well as the corresponding environment structure. In a first loop of the step 2, the stage 0 model was used due to the fact that the complex modelling and reverse FEM activities made a very early availability of stage 1 model within the project not possible. As the stage 1 model was released, the general conclusions of the simulations could be verified and refined in a second loop using this more significant model.

The results obtained from the numerical simulation campaign confirmed that the most severe loading conditions for the CNG composite tank are achieved when the reference vehicle is impacted by the van. In particular, impact configuration no. 9 resulted to be the worst one. Due to the offset and to the “aggressivity” of the van (stiffer and higher main rails, almost double vehicle mass) w.r.t. the reference car, the latter is subjected to very high rear intrusions with the van front structure arriving to interact directly with the tank. Configuration no. 11 (in practice the no. 9 repeated with the speed increased at 80 km/h), despite being more severe in terms of overall target vehicle deformations, was almost similar to configuration no. 9 in terms of loading conditions on the composite tank. This is the case mainly due to the fact that the extra energy introduced by the speed increase was absorbed essentially through more deformation of the vehicle structure in front of the tank area. The deformations for the target vehicle in this crash configuration are presented in Figure 4.

Again no physical tests are foreseen in this step of the VTM.

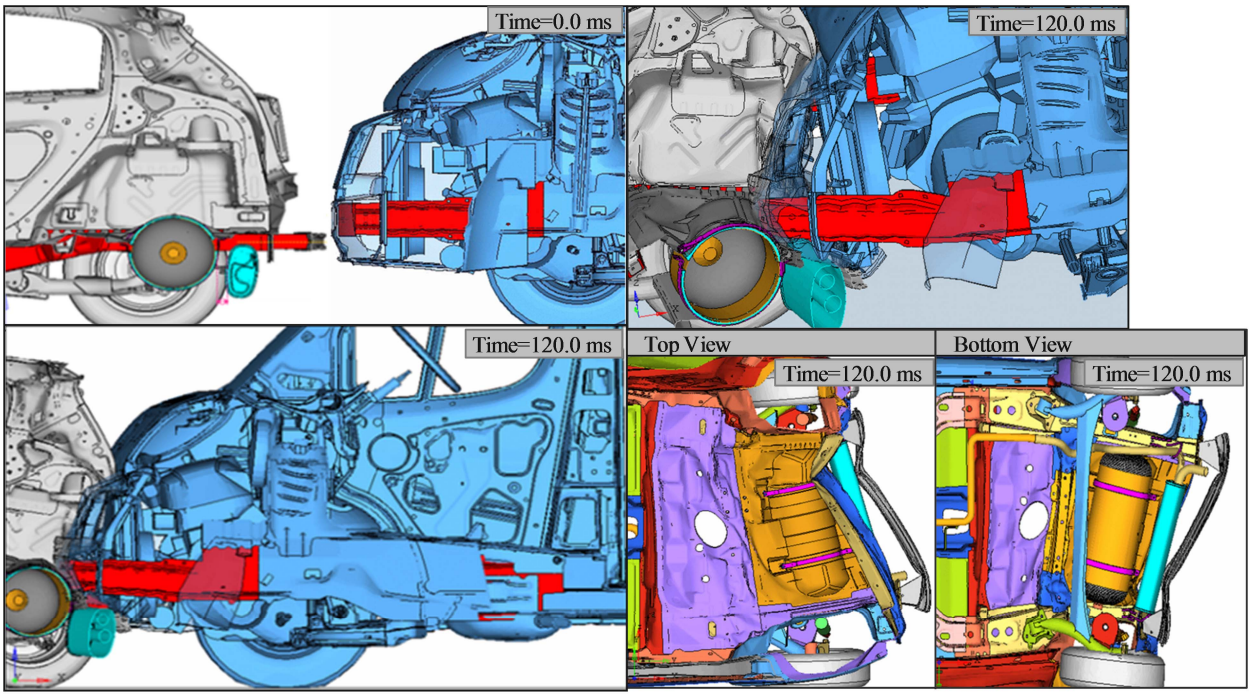

Figure4. Configuration 9: Deformations on target vehicle equipped with Stage 1 tank model

Step 3: Envelop of Crash Loading Conditions

In the third step of the VTM there is a more in depth analysis of the loading to the tank, especially on areas that have potential of hazard to the environment due to damage or even leakage and burst. This includes for example:

- accelerations in different points
- global contact force and maximum interface resultant force
- interface normal pressure
- section forces on the tank
- section forces on tank fixations

Furthermore, this analysis gives information about which boundary conditions and subsystems of the full vehicle impact have to be transferred to the subsequent definition of an adequate simplified test that is significant for the loading of the tank.

Then, the third step of the VTM led to the identification of some important indications towards the definition of an equivalent simplified/reduced subsystem test set-up.

Such indications are recalled in the following:

- An equivalent simplified test-rig should have the possibility to impact the tank on different locations and from different directions.
- This possibility should be realised by an impactor capable to reproduce similar normal pressures on the tank and global contact forces (i.e. having the proper shape and energy level).
- The simplified test-rig should have the possibility to allow some deformation of the tank anchorage points, by acting on their stiffness/strength within a proper range, in order to reproduce the boundary condition seen by the tank when mounted on the specific reference vehicle.

Step 4: Simplified Test Set-up

The step 4 of the VTM is a pivotal step for the application of this methodology since it is not only carried out in the virtual environment but is also performed on physical tanks, thus providing the input for a comparison between the simulation and the tests and allowing a subsequent validation of the approach. In step 4 the task is to accurately reflect the boundary conditions of loading conditions considered to be relevant and significant (i.e. like the already mentioned full vehicle configuration 9) with a test rig that can be set up on the one hand simple and easy and on the other hand reproducible, in order to avoid expensive and complex full vehicle tests. The validation by the experimental test results obtained with such a test-rig shall provide a tank model that can be applied in a validated full vehicle model in order to obtain information about the crash saftey of the CNG tank system. For these in-vehicle applications, the validation process should comprise a final simplification of the tank model in order not to affect the simulation costs too significantly (i.e. the already described stage 3 model).

Starting from the reference case (i.e. the full vehicle configuration 9) a suitable test rig for a crash test facility, considering the above mentioned indications, was developped in several loops of iteration leading to a flexible set-up that allows the application of different tank sizes and mounting systems (e.g. belly and neck mounting) as well as different impact orientations, positions, masses, surfaces and velocities. As a result of such test-rig flexibility, other impact configurations than the one corresponding to the reference case (named test-rig configuration 6) were explored at numerical simulation level, so that a possible test-matrix for the experimental campaign with the reduced set-up was proposed. Among these test-rig configurations, four (including the reference case) were identified as the most relevant ones and subsequently for complexity reasons only this subset of configurations was tested (see test-rig configurations 2, 5, 6 and 7 in Figure 5). The specimen is mounted as it is applied in the vehicle but upside down, since this allows the highest flexibility and accuracy of the test rig set-up on a crash test facility. Here, the tests are documented using load-cells at the mounting plate and high-speed video cameras from different positions.

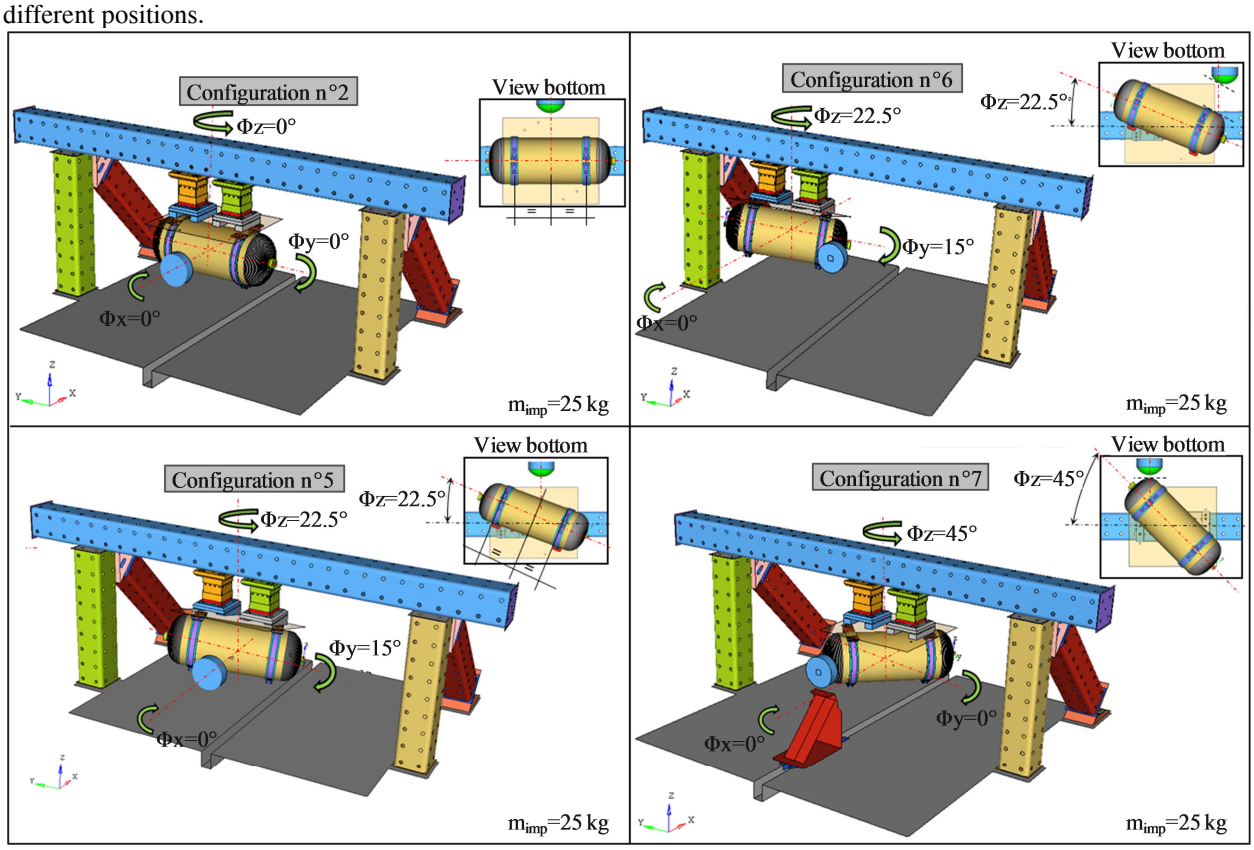

Figure5. Simplified test set-up and analysed impact configurations

After the conduction of the tests several evaluations were carried out. These were analysis of force and acceleration curves measured on the test rig, optical check of tank surface as well as of the mounting straps and interior, microscopy and CT of cut-out specimens as well as burst pressure and cycling pressure tests in order to understand the failure criteria and to see potential areas of hazard (see Figure 6). Furthermore, the experimental results were applied in order to validate the stage 2 model and to subsequently derive the simplified stage 3 model, i.e. the final one that is suitable for the application in all the VTM steps, then closing the methodology loop for potential future structural optimisation or evaluation of different vehicle and tank structures.

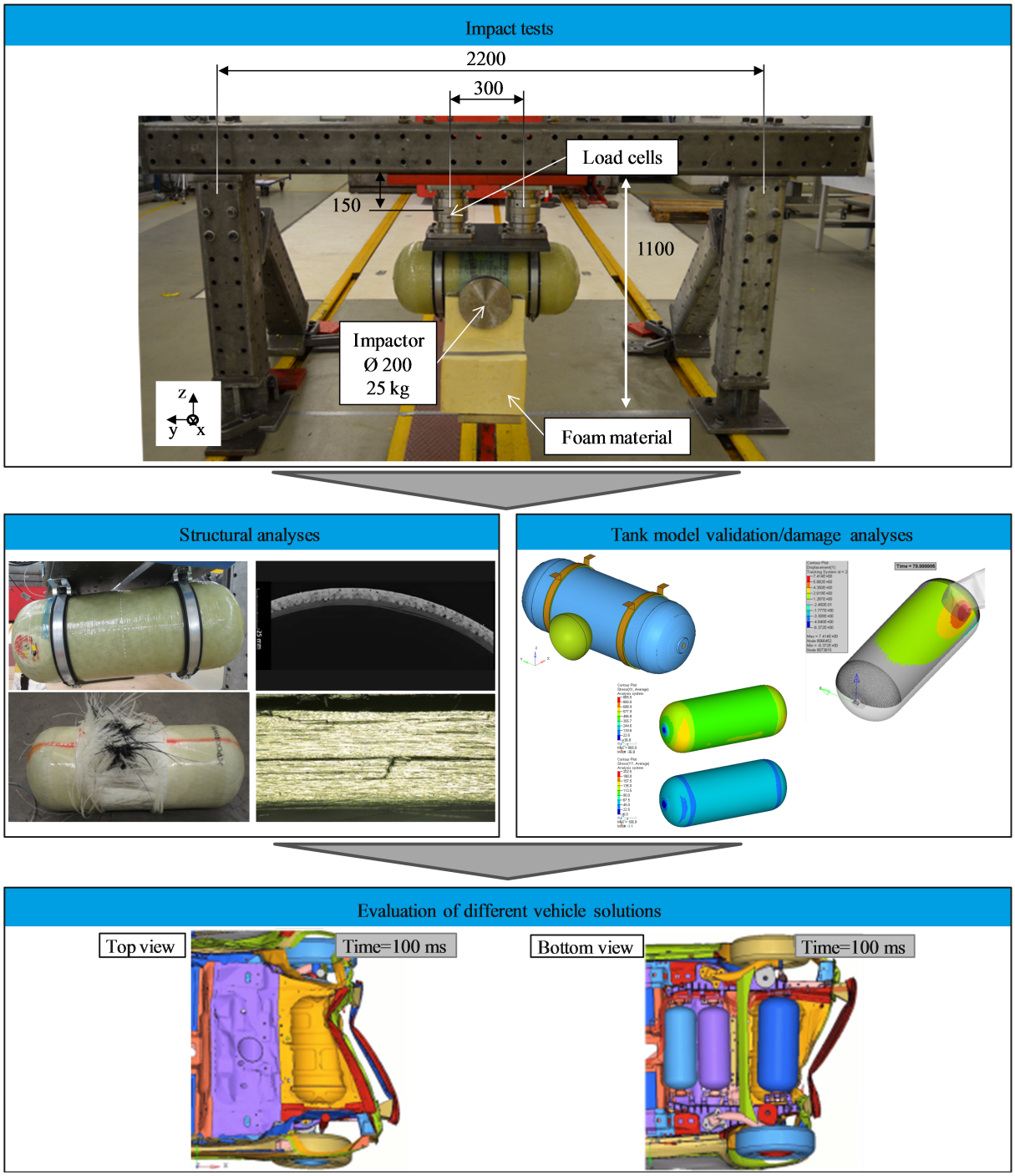

Figure6. Evaluation of CNG tanks after testing

CONCLUSIONS

A stepwise virtual testing methodology for the evaluation and optimisation of vehicles equipped with CNG tanks was developed in the MATISSE project. This methodology allows a reduction of the development effort related to the crash safety design of such a type of APV, on the basis of a validated vehicle simulation model and a simplified experimental test rig set-up that is suitable for the evaluation of the tank crash behaviour as well as for the validation of an appropriate tank model for the crash simulation.

In the course of the methodology a set of relevant crash load cases (at full vehicle level) was defined and subsequently modelled in the FEM environment by using the vehicle model of interest that includes the adopted tank model(s) according to the specific lay-out solution to be examined. Based on the simulation results from this scenario, the most relevant loading conditions acting on the tank(s) can be isolated and further analysed. The results of such an analysis can be used for the definition of a suitable simplified and equivalent test-rig configuration as well as for an adequate experimental test programme. With the conduction of physical tests according to that test programme and together with their corresponding FEM simulations, a tank model can be improved/refined to cover adequately the composite behaviour under impact conditions. Furthermore, it can be validated against the obtained experimental results and subsequently reduced/simplified in order to be more efficiently applied in full vehicle simulations, by maintaining at the same time an appropriate level of failure prediction/detection during the industrial development process of CNG tanks and vehicles equipped with such systems.

ACKNOWLEDGEMENT

All the presented work was carried out within the project MATISSE funded by European Commission's 7th Framework Programme.

The authors would like to acknowledge the MATISSE partners Xperion Energy & Environment GmbH and DYNAmore Nordic AB for the collaboration since the very beginning of the project.

REFERENCES

[1] Eichhorn, U. 2012. "Mobility for the Future"
Proceedings, 21st Aachen Colloquium Automobile and Engine Technology 2012
[2] Wu, J.; Dunn, S. C. 1995. "Environmentally responsible logistics systems"
International Journal of Physical Distribution & Logistics Management, Vol. 25 Iss: 2, pp.20 – 38
[3] N.N.. 2012. "Fortschrittsbericht der Nationalen Plattform Elektromobilität (Dritter Bericht)"
Bundesministerium für Umwelt, Naturschutz, Bau und Reaktorsicherheit, Germany
[4] da Silveria, B. H.; Benvenuti, L. H.; Werninghaus, E.; Coelho, E. P. D.; Silva, C. D.; de Olivera, F. R.; Silva,m J. C. S. 2004. "Development of a Concept Vehicle for Compressed Natural Gas"
SAE Technical Paper Series, Paper No. 2004-01-3452
[5] Gaudio, R.; Volpi, E. 2009. "Position Paper: Natural Gas and CO_2 - Natural gas is a champion in road transport and also saving CO_2 emissions"
Position Paper of NGVA Europe
[6] Hansen, G. P.; Sato, M.; Yan, Y. 2010. "Pressure Vessels for Hydrogen Vehicles: An OEM Perspective"
International Hydrogen Fuel and Pressure Vessel Forum, Beijing
[7] Liu, G. R.; Quek, S. S. 2003. "Finite Element Method – A Practical Course"
Elsevier B.V.
[8] Venkataraman, S.; Haftka, R. T.1999. „Optimization of Composite Panels – A Review"
Proceedings, American Society for Composites
[9] Bueno, P.; Mallen, J.; Rodrigo, J.; Cordero, R.; Garcia, J. 2012. "D3.2 – Overview on accreditation procedures in Europe"
Project Deliverable, imviter Project, FP7–2007–SST–218688
[10] N.N. http://www.ingas-eu.org INGAS Project Final Report and INGAS second annual report - Publishable Executive Summary